Communications in Advanced Mathematical Sciences

VOLUME VIII
ISSUE II

ISSN 2651-4001

VOLUME 8 ISSUE 2
ISSN 2651-4001

June 2025
www.dergipark.org.tr/en/pub/cams

COMMUNICATIONS IN ADVANCED MATHEMATICAL SCIENCES

Technical Editor

Arzu Özkoç Öztürk
Department of Mathematics
Duzce University
Düzce-Türkiye

Zülal Mısır
Department of Mathematics
Sakarya University
Sakarya-Türkiye

Indexing and Abstracting

DOAJ

EBSCO Central & Eastern European Academic Source

EBSCO Applied Science & Technology Source Ultimate

Contents

Research Article

Communications in Advanced Mathematical Sciences
ISSN (Online) 2651-4001

Vol. 8, No. 2, 57-69, 2025
https://doi.org/10.33434/cams.1660607
Research Article

Euler–Maclaurin-type Inequalities for $h-$convex Functions via Riemann-Liouville Fractional Integrals

Fatih Hezenci[1]*, Hüseyin Budak[2]

Abstract
In this paper, some Euler-Maclaurin-type inequalities are established by using $h-$convex functions involving Riemann-Liouville fractional integrals. In precisely, using the properties of h-convex functions, we prove new Euler-Maclaurin-type inequalities. In addition, we present some Euler-Maclaurin-type inequalities for Riemann-Liouville fractional integrals by using Hölder inequality. Moreover, some Euler-Maclaurin-type inequalities are established by using power-mean inequality. Finally, by using the special choices of the obtained results, we obtain some Euler-Maclaurin-type inequalities.

Keywords: Convex functions, Fractional calculus, Maclaurin's formula, Quadrature formula
2020 AMS: 26D07, 26D10, 26D15, 65D32

[1] *Department of Mathematics, Düzce University, Düzce, Türkiye, fatihezenci@gmail.com*
[2] *Department of Mathematics, Kocaeli University, Kocaeli, Türkiye, hsyn.budak@gmail.com*
*__Corresponding author__

Received: 18 March 2025, **Accepted:** 05 May 2025, **Available online:** 14 June 2025
How to cite this article: F. Hezenci, H. Budak, *Euler–Maclaurin-type Inequalities for $h-$convex functions via Riemann-Liouville fractional integrals*, Commun. Adv. Math. Sci., 8(2) (2025), 57-69.

1. Introduction

Inequality theory is a well-established and still fascinating field of research, with a wide range of applications across various areas of mathematics. In mathematical analysis, convex functions play a crucial role in the study of inequalities due to their distinct geometric and analytical properties.

The author of [1] introduces a novel class of functions called h-convex functions.

Definition 1.1. *Let $h:(0,1)\to\mathbb{R}$ be a non-negative function, $h\neq 0$. We say that $f:I\subseteq\mathbb{R}\to\mathbb{R}$ is an h-convex function, if f is non-negative and for all $x,y\in I$, $t\in(0,1)$ we have*

$$f(tx+(1-t)y)\leq h(t)f(x)+h(1-t)f(y). \tag{1.1}$$

If the inequality (1.1) is reversed, then f is said to be h-concave.

By setting

- $h(t)=t$, Definition 1.1 becomes to convex function [2].
- $h(t)=t^s$, Definition 1.1 reduces to s-convex functions [3].
- $h(t)=1$, Definition 1.1 equals to P-functions [4].

Theorem 1.2. *(Hölder inequality). Let $p,q>1$ with $\frac{1}{p}+\frac{1}{q}=1$. If f and g are real functions defined on $[a,b]$ and if $|f|^p$, $|g|^q$ are integrable functions on $[a,b]$, then*

$$\int_a^b |f(t)g(t)|\,dt \le \left(\int_a^b |f(t)|^p\,dt\right)^{\frac{1}{p}} \left(\int_a^b |g(t)|^q\,dt\right)^{\frac{1}{q}}.$$

The power-mean integral inequality, derived from the Hölder inequality, can be expressed as follows:

Theorem 1.3. *(Power mean integral inequality). Let $p\ge 1$ and f, g be two real functions defined on $[a,b]$. If $|f|$, $|f||g|^q$ are integrable functions on $[a,b]$ then*

$$\int_a^b |f(t)g(t)|\,dt \le \left(\int_a^b |f(t)|\,dt\right)^{1-\frac{1}{p}} \left(\int_a^b |f(t)|\,|g(t)|^p\,dt\right)^{\frac{1}{p}}.$$

For further information and clarification of the power-mean integral inequality, go to references [5].

Subsequently, mathematicians have become increasingly interested in fractional calculus due to its fundamental properties and wide-ranging applications. The *Riemann–Liouville integrals* $J_{a+}^{\alpha}f$ and $J_{b-}^{\alpha}f$ of order $\alpha>0$ with $a\ge 0$ are given by

$$J_{a+}^{\alpha}f(x)=\frac{1}{\Gamma(\alpha)}\int_a^x (x-t)^{\alpha-1}f(t)dt,\ \ x>a$$

and

$$J_{b-}^{\alpha}f(x)=\frac{1}{\Gamma(\alpha)}\int_x^b (t-x)^{\alpha-1}f(t)dt,\ \ x<b,$$

respectively [6, 7]. Here, f belongs to $L_1[a,b]$ and $\Gamma(\alpha)$ denotes the Gamma function defining as

$$\Gamma(\alpha):=\int_0^{\infty} e^{-u}u^{\alpha-1}du.$$

The fractional integral coincides with the classical integral for the case of $\alpha=1$.

The formula for Simpson's quadrature, commonly referred as Simpson's $1/3$ rule, is as follows:

$$\int_a^b f(x)\,dx \approx \frac{b-a}{6}\left[f(a)+4f\left(\frac{a+b}{2}\right)+f(b)\right].$$

Theorem 1.4. *Let $f:[a,b]\to\mathbb{R}$ be a four times differentiable and continuous function on (a,b), and let $\left\|f^{(4)}\right\|_{\infty}=\sup\limits_{x\in(a,b)}\left|f^{(4)}(x)\right|<\infty$. Then, the following inequality holds:*

$$\left|\frac{1}{6}\left[f(a)+4f\left(\frac{a+b}{2}\right)+f(b)\right]-\frac{1}{b-a}\int_a^b f(x)dx\right| \le \frac{1}{2880}\left\|f^{(4)}\right\|_{\infty}(b-a)^4.$$

In the paper [8], Dragomir provided an estimate for the remainder in Simpson's formula for functions of bounded variation, with applications in the theory of special means. For further details on Simpson-type inequalities and other related topics involving Riemann–Liouville fractional integrals, readers are referred to [9, 10] and its references.

The Newton-Cotes quadrature formula, frequently referred as Simpson's second formula (also known as Simpson's $3/8$ rule; see [11]), is defined as follows:

$$\int_a^b f(x)\,dx \approx \frac{b-a}{8}\left[f(a)+3f\left(\frac{2a+b}{3}\right)+3f\left(\frac{a+2b}{3}\right)+f(b)\right].$$

Theorem 1.5. *If $f:[a,b]\to\mathbb{R}$ is a four times differentiable and continuous function on (a,b), and $\left\|f^{(4)}\right\|_{\infty}=\sup\limits_{x\in(a,b)}\left|f^{(4)}(x)\right|<\infty$, then one has the inequality*

$$\left|\frac{1}{8}\left[f(a)+3f\left(\frac{2a+b}{3}\right)+3f\left(\frac{a+2b}{3}\right)+f(b)\right]-\frac{1}{b-a}\int_a^b f(x)dx\right| \le \frac{1}{6480}\left\|f^{(4)}\right\|_{\infty}(b-a)^4.$$

In the literature, evaluations for three-step quadrature kernels are frequently referred to as Newton-type results because the three-point Newton-Cotes quadrature is a rule of Simpson's second rule. Newton-type inequalities have been extensively studied by a number of mathematicians. For instance, in paper [12], Erden et al. investigated several Newton-type integral inequalities for functions whose first derivative is arithmetically-harmonically convex in absolute value at a given power. Please refer to [13–15] and its references for more details on Newton-type inequality, which includes convex differentiable functions.

The Maclaurin rule, which is derived from the Maclaurin formula (see to [11]), is equivalent to the corresponding dual Simpson's $3/8$ formula:

$$\int_a^b f(x)\,dx \approx \frac{b-a}{8}\left[3f\left(\frac{5a+b}{6}\right)+2f\left(\frac{a+b}{2}\right)+3f\left(\frac{a+5b}{6}\right)\right].$$

The Maclaurin rule, which is derived from the Maclaurin inequality, is equivalent to the corresponding dual Simpson's $3/8$ formula:

Theorem 1.6. *If $f:[a,b]\to\mathbb{R}$ is a four times differentiable and continuous function on (a,b), and $\left\|f^{(4)}\right\|_\infty=\sup\limits_{x\in(a,b)}\left|f^{(4)}(x)\right|<\infty$, then the following inequality holds:*

$$\left|\frac{1}{8}\left[3f\left(\frac{5a+b}{6}\right)+2f\left(\frac{a+b}{2}\right)+3f\left(\frac{a+5b}{6}\right)\right]-\frac{1}{b-a}\int_a^b f(x)dx\right|\le\frac{7}{51840}\left\|f^{(4)}\right\|_\infty (b-a)^4.$$

Dedić et al. [16] are constructed a set of inequalities using Euler-Maclaurin-type inequalities, and the results were utilized to derive specific error estimates in the case of the Maclaurin quadrature rules. In the paper [17], these results are applied to provide error estimates for the Simpson 3/8 quadrature rules. In [18], several Euler-Maclaurin-type inequalities are considered for differentiable convex functions. Additionally, in [19], several corrected Euler-Maclaurin-type inequalities are established using Riemann-Liouville fractional integrals. For further information on such types of inequalities, the reader is referred to [20–22] and the references therein.

2. A Crucial Equality

In this section, we express integral equality in order to demonstrate the main results of the study.

Lemma 2.1. *[23] If $f:[a,b]\to\mathbb{R}$ is an absolutely continuous function (a,b) such that $f'\in L_1[a,b]$, then the equality*

$$\begin{aligned}&\frac{1}{8}\left[3f\left(\frac{5a+b}{6}\right)+2f\left(\frac{a+b}{2}\right)+3f\left(\frac{a+5b}{6}\right)\right]-\frac{2^{\alpha-1}\Gamma(\alpha+1)}{(b-a)^\alpha}\left[J^\alpha_{\frac{a+b}{2}-}f(a)+J^\alpha_{\frac{a+b}{2}+}f(b)\right]\\&=\frac{b-a}{4}\left[I_1+I_2\right].\end{aligned}$$

is valid. Here,

$$\begin{cases}I_1=\int\limits_0^{\frac{1}{3}}t^\alpha\left[f'\left(\frac{t}{2}b+\frac{2-t}{2}a\right)-f'\left(\frac{t}{2}a+\frac{2-t}{2}b\right)\right]dt,\\ I_2=\int\limits_{\frac{1}{3}}^{1}\left(t^\alpha-\frac{3}{4}\right)\left[f'\left(\frac{t}{2}b+\frac{2-t}{2}a\right)-f'\left(\frac{t}{2}a+\frac{2-t}{2}b\right)\right]dt.\end{cases}$$

3. Euler-Maclaurin-type Inequalities for h-Convex Functions

In this section, we obtain several Euler-Maclaurin-type inequalities for differentiable h-convex functions by using the Riemann-Liouville fractional integrals.

Theorem 3.1. *Suppose that Lemma 2.1 holds and the function $|f'|$ is h-convex on the interval $[a,b]$. Then, one can prove fractional Euler-Maclaurin-type inequality*

$$\begin{aligned}&\left|\frac{1}{8}\left[3f\left(\frac{5a+b}{6}\right)+2f\left(\frac{a+b}{2}\right)+3f\left(\frac{a+5b}{6}\right)\right]-\frac{2^{\alpha-1}\Gamma(\alpha+1)}{(b-a)^\alpha}\left[J^\alpha_{\frac{a+b}{2}-}f(a)+J^\alpha_{\frac{a+b}{2}+}f(b)\right]\right|\\&\le\frac{b-a}{4}\left(\Omega_1(\alpha;h)+\Omega_2(\alpha;h)\right)\left[\left|f'(a)\right|+\left|f'(b)\right|\right].\end{aligned}$$

Here,

$$\Omega_1(\alpha;h)=\int_0^{\frac{1}{3}} t^\alpha \left[h\left(\frac{t}{2}\right)+h\left(\frac{2-t}{2}\right)\right]dt,$$

and

$$\Omega_2(\alpha;h)=\int_{\frac{1}{3}}^{1} \left|t^\alpha-\frac{3}{4}\right| \left[h\left(\frac{t}{2}\right)+h\left(\frac{2-t}{2}\right)\right]dt.$$

Proof. By taking into account the absolute value of Lemma 2.1, one may directly obtain

$$\begin{aligned}&\left|\frac{1}{8}\left[3f\left(\frac{5a+b}{6}\right)+2f\left(\frac{a+b}{2}\right)+3f\left(\frac{a+5b}{6}\right)\right]-\frac{2^{\alpha-1}\Gamma(\alpha+1)}{(b-a)^\alpha}\left[J^\alpha_{\frac{a+b}{2}-}f(a)+J^\alpha_{\frac{a+b}{2}+}f(b)\right]\right| \\ &\leq \frac{b-a}{4}\left\{\int_0^{\frac{1}{3}}|t^\alpha|\left[\left|f'\left(\frac{t}{2}b+\frac{2-t}{2}a\right)\right|+\left|f'\left(\frac{t}{2}a+\frac{2-t}{2}b\right)\right|\right]dt\right. \\ &\left.\quad+\int_{\frac{1}{3}}^{1}\left|t^\alpha-\frac{3}{4}\right|\left[\left|f'\left(\frac{t}{2}b+\frac{2-t}{2}a\right)\right|+\left|f'\left(\frac{t}{2}a+\frac{2-t}{2}b\right)\right|\right]dt\right\}.\end{aligned}\tag{3.1}$$

Since $|f'|$ is h-convex, it yields

$$\begin{aligned}&\left|\frac{1}{8}\left[3f\left(\frac{5a+b}{6}\right)+2f\left(\frac{a+b}{2}\right)+3f\left(\frac{a+5b}{6}\right)\right]-\frac{2^{\alpha-1}\Gamma(\alpha+1)}{(b-a)^\alpha}\left[J^\alpha_{\frac{a+b}{2}-}f(a)+J^\alpha_{\frac{a+b}{2}+}f(b)\right]\right| \\ &\leq \frac{b-a}{4}\left\{\int_0^{\frac{1}{3}}t^\alpha\left[h\left(\frac{t}{2}\right)|f'(b)|+h\left(\frac{2-t}{2}\right)|f'(a)|+h\left(\frac{t}{2}\right)|f'(a)|+h\left(\frac{2-t}{2}\right)|f'(b)|\right]dt\right. \\ &\left.\quad+\int_{\frac{1}{3}}^{1}\left|t^\alpha-\frac{3}{4}\right|\left[h\left(\frac{t}{2}\right)|f'(b)|+h\left(\frac{2-t}{2}\right)|f'(a)|+h\left(\frac{t}{2}\right)|f'(a)|+h\left(\frac{2-t}{2}\right)|f'(b)|\right]dt\right\} \\ &=\frac{b-a}{4}\left(\Omega_1(\alpha)+\Omega_2(\alpha)\right)\left[|f'(a)|+|f'(b)|\right],\end{aligned}$$

which complete the proof of Theorem 3.1. □

Remark 3.2. *If we choose $h(t)=t$ in Theorem 3.1, then the following inequality holds:*

$$\begin{aligned}&\left|\frac{1}{8}\left[3f\left(\frac{5a+b}{6}\right)+2f\left(\frac{a+b}{2}\right)+3f\left(\frac{a+5b}{6}\right)\right]-\frac{2^{\alpha-1}\Gamma(\alpha+1)}{(b-a)^\alpha}\left[J^\alpha_{\frac{a+b}{2}-}f(a)+J^\alpha_{\frac{a+b}{2}+}f(b)\right]\right| \\ &\leq \frac{b-a}{4}\left(\psi_1(\alpha)+\psi_2(\alpha)\right)\left[|f'(a)|+|f'(b)|\right],\end{aligned}$$

$$\psi_1(\alpha)=\int_0^{\frac{1}{3}}t^\alpha dt=\frac{1}{\alpha+1}\left(\frac{1}{3}\right)^{\alpha+1},$$

and

$$\psi_2(\alpha)=\int_{\frac{1}{3}}^{1}\left|t^\alpha-\frac{3}{4}\right|dt=\begin{cases}\frac{1}{\alpha+1}\left(1-\left(\frac{1}{3}\right)^{\alpha+1}\right)-\frac{1}{2}, & 0<\alpha\leq\frac{\ln\left(\frac{3}{4}\right)}{\ln\left(\frac{1}{3}\right)}, \\ \frac{2\alpha}{\alpha+1}\left(\frac{3}{4}\right)^{1+\frac{1}{\alpha}}+\frac{1}{\alpha+1}\left(\frac{1}{3}\right)^{\alpha+1}+\frac{1}{\alpha+1}-1, & \frac{\ln\left(\frac{3}{4}\right)}{\ln\left(\frac{1}{3}\right)}<\alpha.\end{cases}$$

which is established by Gumus et al. in paper [23, Theorem 4].

Corollary 3.3. *Let us consider $h(t)=t^s$ in Theorem 3.1. Then, the following Euler-Maclaurin-type inequality for s-convex functions by using the Riemann-Liouville fractional integrals*

$$\left|\frac{1}{8}\left[3f\left(\frac{5a+b}{6}\right)+2f\left(\frac{a+b}{2}\right)+3f\left(\frac{a+5b}{6}\right)\right]-\frac{2^{\alpha-1}\Gamma(\alpha+1)}{(b-a)^{\alpha}}\left[J_{\frac{a+b}{2}-}^{\alpha}f(a)+J_{\frac{a+b}{2}+}^{\alpha}f(b)\right]\right|$$
$$\leq \frac{b-a}{4}\left(\phi_1(\alpha,s)+\phi_2(\alpha,s)\right)\left[\left|f'(a)\right|+\left|f'(b)\right|\right].$$

Here,

$$\phi_1(\alpha,s)=\int_0^{\frac{1}{3}} t^{\alpha}\left[\left(\frac{t}{2}\right)^s+\left(\frac{2-t}{2}\right)^s\right]dt$$

and

$$\phi_2(\alpha,s)=\int_{\frac{1}{3}}^{1}\left|t^{\alpha}-\frac{3}{4}\right|\left[\left(\frac{t}{2}\right)^s+\left(\frac{2-t}{2}\right)^s\right]dt.$$

Corollary 3.4. *If we assign $h(t)=1$ in Theorem 3.1, then we get the following Euler-Maclaurin-type inequality for $P-$ functions by using the Riemann-Liouville fractional integrals*

$$\left|\frac{1}{8}\left[3f\left(\frac{5a+b}{6}\right)+2f\left(\frac{a+b}{2}\right)+3f\left(\frac{a+5b}{6}\right)\right]-\frac{2^{\alpha-1}\Gamma(\alpha+1)}{(b-a)^{\alpha}}\left[J_{\frac{a+b}{2}-}^{\alpha}f(a)+J_{\frac{a+b}{2}+}^{\alpha}f(b)\right]\right|$$
$$\leq \frac{b-a}{2}\left(\psi_1(\alpha)+\psi_2(\alpha)\right)\left[\left|f'(a)\right|+\left|f'(b)\right|\right].$$

Corollary 3.5. *If we assign $\alpha=1$ in Theorem 3.1, then we can obtain Euler-Maclaurin-type inequality for h-convex functions*

$$\left|\frac{1}{8}\left[3f\left(\frac{5a+b}{6}\right)+2f\left(\frac{a+b}{2}\right)+3f\left(\frac{a+5b}{6}\right)\right]-\frac{1}{b-a}\int_a^b f(t)\,dt\right|$$
$$\leq \frac{b-a}{4}\left(\Omega_1(1;h)+\Omega_2(1;h)\right)\left[\left|f'(a)\right|+\left|f'(b)\right|\right],$$

where

$$\Omega_1(1;h)=\int_0^{\frac{1}{3}} t\left[h\left(\frac{t}{2}\right)+h\left(\frac{2-t}{2}\right)\right]dt,$$

and

$$\Omega_2(1;h)=\int_{\frac{1}{3}}^{1}\left|t-\frac{3}{4}\right|\left[h\left(\frac{t}{2}\right)+h\left(\frac{2-t}{2}\right)\right]dt.$$

Remark 3.6. *If we choose $h(t)=t$ in Corollary 3.5, then we have the following Euler-Maclaurin-type inequality for h-convex functions functions*

$$\left|\frac{1}{8}\left[3f\left(\frac{5a+b}{6}\right)+2f\left(\frac{a+b}{2}\right)+3f\left(\frac{a+5b}{6}\right)\right]-\frac{1}{b-a}\int_a^b f(t)\,dt\right|$$
$$\leq \frac{25(b-a)}{576}\left[\left|f'(a)\right|+\left|f'(b)\right|\right].$$

This is established by Hezenci and Budak in paper [18, Corollary 1].

Corollary 3.7. *Let us consider $h(t)=t^s$ in Corollary 3.5. Then, we obtain the following Euler-Maclaurin-type inequality for s-convex functions*

$$\left|\frac{1}{8}\left[3f\left(\frac{5a+b}{6}\right)+2f\left(\frac{a+b}{2}\right)+3f\left(\frac{a+5b}{6}\right)\right]-\frac{1}{b-a}\int_a^b f(t)\,dt\right|$$
$$\leq \frac{b-a}{4}\left(\varphi_1(s)+\varphi_2(s)\right)\left[\left|f'(a)\right|+\left|f'(b)\right|\right].$$

Here,

$$\varphi_1(s)=\int_0^{\frac{1}{3}} t\left[\left(\frac{t}{2}\right)^s+\left(\frac{2-t}{2}\right)^s\right]dt=\frac{1}{9\cdot 6^s(s+2)}\left[1+\frac{6^{s+2}-5^{s+1}(s+7)}{(s+1)}\right],$$

and

$$\varphi_2(s)=\int_{\frac{1}{3}}^1\left|t-\frac{3}{4}\right|\left[\left(\frac{t}{2}\right)^s+\left(\frac{2-t}{2}\right)^s\right]dt.$$

Corollary 3.8. *If we assign $h(t)=1$ in Corollary 3.5, then we get the following Euler-Maclaurin-type inequality for $P-$functions*

$$\left|\frac{1}{8}\left[3f\left(\frac{5a+b}{6}\right)+2f\left(\frac{a+b}{2}\right)+3f\left(\frac{a+5b}{6}\right)\right]-\frac{1}{b-a}\int_a^b f(t)\,dt\right|$$
$$\leq \frac{25(b-a)}{288}\left[\left|f'(a)\right|+\left|f'(b)\right|\right].$$

Theorem 3.9. *Let us consider the assumptions in Lemma 2.1 and the function $|f'|^q$, $q>1$ is $h-$convex on $[a,b]$. Then, the following Euler-Maclaurin-type inequality holds:*

$$\left|\frac{1}{8}\left[3f\left(\frac{5a+b}{6}\right)+2f\left(\frac{a+b}{2}\right)+3f\left(\frac{a+5b}{6}\right)\right]-\frac{2^{\alpha-1}\Gamma(\alpha+1)}{(b-a)^\alpha}\left[J^\alpha_{\frac{a+b}{2}-}f(a)+J^\alpha_{\frac{a+b}{2}+}f(b)\right]\right|$$
$$\leq \frac{b-a}{4}\left\{\left(\frac{1}{(\alpha p+1)}\left(\frac{1}{3}\right)^{\alpha p+1}\right)^{\frac{1}{p}}\right.$$
$$\times\left[\left(\int_0^{\frac{1}{3}}\left(h\left(\frac{t}{2}\right)\left|f'(b)\right|^q+h\left(\frac{2-t}{2}\right)\left|f'(a)\right|^q\right)dt\right)^{\frac{1}{q}}\right.$$
$$\left.+\left(\int_0^{\frac{1}{3}}\left(h\left(\frac{t}{2}\right)\left|f'(a)\right|^q+h\left(\frac{2-t}{2}\right)\left|f'(b)\right|^q\right)dt\right)^{\frac{1}{q}}\right]$$
$$+\left(\int_{\frac{1}{3}}^1\left|t^\alpha-\frac{3}{4}\right|^p dt\right)^{\frac{1}{p}}\left[\left(\int_{\frac{1}{3}}^1\left(h\left(\frac{t}{2}\right)\left|f'(b)\right|^q+h\left(\frac{2-t}{2}\right)\left|f'(a)\right|^q\right)dt\right)^{\frac{1}{q}}\right.$$
$$\left.\left.+\left(\int_{\frac{1}{3}}^1\left(h\left(\frac{t}{2}\right)\left|f'(a)\right|^q+h\left(\frac{2-t}{2}\right)\left|f'(b)\right|^q\right)dt\right)^{\frac{1}{q}}\right]\right\}.$$

Here, $\frac{1}{p}+\frac{1}{q}=1$.

Proof. If we apply Hölder's inequality to (3.1), then we get

$$\begin{aligned}
&\left|\frac{1}{8}\left[3f\left(\frac{5a+b}{6}\right)+2f\left(\frac{a+b}{2}\right)+3f\left(\frac{a+5b}{6}\right)\right]-\frac{2^{\alpha-1}\Gamma(\alpha+1)}{(b-a)^{\alpha}}\left[J^{\alpha}_{\frac{a+b}{2}-}f(a)+J^{\alpha}_{\frac{a+b}{2}+}f(b)\right]\right| \\
&\leq \frac{b-a}{4}\left\{\left(\int_0^{\frac{1}{3}} t^{\alpha p}dt\right)^{\frac{1}{p}}\left(\int_0^{\frac{1}{3}}\left|f'\left(\frac{t}{2}b+\frac{2-t}{2}a\right)\right|^q dt\right)^{\frac{1}{q}}\right. \\
&+\left(\int_0^{\frac{1}{3}} t^{\alpha p}dt\right)^{\frac{1}{p}}\left(\int_0^{\frac{1}{3}}\left|f'\left(\frac{t}{2}a+\frac{2-t}{2}b\right)\right|^q dt\right)^{\frac{1}{q}} \\
&+\left(\int_{\frac{1}{3}}^{1}\left|t^{\alpha}-\frac{3}{4}\right|^p dt\right)^{\frac{1}{p}}\left(\int_{\frac{1}{3}}^{1}\left|f'\left(\frac{t}{2}b+\frac{2-t}{2}a\right)\right|^q dt\right)^{\frac{1}{q}} \\
&\left.+\left(\int_{\frac{1}{3}}^{1}\left|t^{\alpha}-\frac{3}{4}\right|^p dt\right)^{\frac{1}{p}}\left(\int_{\frac{1}{3}}^{1}\left|f'\left(\frac{t}{2}a+\frac{2-t}{2}b\right)\right|^q dt\right)^{\frac{1}{q}}\right\}.
\end{aligned}$$

Taking advantage of the $h-$convexity $|f'|^q$, we can easily get

$$\begin{aligned}
&\left|\frac{1}{8}\left[3f\left(\frac{5a+b}{6}\right)+2f\left(\frac{a+b}{2}\right)+3f\left(\frac{a+5b}{6}\right)\right]-\frac{2^{\alpha-1}\Gamma(\alpha+1)}{(b-a)^{\alpha}}\left[J^{\alpha}_{\frac{a+b}{2}-}f(a)+J^{\alpha}_{\frac{a+b}{2}+}f(b)\right]\right| \\
&\leq \frac{b-a}{4}\left\{\left(\int_0^{\frac{1}{3}} t^{\alpha p}dt\right)^{\frac{1}{p}}\left(\int_0^{\frac{1}{3}}\left(h\left(\frac{t}{2}\right)\left|f'(b)\right|^q+h\left(\frac{2-t}{2}\right)\left|f'(a)\right|^q\right)dt\right)^{\frac{1}{q}}\right. \\
&+\left(\int_0^{\frac{1}{3}} t^{\alpha p}dt\right)^{\frac{1}{p}}\left(\int_0^{\frac{1}{3}}\left(h\left(\frac{t}{2}\right)\left|f'(a)\right|^q+h\left(\frac{2-t}{2}\right)\left|f'(b)\right|^q\right)dt\right)^{\frac{1}{q}} \\
&+\left(\int_{\frac{1}{3}}^{1}\left|t^{\alpha}-\frac{3}{4}\right|^p dt\right)^{\frac{1}{p}}\left(\int_{\frac{1}{3}}^{1}\left(h\left(\frac{t}{2}\right)\left|f'(b)\right|^q+h\left(\frac{2-t}{2}\right)\left|f'(a)\right|^q\right)dt\right)^{\frac{1}{q}} \\
&\left.+\left(\int_{\frac{1}{3}}^{1}\left|t^{\alpha}-\frac{3}{4}\right|^p dt\right)^{\frac{1}{p}}\left(\int_{\frac{1}{3}}^{1}\left(h\left(\frac{t}{2}\right)\left|f'(a)\right|^q+h\left(\frac{2-t}{2}\right)\left|f'(b)\right|^q\right)dt\right)^{\frac{1}{q}}\right\} \\
&=\frac{b-a}{4}\left\{\left(\frac{1}{(\alpha p+1)}\left(\frac{1}{3}\right)^{\alpha p+1}\right)^{\frac{1}{p}}\right. \\
&\times\left[\left(\int_0^{\frac{1}{3}}\left(h\left(\frac{t}{2}\right)\left|f'(b)\right|^q+h\left(\frac{2-t}{2}\right)\left|f'(a)\right|^q\right)dt\right)^{\frac{1}{q}}\right. \\
&\left.+\left(\int_0^{\frac{1}{3}}\left(h\left(\frac{t}{2}\right)\left|f'(a)\right|^q+h\left(\frac{2-t}{2}\right)\left|f'(b)\right|^q\right)dt\right)^{\frac{1}{q}}\right]
\end{aligned}$$

$$+\left(\int_{\frac{1}{3}}^{1}\left|t^{\alpha}-\frac{3}{4}\right|^{p}dt\right)^{\frac{1}{p}}\left[\left(\int_{\frac{1}{3}}^{1}\left(h\left(\frac{t}{2}\right)\left|f'(b)\right|^{q}+h\left(\frac{2-t}{2}\right)\left|f'(a)\right|^{q}\right)dt\right)^{\frac{1}{q}}\right.$$
$$\left.\left.+\left(\int_{\frac{1}{3}}^{1}\left(h\left(\frac{t}{2}\right)\left|f'(a)\right|^{q}+h\left(\frac{2-t}{2}\right)\left|f'(b)\right|^{q}\right)dt\right)^{\frac{1}{q}}\right]\right\}.$$

This ends the proof of Theorem 3.9. □

Remark 3.10. *If we choose $h(t)=t$ in Theorem 3.9, then the Theorem 3.9 reduces to the result in paper [23, Theorem 5].*

Corollary 3.11. *Let us consider $h(t)=t^{s}$ in Theorem 3.9. Then, the following Euler-Maclaurin-type inequality for s-convex functions by using the Riemann-Liouville fractional integrals*

$$\left|\frac{1}{8}\left[3f\left(\frac{5a+b}{6}\right)+2f\left(\frac{a+b}{2}\right)+3f\left(\frac{a+5b}{6}\right)\right]-\frac{2^{\alpha-1}\Gamma(\alpha+1)}{(b-a)^{\alpha}}\left[J_{\frac{a+b}{2}-}^{\alpha}f(a)+J_{\frac{a+b}{2}+}^{\alpha}f(b)\right]\right|$$
$$\leq\frac{b-a}{4}\left\{\left(\frac{1}{(\alpha p+1)}\left(\frac{1}{3}\right)^{\alpha p+1}\right)^{\frac{1}{p}}\right.$$
$$\times\left[\left(\frac{|f'(b)|^{q}+\left(6^{s+1}-5^{s+1}\right)|f'(a)|^{q}}{3\cdot6^{s}(s+1)}\right)^{\frac{1}{q}}+\left(\frac{|f'(a)|^{q}+\left(6^{s+1}-5^{s+1}\right)|f'(b)|^{q}}{3\cdot6^{s}(s+1)}\right)^{\frac{1}{q}}\right]$$
$$+\left(\int_{\frac{1}{3}}^{1}\left|t^{\alpha}-\frac{3}{4}\right|^{p}dt\right)^{\frac{1}{p}}\left[\left(\frac{\left(3^{s+1}-1\right)|f'(b)|^{q}+\left(5^{s+1}-3^{s+1}\right)|f'(a)|^{q}}{3\cdot6^{s}(s+1)}\right)^{\frac{1}{q}}\right.$$
$$\left.\left.+\left(\frac{\left(3^{s+1}-1\right)|f'(a)|^{q}+\left(5^{s+1}-3^{s+1}\right)|f'(b)|^{q}}{3\cdot6^{s}(s+1)}\right)^{\frac{1}{q}}\right]\right\}.$$

Corollary 3.12. *If we assign $h(t)=1$ in Theorem 3.9, then we get the following Euler-Maclaurin-type inequality for $P-$functions by using the Riemann-Liouville fractional integrals*

$$\left|\frac{1}{8}\left[3f\left(\frac{5a+b}{6}\right)+2f\left(\frac{a+b}{2}\right)+3f\left(\frac{a+5b}{6}\right)\right]-\frac{2^{\alpha-1}\Gamma(\alpha+1)}{(b-a)^{\alpha}}\left[J_{\frac{a+b}{2}-}^{\alpha}f(a)+J_{\frac{a+b}{2}+}^{\alpha}f(b)\right]\right|$$
$$\leq\frac{b-a}{2}\left\{\left(\frac{1}{(\alpha p+1)}\left(\frac{1}{3}\right)^{\alpha p+1}\right)^{\frac{1}{p}}\left(\frac{|f'(b)|^{q}+|f'(a)|^{q}}{3}\right)^{\frac{1}{q}}\right.$$
$$\left.+\left(\int_{\frac{1}{3}}^{1}\left|t^{\alpha}-\frac{3}{4}\right|^{p}dt\right)^{\frac{1}{p}}\left(\frac{2|f'(b)|^{q}+2|f'(a)|^{q}}{3}\right)^{\frac{1}{q}}\right\}.$$

Corollary 3.13. *If we assign $\alpha=1$ in Theorem 3.9, then we can obtain Euler-Maclaurin-type inequality*

$$\left|\frac{1}{8}\left[3f\left(\frac{5a+b}{6}\right)+2f\left(\frac{a+b}{2}\right)+3f\left(\frac{a+5b}{6}\right)\right]-\frac{1}{b-a}\int_{a}^{b}f(t)\,dt\right|$$
$$\leq\frac{b-a}{4}\left\{\left(\frac{1}{(p+1)}\left(\frac{1}{3}\right)^{p+1}\right)^{\frac{1}{p}}\right.$$

$$\times\left[\left(\int_0^{\frac{1}{3}}\left(h\left(\frac{t}{2}\right)\left|f'(b)\right|^q+h\left(\frac{2-t}{2}\right)\left|f'(a)\right|^q\right)dt\right)^{\frac{1}{q}}\right.$$

$$\left.+\left(\int_0^{\frac{1}{3}}\left(h\left(\frac{t}{2}\right)\left|f'(a)\right|^q+h\left(\frac{2-t}{2}\right)\left|f'(b)\right|^q\right)dt\right)^{\frac{1}{q}}\right]$$

$$+\left(\frac{1}{p+1}\left[\left(\frac{1}{4}\right)^{p+1}+\left(\frac{5}{12}\right)^{p+1}\right]\right)^{\frac{1}{p}}\left[\left(\int_{\frac{1}{3}}^{1}\left(h\left(\frac{t}{2}\right)\left|f'(b)\right|^q+h\left(\frac{2-t}{2}\right)\left|f'(a)\right|^q\right)dt\right)^{\frac{1}{q}}\right.$$

$$\left.\left.+\left(\int_{\frac{1}{3}}^{1}\left(h\left(\frac{t}{2}\right)\left|f'(a)\right|^q+h\left(\frac{2-t}{2}\right)\left|f'(b)\right|^q\right)dt\right)^{\frac{1}{q}}\right]\right\}.$$

Remark 3.14. *If we choose $h(t)=t$ in Corollary 3.13, then the following inequality holds:*

$$\left|\frac{1}{8}\left[3f\left(\frac{5a+b}{6}\right)+2f\left(\frac{a+b}{2}\right)+3f\left(\frac{a+5b}{6}\right)\right]-\frac{1}{b-a}\int_a^b f(t)\,dt\right|$$

$$\leq\frac{b-a}{4}\left\{\left(\frac{1}{p+1}\left[\left(\frac{1}{4}\right)^{p+1}+\left(\frac{5}{12}\right)^{p+1}\right]\right)^{\frac{1}{p}}\right.$$

$$\times\left[\left(\frac{4\left|f'(b)\right|^q+2\left|f'(a)\right|^q}{9}\right)^{\frac{1}{q}}+\left(\frac{4\left|f'(a)\right|^q+2\left|f'(b)\right|^q}{9}\right)^{\frac{1}{q}}\right]$$

$$\left.+\left(\frac{1}{p+1}\left(\frac{1}{3}\right)^{p+1}\right)^{\frac{1}{p}}\left[\left(\frac{11\left|f'(b)\right|^q+\left|f'(a)\right|^q}{36}\right)^{\frac{1}{q}}+\left(\frac{11\left|f'(a)\right|^q+\left|f'(b)\right|^q}{36}\right)^{\frac{1}{q}}\right]\right\},$$

which is established by Gumus et al. in paper [23, Corollary 1].

Corollary 3.15. *Let us consider $h(t)=t^s$ in Corollary 3.13. Then, the following inequality*

$$\left|\frac{1}{8}\left[3f\left(\frac{5a+b}{6}\right)+2f\left(\frac{a+b}{2}\right)+3f\left(\frac{a+5b}{6}\right)\right]-\frac{1}{b-a}\int_a^b f(t)\,dt\right|$$

$$\leq\frac{b-a}{4}\left\{\left(\frac{1}{(p+1)}\left(\frac{1}{3}\right)^{p+1}\right)^{\frac{1}{p}}\right.$$

$$\times\left[\left(\frac{\left|f'(b)\right|^q+\left(6^{s+1}-5^{s+1}\right)\left|f'(a)\right|^q}{3\cdot6^s(s+1)}\right)^{\frac{1}{q}}+\left(\frac{\left|f'(a)\right|^q+\left(6^{s+1}-5^{s+1}\right)\left|f'(b)\right|^q}{3\cdot6^s(s+1)}\right)^{\frac{1}{q}}\right]$$

$$+\left(\frac{1}{p+1}\left[\left(\frac{1}{4}\right)^{p+1}+\left(\frac{5}{12}\right)^{p+1}\right]\right)^{\frac{1}{p}}\left[\left(\frac{\left(3^{s+1}-1\right)\left|f'(b)\right|^q+\left(5^{s+1}-3^{s+1}\right)\left|f'(a)\right|^q}{3\cdot6^s(s+1)}\right)^{\frac{1}{q}}\right.$$

$$\left.\left.+\left(\frac{\left(3^{s+1}-1\right)\left|f'(a)\right|^q+\left(5^{s+1}-3^{s+1}\right)\left|f'(b)\right|^q}{3\cdot6^s(s+1)}\right)^{\frac{1}{q}}\right]\right\}.$$

Corollary 3.16. *If we assign $h(t)=1$ in Corollary 3.13, then we get the following inequality*

$$\begin{aligned}&\left|\frac{1}{8}\left[3f\left(\frac{5a+b}{6}\right)+2f\left(\frac{a+b}{2}\right)+3f\left(\frac{a+5b}{6}\right)\right]-\frac{1}{b-a}\int_a^b f(t)\,dt\right|\\&\leq\frac{b-a}{2}\left\{\left(\frac{1}{(p+1)}\left(\frac{1}{3}\right)^{p+1}\right)^{\frac{1}{p}}\left(\frac{|f'(b)|^q+|f'(a)|^q}{3}\right)^{\frac{1}{q}}\right.\\&\quad\left.+\left(\frac{1}{p+1}\left[\left(\frac{1}{4}\right)^{p+1}+\left(\frac{5}{12}\right)^{p+1}\right]\right)^{\frac{1}{p}}\left(\frac{2|f'(b)|^q+2|f'(a)|^q}{3}\right)^{\frac{1}{q}}\right\}.\end{aligned}$$

Theorem 3.17. *Assume that the assumptions of Lemma 2.1 satisfy and the function $|f'|^q$, $q\geq 1$ is $h-$convex on $[a,b]$. Then, we obtain the following Euler-Maclaurin-type inequality*

$$\begin{aligned}&\left|\frac{1}{8}\left[3f\left(\frac{5a+b}{6}\right)+2f\left(\frac{a+b}{2}\right)+3f\left(\frac{a+5b}{6}\right)\right]-\frac{2^{\alpha-1}\Gamma(\alpha+1)}{(b-a)^\alpha}\left[J^\alpha_{\frac{a+b}{2}-}f(a)+J^\alpha_{\frac{a+b}{2}+}f(b)\right]\right|\\&\leq\frac{b-a}{4}\left\{(\varphi_1(\alpha))^{1-\frac{1}{q}}\left[\left[\varphi_3(\alpha;h)\left|f'(b)\right|^q+\varphi_4(\alpha;h)\left|f'(a)\right|^q\right]^{\frac{1}{q}}\right.\right.\\&\quad\left.+\left[\varphi_3(\alpha;h)\left|f'(a)\right|^q+\varphi_4(\alpha;h)\left|f'(b)\right|^q\right]^{\frac{1}{q}}\right]\\&\quad+(\varphi_2(\alpha))^{1-\frac{1}{q}}\left[\left[\varphi_5(\alpha;h)\left|f'(b)\right|^q+\varphi_6(\alpha;h)\left|f'(a)\right|^q\right]^{\frac{1}{q}}\right.\\&\quad\left.\left.+\left[\varphi_5(\alpha;h)\left|f'(a)\right|^q+\varphi_6(\alpha;h)\left|f'(b)\right|^q\right]^{\frac{1}{q}}\right]\right\}.\end{aligned}$$

Here,

$$\varphi_1(\alpha)=\int_0^{\frac{1}{3}}t^\alpha dt=\frac{1}{\alpha+1}\left(\frac{1}{3}\right)^{\alpha+1},$$

$$\begin{aligned}\varphi_2(\alpha)&=\int_{\frac{1}{3}}^1\left|t^\alpha-\frac{3}{4}\right|dt\\&=\begin{cases}\frac{1}{\alpha+1}\left(1-\left(\frac{1}{3}\right)^{\alpha+1}\right)-\frac{1}{2}, & 0<\alpha\leq\frac{\ln\left(\frac{3}{4}\right)}{\ln\left(\frac{1}{3}\right)},\\ \frac{2\alpha}{\alpha+1}\left(\frac{3}{4}\right)^{1+\frac{1}{\alpha}}+\frac{1}{\alpha+1}\left(\frac{1}{3}\right)^{\alpha+1}+\frac{1}{\alpha+1}-1, & \frac{\ln\left(\frac{3}{4}\right)}{\ln\left(\frac{1}{3}\right)}<\alpha.\end{cases}\end{aligned}$$

and

$$\begin{cases}\varphi_3(\alpha;h)=\int_0^{\frac{1}{3}}t^\alpha h\left(\frac{t}{2}\right)dt, & \varphi_5(\alpha;h)=\int_{\frac{1}{3}}^1\left|t^\alpha-\frac{3}{4}\right|h\left(\frac{t}{2}\right)dt,\\ \varphi_4(\alpha;h)=\int_0^{\frac{1}{3}}t^\alpha h\left(\frac{2-t}{2}\right)dt, & \varphi_6(\alpha;h)=\int_{\frac{1}{3}}^1\left|t^\alpha-\frac{3}{4}\right|h\left(\frac{2-t}{2}\right)dt.\end{cases}$$

Proof. When we apply (3.1) to the power-mean inequality, we have

$$\left|\frac{1}{8}\left[3f\left(\frac{5a+b}{6}\right)+2f\left(\frac{a+b}{2}\right)+3f\left(\frac{a+5b}{6}\right)\right]-\frac{2^{\alpha-1}\Gamma(\alpha+1)}{(b-a)^\alpha}\left[J^\alpha_{\frac{a+b}{2}-}f(a)+J^\alpha_{\frac{a+b}{2}+}f(b)\right]\right|$$

$$\leq \frac{b-a}{4}\left\{ \left(\int_0^{\frac{1}{3}} |t^{\alpha}|\, dt \right)^{1-\frac{1}{q}} \left(\int_0^{\frac{1}{3}} |t^{\alpha}| \left| f'\left(\frac{t}{2}b + \frac{2-t}{2}a \right) \right|^q dt \right)^{\frac{1}{q}} \right.$$

$$+ \left(\int_0^{\frac{1}{3}} |t^{\alpha}|\, dt \right)^{1-\frac{1}{q}} \left(\int_0^{\frac{1}{3}} |t^{\alpha}| \left| f'\left(\frac{t}{2}a + \frac{2-t}{2}b \right) \right|^q dt \right)^{\frac{1}{q}}$$

$$+ \left(\int_{\frac{1}{3}}^{1} \left| t^{\alpha} - \frac{3}{4} \right| dt \right)^{1-\frac{1}{q}} \left(\int_{\frac{1}{3}}^{1} \left| t^{\alpha} - \frac{3}{4} \right| \left| f'\left(\frac{t}{2}b + \frac{2-t}{2}a \right) \right|^q dt \right)^{\frac{1}{q}}$$

$$\left. + \left(\int_{\frac{1}{3}}^{1} \left| t^{\alpha} - \frac{3}{4} \right| dt \right)^{1-\frac{1}{q}} \left(\int_{\frac{1}{3}}^{1} \left| t^{\alpha} - \frac{3}{4} \right| \left| f'\left(\frac{t}{2}a + \frac{2-t}{2}b \right) \right|^q dt \right)^{\frac{1}{q}} \right\}.$$

By using the $h-$convexity of $|f'|^q$, it follows

$$\left| \frac{1}{8}\left[3f\left(\frac{5a+b}{6} \right) + 2f\left(\frac{a+b}{2} \right) + 3f\left(\frac{a+5b}{6} \right) \right] - \frac{2^{\alpha-1}\Gamma(\alpha+1)}{(b-a)^{\alpha}} \left[J^{\alpha}_{\frac{a+b}{2}-} f(a) + J^{\alpha}_{\frac{a+b}{2}+} f(b) \right] \right|$$

$$\leq \frac{b-a}{4}\left\{ \left(\int_0^{\frac{1}{3}} t^{\alpha} dt \right)^{1-\frac{1}{q}} \left(\int_0^{\frac{1}{3}} t^{\alpha} \left[h\left(\frac{t}{2} \right) |f'(b)|^q + h\left(\frac{2-t}{2} \right) |f'(a)|^q \right] dt \right)^{\frac{1}{q}} \right.$$

$$+ \left(\int_0^{\frac{1}{3}} t^{\alpha} dt \right)^{1-\frac{1}{q}} \left(\int_0^{\frac{1}{3}} t^{\alpha} \left[h\left(\frac{t}{2} \right) |f'(a)|^q + h\left(\frac{2-t}{2} \right) |f'(b)|^q \right] dt \right)^{\frac{1}{q}}$$

$$+ \left(\int_{\frac{1}{3}}^{1} \left| t^{\alpha} - \frac{3}{4} \right| dt \right)^{1-\frac{1}{q}} \left(\int_{\frac{1}{3}}^{1} \left| t^{\alpha} - \frac{3}{4} \right| \left[h\left(\frac{t}{2} \right) |f'(b)|^q + h\left(\frac{2-t}{2} \right) |f'(a)|^q \right] dt \right)^{\frac{1}{q}}$$

$$\left. + \left(\int_{\frac{1}{3}}^{1} \left| t^{\alpha} - \frac{3}{4} \right| dt \right)^{1-\frac{1}{q}} \left(\int_{\frac{1}{3}}^{1} \left| t^{\alpha} - \frac{3}{4} \right| \left[h\left(\frac{t}{2} \right) |f'(a)|^q + h\left(\frac{2-t}{2} \right) |f'(b)|^q \right] dt \right)^{\frac{1}{q}} \right\}.$$

This finishes the proof of Theorem 3.17. □

4. Summary and Concluding Remarks

In this paper, several Euler-Maclaurin-type inequalities are investigated for differentiable $h-$convex functions by using the Riemann-Liouville fractional integrals. Moreover, by using Hölder inequality, we give some Euler-Maclaurin-type inequalities for Riemann-Liouville fractional integrals. Furthermore, by using the special choices of the obtained results, we obtain the some Euler-Maclaurin-type inequalities.

In future papers, the ideas and strategies behind our results on Euler-Maclaurin-type inequalities using Riemann-Liouville fractional integrals may pave the way for new avenues of research in this field. Improvements or generalizations of our results can be explored by considering different classes of convex functions or other types of fractional integral operators. Additionally, one could derive Euler-Maclaurin-type inequalities for various function classes with the aid of quantum calculus.

5. Article Information

Acknowledgements: The authors express their sincere thanks to the editor and the anonymous reviewers for their helpful comments and suggestions.

Author's Contributions: F. H. was responsible for the original draft preparation. H. B. drafted the introduction and was responsible for reviewing and editing the entire manuscript. All authors read and approved the final manuscript.

Artificial Intelligence Statement: No artificial intelligence tools were used in the preparation of this manuscript.

Conflict of Interest Disclosure: No potential conflict of interest was declared by the authors.

Plagiarism Statement: This article was scanned by the plagiarism program.

References

[1] S. Varosanec, *On h-convexity*, J. Math. Anal. Appl., **326**(1) (2007), 303-311. https://doi.org/10.1016/j.jmaa.2006.02.086

[2] D. S. Mitrinovic, J. E. Pečarić, A. M. Fink, *Classical and New Inequalities in Analysis*, Springer, Dordrecht, 1993.

[3] W. W. Breckner, *Stetigkeitsaussagen für eine Klasse verallgemeinerter konvexer funktionen in topologischen linearen Räumen*, Publ. Inst. Math., **23**(37) (1978), 13-20.

[4] C. E. M. Pearce, A. M. Rubinov, *P-functions, quasi-convex functions and Hadamard-type inequalities*, J. Math. Anal. Appl., **240**(1) (1999), 92-104. https://doi.org/10.1006/jmaa.1999.6593

[5] I. Iscan, *New refinements for integral and sum forms*, J. Inequal. Appl., **2019** (2019), Article ID 304, 11 pages. https://doi.org/10.1186/s13660-019-2258-5

[6] R. Gorenflo, F. Mainardi, *Fractional Calculus: Integral and Differential Equations of Fractional Order*, Springer Verlag, Wien, 1997.

[7] A. A. Kilbas, H. M. Srivastava, J. J. Trujillo, *Theory and Applications of Fractional Differential Equations*, Elsevier, Amsterdam, 2006.

[8] S. S. Dragomir, *On Simpson's quadrature formula for mappings of bounded variation and applications*, Tamkang J. Math., **30**(1) (1999), 53-58. https://doi.org/10.5556/j.tkjm.30.1999.4207

[9] U. S. Kirmaci, *On some Bullen-type inequalities with the kth power for twice differentiable mappings and applications*, J. Inequal. Math. Anal., **1**(1) (2025), 47-64. https://doi.org/10.63286/jima.2025.04

[10] J. Park, *On Simpson-like type integral inequalities for differentiable preinvex functions*, Appl. Math. Sci., **7**(121) (2013), 6009-6021. http://dx.doi.org/10.12988/ams.2013.39498

[11] P. J. Davis, P. Rabinowitz, *Methods of Numerical Integration*, Academic Press, New York-San Francisco-London, 1975.

[12] S. Erden, S. Iftikhar, P. Kumam, M. U. Awan, *Some Newton's like inequalities with applications*, Rev. R. Acad. Cienc. Exactas Fis. Nat. Ser. A Mat. RACSAM, **114** (2020), Article ID 195, 13 pages. https://doi.org/10.1007/s13398-020-00926-z

[13] S. Gao, W. Shi, *On new inequalities of Newton's type for functions whose second derivatives absolute values are convex*, Int. J. Pure Appl. Math., **74**(1) (2012), 33-41.

[14] S. Iftikhar, P. Kumam, S. Erden, *Newton's-type integral inequalities via local fractional integrals*, Fractals, **28**(3) (2020), Article ID 2050037. https://doi.org/10.1142/S0218348X20500371

[15] M. A. Noor, K. I. Noor, S. Iftikhar, *Newton inequalities for p-harmonic convex functions*, Honam Math. J., **40**(2) (2018), 239-250. https://dx.doi.org/10.5831/HMJ.2018.40.2.239

[16] Lj. Dedić, M. Matić, J. Pečarić, *Euler-Maclaurin formulae*, Math. Inequal. Appl., **6**(2) (2003), 247–275.

[17] Lj. Dedić, M. Matić, J. Pečarić, A. Vukelic, *On Euler-Simpson* $3/8$ *formulae*, Nonlinear Stud., **18**(1) (2011), 1-26.

[18] F. Hezenci, H. Budak, *Maclaurin-type inequalities for Riemann-Liouville fractional integrals*, Ann. Univ. Mariae Curie-Skłodowska Sect. A Math., **76**(2) (2022), 15-32. http://dx.doi.org/10.17951/a.2022.76.2.15-32

[19] F. Hezenci, *Fractional inequalities of corrected Euler-Maclaurin-type for twice-differentiable functions*, Comput. Appl. Math., **42** (2023), 1-15, Article ID 92. https://doi.org/10.1007/s40314-023-02235-8

[20] F. Hezenci, *Fractional Maclaurin-type inequalities for twice-differentiable functions*, Rocky Mountain J. Math., **55**(1) (2025), 155-165. https://doi.org/10.1216/rmj.2025.55.155

[21] I. Franjic, J. Pečarić, I. Perić, A. Vukelić, *Euler Integral Identity, Quadrature Formulae and Error Estimations*, Element, Zagreb, 2011.

[22] J. E. Pečarić, F. Proschan, Y. L. Tong, *Convex Functions, Partial Orderings and Statistical Applications*, Academic Press, Boston, 1992.

[23] M. Gümüş, F. Hezenci, H. Budak, *Some new approaches to fractional Euler–Maclaurin-Type inequalities via various function classes*, Fractal Fract., **8**(7) (2024), Article ID 372, 19 pages. https://doi.org/10.3390/fractalfract8070372

Communications in Advanced Mathematical Sciences
ISSN (Online) 2651-4001

Vol. 8, No. 2, 70-85, 2025
https://doi.org/10.33434/cams.1581561
Research Article

Effect of Coefficient of Variation on Variable Sampling Scheme Indexed in AQL and AOQL under Measurement Error

Uttama Mishra

Abstract
This study investigates the impact of measurement error on variable sampling schemes indexed by Acceptance Quality Limit (AQL) and Average Outgoing Quality Level (AOQL) while considering a known Coefficient of Variation (CV). We present procedures and tables for selecting appropriate variable sampling plans based on specified AQL and AOQL values. In our approach, rejected lots undergo 100% inspection to replace non-conforming items. The operating characteristic (OC) function is analyzed for various CV values, highlighting how measurement error influences the classification of product quality. Our findings emphasize the importance of understanding the relationship between measurement error, CV, AQL, and AOQL in quality control processes, ultimately aiming to enhance product quality and optimize inspection resources.

Keywords: AOQL, AQL, Coefficient of variation, Measurement error, OC function, Variable sampling scheme
2020 AMS: 62C99, 62D05

Shri Vaishnav Vidyapeeth Vishwavidyalaya, Indore, Madhya Pradesh, India, uttamamishra@svvv.edu.in, uttamamishra@gmail.com
Received: 08 November 2024, **Accepted:** 29 April 2025, **Available online:** 14 June 2025
How to cite this article: U. Mishra, *Effect of coefficient of variation on variable sampling scheme indexed in AQL and AOQL under measurement error*, Commun. Adv. Math. Sci., 8(2) (2025), 70-85.

1. Introduction

The primary objective of quality control is to ensure that a product or service meets the required standards and satisfies customer expectations. This involves maintaining consistency in production processes and ensuring product reliability. To achieve this, the acceptance of an application is recognized as part of a process that involves detecting and analyzing product quality, implementing quality control measures, and making necessary improvements, particularly in identifying and managing defective components.Replacement plan is one of the classifications of warranty that requires fewer instances but provides the same protection to manufacturers and consumers [1]. To check the stability of the product. CV is defined as the ratio of the standard deviation to the mean; This is better than the overall effect. It is considered an important metric to identify and compare changes. It is more important to use CV to describe variance than standard deviation. CV allows investors to determine how unpredictable or risky the assumption is compared to the expected return on investment. In recent years, a lot of work has been done on different models for different situations. [2] proposed a two-stage regression model based on the dependent variable. [3] investigated the robustness of one-shot methods measured by AQL and AOQL. [4] and [5] investigated that CV can be used as a negative factor. Obtaining a high level of final product while controlling the production cost is a challenge in the production process. Analytical techniques have been used effectively to solve this problem; For this purpose, the product is analysed. All audits have the potential for errors, such as accepting the wrong product and rejecting the appropriate product.

These errors are called observational errors, are mostly due to chance and can be predicted. The requirement that a product measure be within certain limits is often more important than the requirement that the product mean and variance be at or near a decision. Many authors have proposed acceptance criteria as a measure of error. [6] proposed acceptance through change as a measure of uncertainty. [7] presents a model based on measurement error for variables. [8] proposed a two-stage variable sampling plan to compare its performance with the single sampling plan by minimizing the ASN using the two-point approach on the OC curve. [9] have used three forms of acceptance criteria(σ-method, s-method and R-method) for the selection of single sampling plan for variables. [10] introduced a new variable sampling plan based on the process capability index to deal with product acceptance determination. [11] studied the impact of the coefficient of variation (CV) on single-sampling plans, highlighting its role in improving quality control under normality assumptions. [12] determines plan parameters using the classical two-point condition on the operating characteristic curve to meet both producer and consumer risk requirements. The proposed sampling plan achieves the same protection with a smaller sample size, particularly for high-quality lots. [13] investigates the performance of the coefficient of variation chart in the presence of measurement errors for a finite production horizon. Also, studies a two-sided Shewhart coefficient of variation chart with measurement errors for detecting both increases and decreases in the coefficient of variation for short run processes using an error model with a linear covariate. [14] considered a generalized multiple dependent state (GMDS) sampling plan for accepting a lot based on the coefficient of variation when a quality characteristic comes from a normal distribution. [15] aimed to develop a coefficient of variation (CV) control chart utilizing the generalized multiple dependent state (GMDS) sampling approach for CV monitoring. [16] developed some novel calibration-based coefficient of variation estimators for the study variable under double-stratified random sampling (DSRS) using the robust features of linear (L and TL) moments, which offer appropriate coefficient of variation estimates.

The remaining article is structured as follows: Section 2 discusses the methodology of the sampling plan. Section 3 presents the numerical tables, calculations, and results. Section 4 provides a discussion on the effect of CV on AQL, AOQL, and measurement error. Finally, the conclusion of this study is presented in Section 5.

2. Variable Sampling with Known Coefficient of Variation Under Measurement Error

In connection with the variable sampling plan when σ is known, the density function is given by:

$$\phi(y_e) = \int_{\infty}^{y_e} \frac{1}{\sqrt{2\pi}} e^{\frac{-1}{2}Z^2} dZ$$

where $Z \sim N(0,1)$. The acceptance criterion for the inspection plan with upper specification limit, U_e, is:

accept the lot if $\bar{x} + k_{\sigma_e} \leq U_e$

where k_{σ_e} is the acceptance parameter. Now, the acceptance criterion for the lower specification limit, L_e, is:

accept the lot if $\bar{x} + k_{\sigma_e} \geq L_e$.

The fraction non-conformities in a lot given will be:

$$\phi(-\nu_e) = p_e \tag{2.1}$$

with

$$\nu_e = \frac{U_e - \mu}{\sigma_e}.$$

If the proportion defective in the lot is p_e, then $\nu_e \sigma_e + \mu = U_e$ and its probability of acceptance will be:

$$P_a(p_e) = \phi(w_e) \tag{2.2}$$

where

$$w_e = (\nu_e - k_{\sigma_e}) \sqrt{n_{\sigma_e} \rho_e^2 + v_e^2}$$

whenever ρ_e is the measurement error, given by the equation $\left(\frac{\sigma_p}{\sigma_e} = \frac{\rho_e}{\sqrt{1-\rho_e^2}} \right)$ and v_e is the coefficient of variation.

If all the fallacies originated in the rejected lots are reinstated by the conformities in a rectifying inspection plan. The determination of AOQ is approximated by:

$$AOQ = p_e P_a(p_e).$$

If p_{em} is the proportion non-conformity at the maximum value of AOQ, then AOQL is given by:

$$AOQ = p_{em} P_a(p_{em}). \tag{2.3}$$

If AQL(p_{e1}) is specified, then the corresponding value of v_{AQL} or v_{e1} will be fixed and if $P_a(p_{e1})$ is fixed at 95%, then $w_{AQL} = w_1 = 1.645$. Hence, we have:

$$1.645 = (v_{e1} - k_{\sigma_e})\sqrt{n_{\sigma_e}\rho_e^2 + v_e^2}. \tag{2.4}$$

So that for a given AQL, k_{σ_e} is determined by the sample n_{σ_e}. For calculating the optimal value of n_{σ_e} and k_{σ_e}, a trial value is assumed and the probability of acceptance at p_{em} is found from equation (2.3) as:

$$P_a(p_{em}) = \frac{AOQL}{p_{em}}. \tag{2.5}$$

The auxiliary variables v_{em} and w_{em} corresponding to the values of p_{em} and $P_a(p_{em})$ respectively, can be obtained using the equation (2.1) and (2.2). The values of v_{e1} and $w_{e1} = 1.645$ are known for a given value of p_{e1}. By using values of v_{e1}, w_{e1}, v_{em} and w_{em}, we can calculate n_{σ_e} by the following equation given by Wallis (1948):

$$n_{\sigma_e} = \frac{(w_{e1} - w_{em})^2}{(v_{e1} - v_{em})^2}. \tag{2.6}$$

By using the value of n_{σ_e} given in equation (2.6), it is observed whether or not the trial value of p_{em} satisfies the following equation:

$$AOQL - p_{em}^2\sqrt{n_{\sigma_e}\exp\left[-(w_{em}^2 - v_{em}^2)\right]} = 0. \tag{2.7}$$

The equation (2.7) can be obtained by following the formula:

$$\frac{dAOQ}{dp_e} = P_a(p_e) + p_e\frac{dP_a(p_e)}{dp_e} = 0 \tag{2.8}$$

where

$$\frac{dP_a(p_e)}{dp_e} = -\sqrt{n_{\sigma_e}\exp[-(w_{em}^2 - v_{em}^2)]}.$$

If the trial value of p_{em} would not satisfy equation (2.8), then another value will be obtained from the same equation, and the method of successive substitution is often found for the optimal result, and equation (2.8) can be rewritten as:

$$p_{em} = \frac{AOQL}{p_{em}\sqrt{n_{\sigma_e}\exp\left[-(w_{em}^2 - v_{em}^2)\right]}}.$$

This iterative process continues till the convergence of p_{em} is achieved. Furthermore, the value of k_{σ_e} can be calculated using equation (2.4).

3. Numerical Illustration and Result

For illustrating the calculation numerically, we have considered a single sampling plan for variables under measurement error with the effect of the coefficient of variation. For examining the sampling scheme following values are considered: ρ_e=∞(error free),2,4,6, v_e=0,1,4,8,16.

Furthermore, Table 4.1, Table 4.2, Table 4.3, Table 4.4 is used for the selection of σ-method single sampling plan. For example, if we fix the AQL=1% and AOQL=1.25% then Table 4.1 provides $n_{\sigma_e} = 23$ and $k_{\sigma_e} = 1.984$ when $v_e = 0$. Suppose that it is decided to use the σ-method acceptance criterion when $\sigma_e = 2.0$, there is an upper specification limit $U_e = 10$ exists, and a unit for which the quality characteristic $x > U_e$ is considered as non-conforming. In such a case, Table 4.5, Table 4.6,

Table 4.7, Table 4.8 shows the performance characteristics of the plan with $n_{\sigma_e} = 23$ and $k_{\sigma_e} = 2$ under a rectifying inspection scheme. If the true process average quality is operating at AQL(μ=3.82) then 95% of the submitted lots will be accepted and 5% of the rejected lots will be rectified by replacing non-conforming units with conforming units. In that case, the AOQ will be only 0.95%. If the submitted lot quality deteriorates to 0.19%, only about 67% of the lots will be accepted by the sampling plan, and one out of every three lots will be rejected and rectified. The AOQ in such a case does not exceed the AOQL=1.25%, which means, irrespective of the product quality submitted by the producer, the consumer will receive an average quality not worse than 1.25% under the rectification scheme.

The user of Table 4.1, Table 4.2, Table 4.3, Table 4.4 given here should understand the limitations of plans indexed by AOQL. Sampling with rectification of rejected lots on the one hand reduces the average percentage of nonconforming items in the lots, but on the other hand, introduces non-homogeneity in the series of lots finally accepted. That is, any lot will have a quality of p_e% or 0% nonconforming, depending on whether the lot is accepted or rectified. Thus, the assumption underlying the AOQL principle is that the homogeneity in the qualities of individual lots is unimportant and only the average quality matters. For plans listed in Table 4.1 if the individual lot quality happens to be the product quality p_{em} at which AOQL occurs, then the associated probability of acceptance will be poor. For example, at an AQL=0.25% and an AOQL=1.25% Table 4.9 gives $p_a(p_{em}) = 0.32$, then, from equation (2.5), $p_{em} = 3.90\%$, then on an average of every three lots passed on to the customer, two will be free from non-conforming items, the third lot will contain 3.90% non-conforming items, which is 16 times the AQL specified for $v_e = 0$. In a similar way, we can interpret the results for other values of v_e. Furthermore, if we consider the plan given in Table 4.2, the AQL is set at 0.15%, which means, a lot must produce no more than 0.15% defective items during the production process to be acceptable. AOQL of 0.5% means the average proportion of defective products after inspection shall not rise above 0.5%. The acceptance probability is comparatively low $p_a(p_{em}) = 0.414$ i.e. 41.4% given in Table 4.10, this low likelihood indicates that the lot will probably be rejected more than half the time, then equation (2.5) gives lot quality $p_{em} = 1.208\%$, a substantial increase over the AQL of 0.15%. This indicates that the lot's defect rate is significantly higher (almost 8 times) than what is adequate. In addition to, The sample plan given in Table 4.3 may be sufficiently tolerant to accept lots with defect rates higher than the acceptable threshold, as indicated by the high likelihood of acceptance 80.3% given in Table 4.11, due to the lot quality of 0.0996%, obtained by using equation (2.5), being greater than the permissible limit of both AQL= 0.065% and AOQL=0.08%. This implies that even if the lot frequently passes inspection, there are still more defects than is ideal. The high CV of 8 indicates a high degree of process variability, which raises the risk of variable product quality and adds to greater failure rates. Table 4.12 provides values of the probability of acceptance for different values of v_e when $\rho_e = \infty$.

To avoid such inconvenience, the producer should maintain the process quality more or less at the AQL. The high rate of rejection of lots at $p_e = p_{em}$ will also indirectly put pressure on the producer to improve the submitted quality.

4. Discussion

In addition to, CV plays a significant role in variable sampling scheme indexing in terms of AQL and AOQL, especially in the presence of measurement error. Here's how it affects these parameters:

1. AQL:

- In variable sampling schemes, AQL represents the maximum acceptable level of non-conforming items in a batch or lot.
- The impact of CV on AQL is primarily through its influence on measurement error. A higher CV can lead to increased measurement variability, which may affect the determination of whether a batch meets the AQL criteria.
- When there's measurement error, a higher CV can result in wider variability in measured values, potentially leading to misclassification of batches as conforming or non-conforming.

2. AOQL:

- AOQL represents the average quality level of outgoing lots over time when the process is operating at its AQL.
- Measurement error, influenced by the CV, can affect the AOQL by introducing variability in the measurement process.
- A higher CV can lead to increased uncertainty in measuring the quality of outgoing lots, potentially impacting the AOQL calculations.
- In variable sampling schemes, where measurement error is considered, adjustments may need to be made to the AOQL calculations to account for the variability introduced by the CV.

CV		AQL%											
	AOQL%	0.04	0.065	0.1	0.15	0.25	0.4	0.65	1	1.5	2.5	4	6.5
	0.05	44,3.105											
	0.08	16,2.935	43,2.965										
	0.125	9,2.800	15,2.794	38,2.823									
	0.2	6,2.666	8,2.644	13,2.638	29,2.660								
	0.32	4,2.533	5,2.502	7,2.482	11,2.475	29,2.504							
v_e=0	0.5	3,2.404	4,2.367	5,2.339	6,2.319	11,2.311	29,2.346						
	0.8	2,2.260	3,2.219	3,2.186	4,2.159	6,2.134	10,2.129	27,2.169					
	1.25		2,2.070	2,2.033	3,2.002	4,1.968	5,1.947	9,1.945	23,1.984				
	2			2,1.967	2,1.825	3,1.786	3,1.756	5,1.735	8,1.733	17,1.766			
	3.2					2,1.587	2,1.552	3,1.522	4,1.504	6,1.502	16,1.548		
	5							2,1.301	2,1.276	3,1.261	6,1.263	14,1.319	
	8								2,1.004	2,0.983	3,0.968	5,0.975	12,1.045
	0.05	45,3.107											
	0.08	17,2.948	44,2.968										
	0.125	10,2.829	16,2.808	39,2.827									
	0.2	7,2.719	9,2.676	14,2.655	30,2.666								
	0.32	5,2.619	6,2.561	8,2.519	12,2.495	30,2.509							
v_e=1	0.5	4,2.529	5,2.460	6,2.406	7,2.364	12,2.333	30,2.351						
	0.8	3,2.439	4,2.361	4,2.296	5,2.241	7,2.184	11,2.154	28,2.175					
	1.25		3,2.271	3,2.198	4,2.133	5,2.059	6,2.004	10,1.971	12,1.867				
	2			3,2.099	3,2.025	4,1.937	4,1.864	6,1.802	24,1.991	18,1.778			
	3.2					3,1.822	3,1.734	4,1.651	9,1.769	7,1.551	17,1.561		
	5							3,1.519	5,1.590	4,1.373	7,1.318	16,1.333	
	8								3,1.438	3,1.203	4,1.108	5,1.049	13,1.064
	0.05	59,3.139											
	0.08	31,3.055	59,3.001										
	0.125	24,3.015	30,2.917	53,2.865									
	0.2	21,2.990	23,2.874	28,2.780	44,2.720								
	0.32	19,2.975	20,2.849	22,2.740	26,2.645	45,2.684							
v_e=4	0.5	18,2.965	19,2.835	20,2.719	21,2.611	26,2.645	44,2.528						
	0.8	17,2.958	18,2.825	18,2.705	19,2.590	21,2.627	25,2.487	43,2.358					
	1.25		17,2.819	17,2.697	18,2.579	19,2.617	20,2.469	24,2.316	38,2.193				
	2			17,2.691	17,2.571	18,2.611	18,2.460	20,2.298	22,2.153	31,1.877			
	3.2					17,2.607	17,2.454	18,2.289	19,2.137	21,1.809	24,1.719		
	5							17,2.285	17,2.129	18,1.784	19,1.677	29,1.447	
	8								17,1.924	17,1.771	17,1.658	19,1.370	27,1.197
	0.05	103,3.190											
	0.08	74,3.162	101,3.052										
	0.125	69,3.154	74,3.025	96,2.922									
	0.2	66,3.151	68,3.017	72,2.896	87,2.791								
	0.32	65,3.149	66,3.014	67,2.889	70,2.771	87,2.631							
v_e=8	0.5	65,3.148	65,3.012	66,2.887	67,2.766	70,2.610	87,2.475						
	0.8	65,3.148	65,3.011	65,2.886	65,2.764	66,2.605	69,2.454	85,2.305					
	1.25		65,3.011	65,2.886	65,2.763	65,2.603	66,2.450	69,2.285					
	2			64,2.885	64,2.763	65,2.602	65,2.448	66,2.281	67,2.126	74,1.979			
	3.2					64,2.602	65,2.447	65,2.279	65,2.123	66,1.968	74,1.768		
	5							64,2.381	64,2.121	65,1.966	66,1.757	72,1.557	
	8								64,2.121	64,1.965	65,1.755	66,1.547	70,1.317
	0.05	275,3.25											
	0.08	259,3.25	273,3.12										
	0.125	257,3.25	259,3.11	270,2.990									
	0.2	257,3.25	257,3.11	258,2.988	264,2.866								
	0.32	256,3.25	256,3.11	257,2.988	257,2.865	264,2.706							
v_e=16	0.5	256,3.25	256,3.11	256,2.987	257,2.865	257,2.704	263,2.551						
	0.8	256,3.25	256,3.11	256,2.987	256,2.865	256,2.704	257,2.549	262,2.382					
	1.25		256,3.11	256,2.987	256,2.865	256,2.704	256,2.549	257,2.381	260,2.224				
	2			256,2.987	256,2.865	256,2.704	256,2.549	256,2.381	256,2.224	258,2.068			
	3.2					256,2.704	256,2.549	256,2.381	256,2.224	256,2.067	257,1.857		
	5							256,2.381	256,2.224	256,2.067	256,1.857	257,1.648	
	8								256,2.224	256,2.067	256,1.857	256,1.648	256,1.411

Table 4.1. Values of n_{σ_e} and k_{σ_e} for different values of v_e when $\rho_e = 4$

CV						AOQL%							
	AOQL(%)	0.04	0.065	0.1	0.15	0.25	0.4	0.65	1	1.5	2.5	4	6.5
	0.05	45,3.108											
	0.08	16,2.942	43,2.966										
	0.125	9,2.810	16,2.802	39,2.827									
	0.2	6,2.678	9,2.654	14,2.646	30,2.666								
	0.32	4,2.547	5,2.514	8,2.492	12,2.483	30,2.509							
v_e=0	0.5	3,2.420	4,2.381	5,2.351	7,2.330	11,2.320	30,2.351						
	0.8	2,2.278	3,2.236	3,2.201	4,2.172	6,2.145	10,2.138	28,2.174					
	1.25		2,2.089	3,2.051	3,2.018	4,1.982	6,1.959	10,1.954	24,1.990				
	2			2,1.990	2,1.844	3,1.803	3,1.771	5,1.747	8,1.743	17,1.773			
	3.2					2,1.607	2,1.570	3,1.538	4,1.518	6,1.513	17,1.555		
	5							2,1.321	3,1.294	3,1.276	6,1.274	15,1.326	
	8								2,1.026	2,1.003	3,0.984	5,0.988	13,1.053
	0.05	46,3.111											
	0.08	17,2.954	46,2.972										
	0.125	10,2.837	17,2.814	40,2.831									
	0.2	7,2.728	10,2.684	15,2.661	31,2.671								
	0.32	5,2.628	6,2.569	9,2.527	13,2.502	31,2.514							
v_e=1	0.5	4,2.539	5,2.470	6,2.415	8,2.372	12,2.340	31,2.356						
	0.8	3,2.449	4,2.371	4,2.306	5,2.250	7,2.193	11,2.161	29,2.180					
	1.25		3,2.281	3,2.208	4,2.143	5,2.068	7,2.013	11,1.979					
	2			3,2.109	3,2.035	4,1.947	4,1.873	6,1.811	25,1.997	18,1.784			
	3.2					3,1.832	3,1.744	4,1.661	9,1.777	7,1.560	18,1.567		
	5							3,1.529	5,1.599	4,1.383	7,1.326	16,1.339	
	8								4,1.448	3,1.213	4,1.118	6,1.058	14,1.070
	0.05	61,3.142											
	0.08	31,3.057	60,3.004										
	0.125	24,3.017	31,2.919	55,2.867									
	0.2	21,2.991	23,2.875	29,2.782	45,2.722								
	0.32	19,2.975	20,2.851	22,2.742	26,2.647	46,2.685							
v_e=4	0.5	18,2.966	19,2.836	20,2.720	21,2.612	26,2.646	45,2.529						
	0.8	17,2.958	18,2.826	18,2.706	19,2.591	21,2.627	25,2.487	43,2.359					
	1.25		17,2.820	18,2.697	18,2.579	19,2.617	20,2.470	24,2.317	39,2.194				
	2			17,2.691	17,2.571	18,2.611	18,2.460	20,2.299	23,2.153	32,1.879			
	3.2					17,2.608	17,2.455	18,2.290	19,2.137	21,1.811	24,1.721		
	5							17,2.285	18,2.130	18,1.785	19,1.678	30,1.449	
	8								17,1.925	17,1.772	17,1.659	19,1.376	27,1.199
	0.05	103,3.191											
	0.08	75,3.162	102,3.053										
	0.125	69,3.155	74,3.025	97,2.923									
	0.2	66,3.151	68,3.017	72,2.897	87,2.792								
	0.32	65,3.149	66,3.014	67,2.890	70,2.772	88,2.632							
v_e=8	0.5	65,3.149	65,3.012	66,2.888	67,2.766	70,2.611	87,2.476						
	0.8	65,3.148	65,3.012	65,2.886	65,2.764	67,2.605	69,2.454	85,2.306					
	1.25		65,3.011	65,2.886	65,2.763	65,2.603	66,2.450	69,2.285					
	2			64,2.885	64,2.763	65,2.602	65,2.448	66,2.281	67,2.126	75,1.980			
	3.2					64,2.602	64,2.447	65,2.279	65,2.123	66,1.968	74,1.768		
	5							64,2.381	64,2.122	65,1.966	66,1.757	72,1.557	
	8								64,2.121	64,1.965	65,1.755	65,1.547	70,1.317
	0.05	275,3.254											
	0.08	260,3.251	274,3.117										
	0.125	257,3.250	259,3.114	270,2.990									
	0.2	257,3.250	257,3.113	259,2.988	264,2.867								
	0.32	256,3.250	256,3.113	257,2.988	258,2.865	264,2.706							
v_e=16	0.5	256,3.250	256,3.113	256,2.987	257,2.865	257,2.704	263,2.551						
	0.8	256,3.250	256,3.113	256,2.987	256,2.865	256,2.704	257,2.549	262,2.382					
	1.25		256,3.113	256,2.987	256,2.865	256,2.704	256,2.549	257,2.381	260,2.224				
	2			256,2.987	256,2.865	256,2.704	256,2.549	256,2.381	256,2.224	258,2.068			
	3.2					256,2.704	256,2.549	256,2.381	256,2.224	256,2.067	257,1.857		
	5							256,2.381	256,2.224	256,2.067	256,1.857	257,1.648	
	8								256,2.224	256,2.067	256,1.857	256,1.648	256,1.411

Table 4.2. Values of n_{σ_e} and k_{σ_e} for different values of v_e when $\rho_e = 6$

CV		AQL %											
	AOQL(%)	0.04	0.065	0.1	0.15	0.25	0.4	0.65	1	1.5	2.5	4	6.5
	0.05	37,3.082											
	0.08	13,2.898	36,2.943										
	0.125	7,2.751	13,2.757	32,2.799									
	0.2	5,2.606	7,2.593	11,2.598	24,2.633								
	0.32	3,2.461	4,2.438	6,2.427	9,2.431	25,2.477							
v_e=0	0.5	3,2.320	3,2.292	4,2.272	5,2.261	9,2.267	24,2.319						
	0.8	2,2.164	2,2.131	3,2.106	3,2.087	5,2.074	8,2.082	23,2.141					
	1.25		2,1.969	2,1.941	2,1.917	3,1.894	5,1.885	8,1.897	19,1.953				
	2			2,1.835	2,1.725	2,1.696	3,1.677	4,1.669	6,1.681	14,1.730			
	3.2					2,1.480	2,1.455	2,1.437	3,1.432	5,1.443	13,1.511		
	5							2,1.198	2,1.184	3,1.181	5,1.201	12,1.280	
	8								1,0.889	2,0.879	2,0.880	4,0.907	10,1.003
	0.05	53,3.127											
	0.08	29,3.045	53,2.989										
	0.125	23,3.007	54,2.992	48,2.853									
	0.2	20,2.984	22,2.866	27,2.771	40,2.708								
v_e=4	0.32	19,2.971	20,2.844	21,2.734	25,2.636	41,2.678							
	0.5	18,2.963	18,2.831	19,2.714	21,2.604	25,2.641	40,2.522						
	0.8	17,2.958	17,2.823	18,2.702	19,2.586	20,2.624	23,2.482	39,2.352					
	1.25		17,2.817	17,2.694	18,2.576	18,2.615	20,2.466	23,2.312	36,2.188				
	2			17,2.689	17,2.569	17,2.610	18,2.458	19,2.296	21,2.149	30,1.867			
	3.2					17,2.607	17,2.453	18,2.288	18,2.135	20,1.804	23,1.711		
	5							17,2.284	17,2.128	18,1.781	19,1.673	27,1.437	
	8								17,1.923	17,1.770	17,1.656	19,1.371	26,1.188
	0.05	97,3.186											
	0.08	74,3.161	96,3.048										
	0.125	68,3.153	72,3.023	92,2.918									
	0.2	66,3.150	67,3.015	71,2.895	84,2.788								
	0.32	65,3.149	66,3.013	67,2.889	70,2.770	87,2.630							
v_e=8	0.5	65,3.148	65,3.012	66,2.887	66,2.766	69,2.609	85,2.473						
	0.8	64,3.148	65,3.011	65,2.886	65,2.764	66,2.605	69,2.453	82,2.302					
	1.25		65,3.011	65,2.885	65,2.763	65,2.603	66,2.449	68,2.284	78,2.140				
	2			64,2.885	64,2.763	65,2.602	65,2.448	65,2.280	67,2.125	73,1.977			
	3.2					64,2.602	64,2.447	64,2.278	65,2.122	66,1.967	72,1.766		
	5							64,2.381	64,2.121	65,1.966	66,1.757	71,1.555	
	8								64,2.121	64,1.965	64,1.755	65,1.547	69,1.316
	0.05	272,3.253											
	0.08	259,3.251	271,3.116										
	0.125	257,3.250	259,3.114	268,2.990									
	0.2	257,3.250	257,3.113	258,2.988	263,2.866								
v_e=16	0.32	256,3.250	256,3.113	257,2.988	257,2.865	263,2.706							
	0.5	256,3.250	256,3.113	256,2.987	256,2.865	257,2.704	262,2.550						
	0.8	256,3.250	256,3.113	256,2.987	256,2.865	256,2.704	257,2.549	261,2.382					
	1.25		256,3.113	256,2.987	256,2.865	256,2.704	256,2.549	257,2.381	259,2.224				
	2			256,2.987	256,2.865	256,2.704	256,2.549	256,2.381	256,2.224	258,2.068			
	3.2					256,2.704	256,2.549	256,2.381	256,2.224	256,2.067	257,1.857		
	5							256,2.381	256,2.224	256,2.067	257,1.857	257,1.648	
	8								256,2.224	256,2.067	256,1.857	256,1.648	256,1.411

Table 4.3. Values of n_{σ_e} and k_{σ_e} for different values of v_e when $\rho_e = 2$

CV		AQL%											
	AOQL%	0.04	0.065	0.1	0.15	0.25	0.4	0.65	1	1.5	2.5	4	6.5
	0.05	47,3.112											
	0.08	17,2.900	46,2.972										
	0.125	9,2.754	16,2.807	40,2.831									
	0.2	6,2.608	9,2.661	14,2.652	30,2.670								
	0.32	4,2.464	6,2.523	8,2.500	12,2.489	31,2.513							
v_e=0	0.5	3,2.324	4,2.392	5,2.361	7,2.338	12,2.327	31,2.355						
	0.8	2,2.168	3,2.249	4,2.213	4,2.183	6,2.154	11,2.145	29,2.178					
	1.25		2,2.104	3,2.065	3,2.031	4,1.994	6,1.968	10,1.961	25,1.994				
	2			2,2.006	2,1.860	3,1.817	4,1.783	5,1.748	8,1.741	18,1.788			
	3.2					2,1.623	2,1.585	3,1.551	4,1.529	6,1.522	17,1.561		
	5							2,1.337	3,1.308	3,1.288	6,1.284	15,1.332	
	8								2,1.044	2,1.019	3,1.998	5,0.999	13,1.060

	0.05	45,3.142											
	0.08	16,3.061	45,3.006										
	0.125	8,3.019	15,2.922	39,2.869									
	0.2	5,2.994	8,2.877	13,2.785	30,2.726								
	0.32	3,2.978	4,2.852	6,2.743	11,2.649	30,2.686							
v_e=4	0.5	2,2.969	3,2.838	4,2.721	6,2.614	11,2.647	30,2.531						
	0.8	2,2.962	2,2.829	3,2.710	3,2.592	5,2.628	9,2.488	30,2.358					
	1.25		2,2.823	2,2.703	2,2.614	3,2.618	5,2.470	9,2.313	24,2.197				
	2			1,1.697	2,2.612	2,2.614	3,2.463	4,2.294	7,2.154	17,1.882			
	3.2					2,2.612	2,2.458	2,2.286	3,2.138	5,1.813	9,1.723		
	5							2,2.283	2,2.131	3,1.790	4,1.683	14,1.452	
	8								1,1.931	2,1.778	2,1.669	3,1.378	12,1.203

	0.05	109,3.195											
	0.08	78,3.166	105,3.055										
	0.125	71,3.157	77,3.029	34,2.924									
	0.2	68,3.154	71,3.021	9,2.897	24,2.792								
	0.32	67,3.152	68,3.017	5,2.891	6,2.771	25,2.632							
v_e=8	0.5	66,3.151	67,3.015	3,2.889	4,2.768	6,2.611	24,2.476						
	0.8	66,3.150	66,3.014	2,2.888	2,2.765	3,2.606	7,2.457	22,2.306					
	1.25		66,3.013	2,2.887	2,2.765	2,2.605	4,2.452	7,2.288	19,2.145				
	2			1,2.887	1,2.764	2,2.604	3,2.451	4,2.284	5,2.128	11,1.980			
	3.2					2,2.604	2,2.449	2,2.282	3,2.125	4,1.970	12,1.772		
	5							2,2.382	2,2.123	2,1.968	4,1.760	8,1.557	
	8								1,2.123	1,1.966	2,1.758	3,1.550	6,1.318

	0.05	43,3.232											
	0.08	12,3.221	39,3.094										
	0.125	7,3.219	21,3.097	27,2.964									
	0.2	4,3.218	5,3.081	8,2.957	19,2.839								
	0.32	3,3.217	4,3.081	4,2.955	6,2.883	19,2.678							
v_e=12	0.5	2,3.217	3,3.080	3,2.954	3,2.832	6,2.673	19,2.523						
	0.8	2,3.216	2,3.080	2.2.954	2,2.832	3,2.671	5,2.517	17,2.413					
	1.25		2,3.080	2,2.954	2,2.831	2,2.671	4,2.517	7,2.411	12,2.199				
	2			1,2.954	1,2.831	2,2.671	2,2.517	4,2.411	1,2.190	6,2.036			
	3.2					1,2.671	2,2.516	3,2.342	1,2.258	1,2.034	2,1.918		
	5							2,2.342	1,2.258	1,2.034	2,1.918	4,1.616	
	8								1,2.190	1,2.033	1,2.917	3,1.615	4,1.379

	0.05	28,3.255											
	0.08	6,3.251	22,3.117										
	0.125	5,3.251	7,3.115	22,2.991									
	0.2	3,3.251	5,3.114	8,2.989	18,2.868								
	0.32	2,3.250	4,3.114	4,2.988	5,2.866	9,2.706							
v_e=16	0.5	2,3.250	3,3.114	2,2.988	3,2.866	5,2.705	9,2.551						
	0.8	2,3.250	2,3.114	2,2.988	2,2.865	3,2.705	3,2.550	7,2.382					
	1.25		2,3.113	1,2.988	1,2.865	2,2.705	3,2.550	6,2.382	4,2.224				
	2			1,2.988	1,2.865	2,2.705	2,2.550	4,2.382	4,2.224	2,2.068			
	3.2					1,2.705	2,2.550	2,2.381	2,2.224	1,2.067	7,1.858		
	5							2,2.381	2,2.224	1,2.067	1,1.857	2,1.648	
	8								1,2.224	1.2.067	1,1.857	2,1.648	3,1.412

Table 4.4. Values of n_{σ_e} and k_{σ_e} for different values of v_e when $\rho_e = \infty$

CV	μ	v_e	p(%)	w	Pa	AOQ
	3.82	3.09	0.1	1.6381	0.9493	0.095
	4.2	2.9	0.19	0.4364	0.6687	0.1248
	4.5	2.75	0.3	-0.5123	0.3042	0.0907
v_e=0	5	2.5	0.62	-2.0934	0.0182	0.0113
	5.3	2.35	0.94	-3.0421	0.0012	0.0011
	5.6	2.2	1.39	-3.9908	0	0
	3.82	3.09	0.1	1.639	0.9494	0.095
	4.2	2.9	0.19	0.2299	0.5909	0.1103
	4.5	2.75	0.3	-0.8825	0.1887	0.0562
v_e=4	5	2.5	0.62	-2.7366	0.0031	0.0019
	5.3	2.35	0.94	-3.849	0.0001	0.0001
	5.6	2.2	1.39	-4.9614	0	0
	3.82	3.09	0.1	1.6433	0.9498	0.0951
	4.2	2.9	0.19	-0.2376	0.4061	0.0758
	4.5	2.75	0.3	-1.7225	0.0425	0.0127
v_e=8	5	2.5	0.62	-4.1974	0	0
	5.3	2.35	0.94	-5.6823	0	0
	5.6	2.2	1.39	-7.1672	0	0
	3.82	3.09	0.1	1.6477	0.9503	0.0951
	4.2	2.9	0.19	-0.8369	0.2013	0.0376
	4.5	2.75	0.3	-2.7984	0.0026	0.0008
v_e=12	5	2.5	0.62	-6.0676	0	0
	5.3	2.35	0.94	-8.0291	0	0
	5.6	2.2	1.39	-9.9906	0	0
	3.82	3.09	0.1	1.6387	0.9494	0.095
	4.2	2.9	0.19	-1.5063	0.066	0.0123
	4.5	2.75	0.3	-3.9893	0	0
v_e=16	5	2.5	0.62	-8.1275	0	0
	5.3	2.35	0.94	-10.6104	0	0
	5.6	2.2	1.39	-13.0934	0	0

Table 4.5. Performance characteristic for variable plan under known CV under measurement error when $\rho_e = 4$

CV	μ	v_e	p(%)	w	Pa	AOQ
	3.82	3.09	0.1	1.6381	0.9493	0.095
	4.2	2.9	0.19	0.4364	0.6687	0.1248
	4.5	2.75	0.3	-0.5123	0.3042	0.0907
v_e=0	5	2.5	0.62	-2.0934	0.0182	0.0113
	5.3	2.35	0.94	-3.0421	0.0012	0.0011
	5.6	2.2	1.39	-3.9908	0	0
	3.82	3.09	0.1	1.639	0.9494	0.095
	4.2	2.9	0.19	0.2299	0.5909	0.1103
	4.5	2.75	0.3	-0.8825	0.1887	0.0562
v_e=4	5	2.5	0.62	-2.7366	0.0031	0.0019
	5.3	2.35	0.94	-3.849	0.0001	0.0001
	5.6	2.2	1.39	-4.9614	0	0
	3.82	3.09	0.1	1.6433	0.9498	0.0951
	4.2	2.9	0.19	-0.2376	0.4061	0.0758
	4.5	2.75	0.3	-1.7225	0.0425	0.0127
v_e=8	5	2.5	0.62	-4.1974	0	0
	5.3	2.35	0.94	-5.6823	0	0
	5.6	2.2	1.39	-7.1672	0	0
	3.82	3.09	0.1	1.6477	0.9503	0.0951
	4.2	2.9	0.19	-0.8369	0.2013	0.0376
	4.5	2.75	0.3	-2.7984	0.0026	0.0008
v_e=12	5	2.5	0.62	-6.0676	0	0
	5.3	2.35	0.94	-8.0291	0	0
	5.6	2.2	1.39	-9.9906	0	0
	3.82	3.09	0.1	1.6387	0.9494	0.095
	4.2	2.9	0.19	-1.5063	0.066	0.0123
	4.5	2.75	0.3	-3.9893	0	0
v_e=16	5	2.5	0.62	-8.1275	0	0
	5.3	2.35	0.94	-10.6104	0	0
	5.6	2.2	1.39	-13.0934	0	0

Table 4.6. Performance characteristic for variable plan under known CV under measurement error when $\rho_e = 6$

CV	μ	ν_e	p(%)	w	Pa	AOQ
ν_e=0	3.8196	3.0902	0.1	1.4711	0.9294	0.0929
	4.2	2.9	0.19	0.5102	0.6951	0.1297
	4.5	2.75	0.3	-0.2475	0.4022	0.1199
	5	2.5	0.62	-1.5105	0.0655	0.0406
	5.3	2.35	0.94	-2.2682	0.0117	0.0109
	5.6	2.2	1.39	-3.026	0.0012	0.0017
ν_e=1	3.8196	3.0902	0.1	1.4977	0.9329	0.0933
	4.2	2.9	0.19	0.5024	0.6923	0.1292
	4.5	2.75	0.3	-0.2826	0.3887	0.1158
	5	2.5	0.62	-1.5908	0.0558	0.0347
	5.3	2.35	0.94	-2.3758	0.0088	0.0082
	5.6	2.2	1.39	-3.1607	0.0008	0.0011
ν_e=4	3.82	3.09	0.1	1.7484	0.9598	0.0961
	4.2	2.9	0.19	0.3467	0.6356	0.1186
	4.5	2.75	0.3	-0.7599	0.2237	0.0666
	5	2.5	0.62	-2.6042	0.0046	0.0029
	5.3	2.35	0.94	-3.7108	0.0001	0.0001
	5.6	2.2	1.39	-4.8174	0	0
ν_e=8	3.82	3.09	0.1	2.0151	0.9781	0.0979
	4.2	2.9	0.19	-0.2109	0.4165	0.0777
	4.5	2.75	0.3	-1.9683	0.0245	0.0073
	5	2.5	0.62	-4.8973	0	0
	5.3	2.35	0.94	-6.6547	0	0
	5.6	2.2	1.39	-8.4121	0	0
ν_e=16	3.82	3.09	0.1	2.1682	0.9849	0.0986
	4.2	2.9	0.19	-1.9514	0.0255	0.0048
	4.5	2.75	0.3	-5.2036	0	0
	5	2.5	0.62	-10.624	0	0
	5.3	2.35	0.94	-13.8763	0	0
	5.6	2.2	1.39	-17.1285	0	0

Table 4.7. Performance Characteristic for Variable plan under Known CV under Measurement Error when ρ_e = 2

CV	μ	ν_e	p(%)	w	Pa	AOQ
ν_e=0	3.82	3.09	0.1	1.6381	0.9493	0.095
	4.2	2.9	0.19	0.4364	0.6687	0.1248
	4.5	2.75	0.3	-0.5123	0.3042	0.0907
	5	2.5	0.62	-2.0934	0.0182	0.0113
	5.3	2.35	0.94	-3.0421	0.0012	0.0011
	5.6	2.2	1.39	-3.9908	0	0
ν_e=4	3.82	3.09	0.1	1.639	0.9494	0.095
	4.2	2.9	0.19	0.2299	0.5909	0.1103
	4.5	2.75	0.3	-0.8825	0.1887	0.0562
	5	2.5	0.62	-2.7366	0.0031	0.0019
	5.3	2.35	0.94	-3.849	0.0001	0.0001
	5.6	2.2	1.39	-4.9614	0	0
ν_e=8	3.82	3.09	0.1	1.6433	0.9498	0.0951
	4.2	2.9	0.19	-0.2376	0.4061	0.0758
	4.5	2.75	0.3	-1.7225	0.0425	0.0127
	5	2.5	0.62	-4.1974	0	0
	5.3	2.35	0.94	-5.6823	0	0
	5.6	2.2	1.39	-7.1672	0	0
ν_e=12	3.82	3.09	0.1	1.6477	0.9503	0.0951
	4.2	2.9	0.19	-0.8369	0.2013	0.0376
	4.5	2.75	0.3	-2.7984	0.0026	0.0008
	5	2.5	0.62	-6.0676	0	0
	5.3	2.35	0.94	-8.0291	0	0
	5.6	2.2	1.39	-9.9906	0	0
ν_e=16	3.82	3.09	0.1	1.6387	0.9494	0.095
	4.2	2.9	0.19	-1.5063	0.066	0.0123
	4.5	2.75	0.3	-3.9893	0	0
	5	2.5	0.62	-8.1275	0	0
	5.3	2.35	0.94	-10.6104	0	0
	5.6	2.2	1.39	-13.0934	0	0

Table 4.8. Performance characteristic for variable plan under known CV under measurement error when $\rho_e = \infty$

CV		AQL%											
	AOQL(%)	0.04	0.065	0.1	0.15	0.25	0.4	0.65	1	1.5	2.5	4	6.5
	0.05	0.68462											
	0.08	0.48678	0.6899										
	0.125	0.37398	0.5014	0.67466									
	0.2	0.29645	0.38101	0.49125	0.65077								
	0.32	0.24546	0.30439	0.37744	0.47488	0.67303							
v_e=0	0.5	0.21404	0.25693	0.30818	0.37456	0.49724	0.68675						
	0.8	0.19258	0.22477	0.26136	0.30783	0.38869	0.50119	0.69534					
	1.25		0.20694	0.23425	0.26838	0.32534	0.40026	0.5173	0.68964				
	2			0.1003	0.24467	0.28546	0.33675	0.41206	0.51112	0.68165			
	3.2					0.26547	0.30185	0.35283	0.4161	0.50142	0.68164		
	5							0.32483	0.36793	0.42307	0.52727	0.69684	
	8								0.34829	0.38443	0.4484	0.53969	0.70863
	0.05	0.68											
	0.08	0.50133	0.71161										
	0.125	0.39951	0.51594	0.68322									
	0.2	0.33297	0.40798	0.50786	0.65699								
	0.32	0.29212	0.34321	0.40728	0.4945	0.67753							
v_e=1	0.5	0.26937	0.30617	0.35042	0.40758	0.5165	0.69107						
	0.8	0.25792	0.28473	0.31583	0.3544	0.42336	0.52198	0.70293					
	1.25		0.27702	0.29985	0.32729	0.37423	0.43717	0.53889					
	2			0.29692	0.31654	0.34888	0.39009	0.45203	0.69616	0.66956			
	3.2					0.3435	0.3713	0.41098	0.53672	0.53237	0.69074		
	5							0.39997	0.46154	0.4746	0.55902	0.7065	
	8								0.43228	0.45784	0.50469	0.57584	0.71918
	0.05	0.73071											
	0.08	0.62803	0.74037										
	0.125	0.59635	0.64404	0.73587									
	0.2	0.58582	0.60883	0.6465	0.71357								
	0.32	0.58969	0.60239	0.62031	0.64894	0.73526							
v_e=4	0.5	0.5999	0.60744	0.61737	0.6328	0.66659	0.7485						
	0.8	0.61693	0.62091	0.62626	0.63389	0.65032	0.68018	0.7613					
	1.25		0.63889	0.64175	0.64601	0.65744	0.6676	0.69247	0.76246				
	2			0.65998	0.66431	0.66561	0.67561	0.68326	0.70747	0.75713			
	3.2					0.69041	0.69312	0.69519	0.70777	0.72198	0.74111		
	5							0.72061	0.72411	0.72712	0.73639	0.7896	
	8								0.75019	0.75309	0.75577	0.80709	0.80716
	0.05	0.79835											
	0.08	0.7729	0.80981										
	0.125	0.77208	0.78092	0.81269									
	0.2	0.7783	0.78313	0.78856	0.80966								
	0.32	0.7794	0.79105	0.80421	0.79575	0.82136							
v_e=8	0.5	0.79929	0.78443	0.80158	0.79802	0.80837	0.82893						
	0.8	0.80177	0.80842	0.79893	0.81456	0.81615	0.81486	0.83862					
	1.25		0.80621	0.82423	0.82141	0.8249	0.8198	0.82848					
	2			0.83556	0.83815	0.83407	0.83822	0.83843	0.84074	0.84955			
	3.2					0.84571	0.84147	0.84725	0.85269	0.85205	0.86114		
	5							0.86579	0.86572	0.8208	0.86607	0.87407	
	8								0.88105	0.87949	0.87999	0.86502	0.88712
	0.05	0.88906											
	0.08	0.88521	0.89379										
	0.125	0.88223	0.89252	0.89739									
	0.2	0.89558	0.88861	0.89561	0.90112								
	0.32	0.89634	0.89851	0.90249	0.91397	0.90623							
v_e=16	0.5	0.90596	0.90412	0.90585	0.90882	0.90806	0.91121						
	0.8	0.90802	0.91078	0.91484	0.90974	0.91091	0.90926	0.91585					
	1.25		0.91638	0.9184	0.91651	0.9187	0.91936	0.91965	0.91745				
	2			0.92472	0.92605	0.92469	0.92549	0.92502	0.92538	0.92698			
	3.2					0.93171	0.93337	0.93299	0.93216	0.93082	0.93224		
	5							0.93835	0.93635	0.93904	0.93642	0.93732	
	8								0.94472	0.94488	0.94531	0.94667	0.94633

Table 4.9. Values of probability of acceptance for different values of v_e when $\rho_e = 4$

		AQL%											
CV	AOQL%	0.04	0.065	0.1	0.15	0.25	0.4	0.65	1	1.5	2.5	4	6.5
	0.05	0.657											
	0.08	0.4946	0.6368										
	0.125	0.382	0.5091	0.6608									
	0.2	0.304	0.389	0.4989	0.6549								
	0.32	0.2524	0.312	0.3853	0.4826	0.6618							
v_e=0	0.5	0.2199	0.2637	0.3159	0.3823	0.5047	0.6788						
	0.8	0.1982	0.2309	0.2686	0.315	0.3963	0.5078	0.7007					
	1.25		0.2124	0.2409	0.2749	0.3324	0.4077	0.5244	0.6938				
	2			0.1038	0.2507	0.2919	0.3436	0.4193	0.5146	0.6637			
	3.2					0.2712	0.308	0.3595	0.423	0.5085	0.6868		
	5							0.3307	0.3742	0.4296	0.534	0.7022	
	8								0.353	0.3903	0.4546	0.5459	0.713
	0.05	0.6911											
	0.08	0.5084	0.6929										
	0.125	0.4065	0.5229	0.6895									
	0.2	0.3394	0.4149	0.5147	0.662								
	0.32	0.2978	0.3495	0.414	0.5011	0.6809							
v_e=1	0.5	0.2744	0.3117	0.3564	0.414	0.5231	0.6918						
	0.8	0.2623	0.2895	0.3211	0.3601	0.4296	0.5285	0.7017					
	1.25		0.2812	0.3044	0.3323	0.3798	0.4432	0.5449					
	2			0.3008	0.3208	0.3536	0.3953	0.4577	0.7016	0.6744			
	3.2					0.3474	0.3757	0.4158	0.5426	0.5379	0.6965		
	5							0.404	0.4668	0.4796	0.5643	0.7118	
	8								0.4367	0.4616	0.5091	0.5806	0.7241
	0.05	0.7345											
	0.08	0.633	0.7293										
	0.125	0.5985	0.6461	0.7395									
	0.2	0.588	0.6106	0.6491	0.723								
	0.32	0.5909	0.6037	0.6223	0.6495	0.7414							
v_e=4	0.5	0.601	0.6084	0.6187	0.6331	0.6688	0.7534						
	0.8	0.6174	0.6216	0.6272	0.6347	0.6513	0.6814	0.7637					
	1.25		0.6394	0.6424	0.6466	0.6548	0.6688	0.6975	0.7655				
	2			0.6628	0.6658	0.6701	0.6766	0.6883	0.71	0.7582			
	3.2					0.6922	0.695	0.7004	0.7087	0.7238	0.7438		
	5							0.7214	0.7248	0.7317	0.7366	0.7927	
	8								0.7516	0.7537	0.7557	0.7693	0.8087
	0.05	0.8042											
	0.08	0.7722	0.8103										
	0.125	0.7729	0.7832	0.8075									
	0.2	0.7767	0.7854	0.7791	0.8113								
	0.32	0.7869	0.7901	0.7903	0.7977	0.822							
v_e=8	0.5	0.7989	0.7856	0.7934	0.8031	0.8083	0.8305						
	0.8	0.8024	0.8093	0.811	0.8064	0.8085	0.8173	0.8397					
	1.25		0.8069	0.7935	0.8227	0.8179	0.8261	0.828	0.8454				
	2			0.8323	0.8344	0.8354	0.832	0.8386	0.8409	0.8505			
	3.2					0.8467	0.849	0.8493	0.8516	0.852	0.8624		
	5							0.8655	0.866	0.8662	0.867	0.8741	
	8								0.8772	0.8813	0.8815	0.8816	0.8872
	0.05	0.8893											
	0.08	0.8749	0.8923										
	0.125	0.8844	0.8934	0.8974									
	0.2	0.8967	0.8907	0.888	0.9011								
	0.32	0.897	0.8995	0.9043	0.8988	0.9063							
v_e=16	0.5	0.9064	0.9047	0.9068	0.9029	0.909	0.9112						
	0.8	0.9083	0.9111	0.9153	0.9105	0.9123	0.9126	0.915					
	1.25		0.9166	0.9187	0.9169	0.9193	0.9205	0.9177	0.9179				
	2			0.9249	0.9263	0.9267	0.9268	0.9269	0.9271	0.9273			
	3.2					0.9318	0.9299	0.9333	0.9327	0.9319	0.9328		
	5							0.9384	0.9365	0.9393	0.937	0.9377	
	8								0.9444	0.9449	0.9453	0.9441	0.9459

Table 4.10. Values of probability of acceptance for different values of v_e when $\rho_e = 6$

		AQL%											
CV	AOQL%	0.04	0.065	0.1	0.15	0.25	0.4	0.65	1	1.5	2.5	4	6.5
	0.05	0.6533											
	0.08	0.4465	0.6618										
	0.125	0.3298	0.4618	0.6543									
	0.2	0.259	0.341	0.4518	0.6174								
	0.32	0.2119	0.2674	0.3382	0.4356	0.6416							
v_e=0	0.5	0.1837	0.2236	0.2723	0.3361	0.4588	0.6574						
	0.8	0.1659	0.195	0.2295	0.2727	0.3508	0.4634	0.6672					
	1.25		0.1803	0.2058	0.2369	0.2906	0.3632	0.4805	0.6589				
	2			0.0795	0.2168	0.2545	0.3031	0.3761	0.4751	0.6285			
	3.2					0.2382	0.2721	0.3204	0.3816	0.4666	0.6525		
	5							0.2963	0.3371	0.3904	0.4941	0.6694	
	8								0.3218	0.356	0.4178	0.5083	0.6821
	0.05	0.7167											
	0.08	0.6167	0.7154										
	0.125	0.5876	0.6289	0.7236									
	0.2	0.5802	0.5983	0.629	0.6912								
	0.32	0.5753	0.5963	0.6116	0.6404	0.7157							
v_e=4	0.5	0.5748	0.6033	0.6119	0.6254	0.6578	0.7378						
	0.8	0.5605	0.6174	0.6219	0.6299	0.644	0.6717	0.7458					
	1.25		0.6375	0.6388	0.6435	0.6504	0.6624	0.6978	0.7227				
	2			0.6657	0.6556	0.6665	0.6723	0.6895	0.7117	0.7388			
	3.2					0.6885	0.6918	0.651	0.7044	0.7142	0.7373		
	5							0.5324	0.72	0.7274	0.7319	0.7831	
	8								0.7493	0.751	0.7542	0.7646	0.8015
	0.05	0.7976											
	0.08	0.7453	0.803										
	0.125	0.7737	0.7803	0.8075									
	0.2	0.7709	0.7725	0.7791	0.8021								
	0.32	0.7666	0.7884	0.7903	0.7889	0.7815							
v_e=8	0.5	0.7921	0.7792	0.7934	0.7972	0.8047	0.811						
	0.8	0.7988	0.8044	0.811	0.8066	0.8015	0.8113	0.833					
	1.25		0.7688	0.7935	0.8159	0.8161	0.8259	0.8236	0.8414				
	2			0.8323	0.834	0.8344	0.8373	0.8359	0.8398	0.8469			
	3.2					0.8263	0.8356	0.9076	0.844	0.8524	0.8604		
	5							0.8394	0.8553	0.8615	0.8658	0.8724	
	8								0.8755	0.844	0.8762	0.8766	0.8852
	0.05	0.8887											
	0.08	0.8835	0.8915										
	0.125	0.8771	0.88	0.8969									
	0.2	0.8906	0.8913	0.8988	0.8977								
	0.32	0.9026	0.8939	0.8945	0.8971	0.906							
v_e=16	0.5	0.9041	0.9098	0.9099	0.9099	0.9027	0.911						
	0.8	0.9068	0.9092	0.9126	0.9124	0.9108	0.9125	0.9155					
	1.25		0.9203	0.9209	0.9197	0.9159	0.9192	0.9162	0.9197				
	2			0.924	0.9251	0.9233	0.9234	0.9211	0.9248	0.9231			
	3.2					0.9311	0.9325	0.9316	0.9298	0.9333	0.9316		
	5							0.9379	0.9391	0.938	0.9371	0.9374	
	8								0.9447	0.9448	0.9452	0.9463	0.9461

Table 4.11. Values of probability of acceptance for different values of v_e when $\rho_e = 2$

		AQL(%)											
CV	AOQL(%)	0.04	0.065	0.1	0.15	0.25	0.4	0.65	1	1.5	2.5	4	6.5
	0.05	0.7											
	0.08	0.501	0.727										
	0.125	0.389	0.515	0.7									
	0.2	0.311	0.395	0.505	0.663								
	0.32	0.258	0.318	0.392	0.489	0.696							
v_e=0	0.5	0.226	0.27	0.322	0.389	0.51	0.714						
	0.8	0.203	0.236	0.274	0.321	0.402	0.514	0.719					
	1.25		0.227	0.246	0.281	0.338	0.413	0.53	0.702				
	2			0.104	0.255	0.297	0.349	0.425	0.524	0.672			
	3.2					0.276	0.313	0.365	0.428	0.514	0.696		
	5							0.336	0.379	0.435	0.54	0.714	
	8								0.358	0.395	0.46	0.553	0.72
	0.05	0.618											
	0.08	0.613	0.739										
	0.125	0.59	0.633	0.743									
	0.2	0.571	0.61	0.644	0.66								
	0.32	0.565	0.597	0.623	0.645	0.741							
v_e=4	0.5	0.556	0.556	0.616	0.63	0.666	0.744						
	0.8	0.533	0.485	0.571	0.635	0.65	0.684	0.746					
	1.25		0.446	0.521	0.568	0.635	0.667	0.698	0.715				
	2			0.509	0.513	0.559	0.581	0.689	0.71	0.748			
	3.2					0.439	0.559	0.651	0.709	0.718	0.738		
	5							0.532	0.679	0.665	0.698	0.786	
	8								0.606	0.639	0.576	0.767	0.801
	0.05	0.76											
	0.08	0.704	0.802										
	0.125	0.689	0.716	0.814									
	0.2	0.656	0.626	0.784	0.811								
	0.32	0.617	0.601	0.747	0.806	0.821							
v_e=8	0.5	0.566	0.589	0.732	0.764	0.808	0.831						
	0.8	0.552	0.521	0.672	0.756	0.799	0.779	0.84					
	1.25		0.478	0.629	0.713	0.755	0.717	0.779	0.835				
	2			0.548	0.651	0.661	0.606	0.694	0.798	0.847			
	3.2					0.532	0.574	0.666	0.739	0.79	0.837		
	5							0.579	0.702	0.751	0.793	0.874	
	8								0.625	0.72	0.718	0.798	0.887
	0.05	0.782											
	0.08	0.754	0.813										
	0.125	0.693	0.785	0.851									
	0.2	0.662	0.745	0.795	0.848								
	0.32	0.62	0.675	0.759	0.82	0.861							
v_e=12	0.5	0.575	0.613	0.74	0.784	0.819	0.861						
	0.8	0.567	0.548	0.689	0.764	0.807	0.824	0.879					
	1.25		0.493	0.645	0.719	0.757	0.743	0.78	0.883				
	2			0.551	0.661	0.678	0.675	0.696	0.901	0.894			
	3.2					0.571	0.584	0.605	0.899	0.886	0.894		
	5							0.498	0.877	0.84	0.832	0.909	
	8								0.813	0.815	0.814	0.818	0.909
	0.05	0.865											
	0.08	0.849	0.883										
	0.125	0.784	0.84	0.873									
	0.2	0.748	0.756	0.806	0.855								
	0.32	0.683	0.68	0.773	0.828	0.904							
v_e=16	0.5	0.638	0.65	0.753	0.791	0.832	0.904						
	0.8	0.612	0.584	0.708	0.776	0.812	0.865	0.912					
	1.25		0.531	0.661	0.726	0.762	0.779	0.808	0.921				
	2			0.573	0.674	0.686	0.678	0.715	0.821	0.924			
	3.2					0.583	0.607	0.632	0.769	0.907	0.974		
	5							0.55	0.625	0.883	0.882	0.923	
	8								0.518	0.868	0.865	0.866	0.913

Table 4.12. Values of probability of acceptance for different values of v_e when $\rho_e = \infty$

5. Conclusion

The difference between parameters significantly impacts the variation in measurement parameters, specifically in Acceptance Quality Limit (AQL) and Average Outgoing Quality Level (AOQL), by influencing the measurement error and subsequently the measurement process. Measurement errors introduce biases that can lead to overestimation or underestimation of the Coefficient of Variation (CV), which can severely affect the reliability of AQL and AOQL determinations, leading to erroneous acceptance or rejection decisions in quality control. CV plays an essential role in variable sampling schemes indexed by AQL and AOQL, as higher CV values introduce greater variability, leading to batch misclassification and significantly impacting AOQL assessments. Addressing and mitigating the effects of high CV values are crucial to ensure consistent quality control outcomes, and modifications to quality control methods can improve the accuracy of AQL and AOQL assessments while optimizing inspection resources. Reducing variability not only enhances product quality but also ensures the robustness and reliability of the entire quality control process. This paper explores how CV affects variable sampling plans under AQL and AOQL, examining how measurement errors influence the performance of these plans, and provides valuable insights into designing sampling plans that maintain specific quality levels despite inherent measurement errors, which is critical for balancing quality assurance with operational efficiency in production.

Article Information

Acknowledgements: The author would like to express her sincere thanks to the editor and the anonymous reviewers for their helpful comments and suggestions.

Artificial Intelligence Statement: The author declares there is no use of Artificial Intelligence in this article.

Conflict of Interest Disclosure: The author declares no potential conflict of interest.

Plagiarism Statement: This article was scanned by the plagiarism program.

References

[1] D. C. Montgomery, *Introduction to Statistical Quality Control*, John Wiley & Sons, 8 edition, Aug. 2019.

[2] Y. Ching-Ho, A. Muhammad, C. Chia-Hao, S. R. A. Khan, A. Liaquat, J. Chi-Hyuck, *A variable sampling plan based on the coefficient of variation for lots resubmission*, Sci. Rep., **13** (2023), 1-18, Article ID 22986. http://dx.doi.org/10.1038/s41598-023-50498-2

[3] R. Sankle, J. Singh, *Single sampling plans for variables indexed by aql and aoql with measurement error*, J. Mod. Appl. Stat. Methods, **11**(2) (2012), 396-406. http://dx.doi.org/10.22237/jmasm/1351743060

[4] Y. Tong, Q. Chen, *Sampling inspection by variables for coefficient of variation*, Theor. Appl. Probab., **3** (1991), 315-327.

[5] J. Wang, H. Xiao, *A sampling test with varied coefficients as the quality indices*, The Journal of Quantitative and Technical Economics, **2001**(3) (2001), 117-119.

[6] H. Melgaard, P. Thyregod, *Acceptance sampling by variables under measurement uncertainty*, Physica-Verlag HD, **6** (2001), 47-57. http://dx.doi.org/10.1007/978-3-642-57590-7_4

[7] P. Wilrich, *Variables Sampling Under Measurement Error*, Wiley, Sept. 2014. http://dx.doi.org/10.1002/9781118445112.stat04214

[8] Y. Aijun, L. Sanyang, D. Xiaojuan, *Variables two stage sampling plans based on the coefficient of variation*, J. Adv. Mech. Des. Syst. Manuf., **10**(1) (2016), 1-12. http://dx.doi.org/10.1299/JAMDSM.2016JAMDSM0002

[9] K. Govindaraju, V. Soundararajan, *Selection of single sampling plans for variables matching the mil-std-105 scheme*, J. Qual. Technol., **18**(4) (1986), 234-238. http://dx.doi.org/10.1080/00224065.1986.11979017

[10] C.W. Wu, W. Pearn, *A variables sampling plan based on cpmk for product acceptance determination*, Eur. J. Oper. Res., **184**(2) (2008), 549-560. http://dx.doi.org/10.1016/j.ejor.2006.11.032

[11] J. R. Singh, A. Sanvalia, *Single sampling plan for variable indexed by aql and aoql with known coefficient of variation*, Int. J. Comput. Sci. Eng., **5**(10) (2017), 20-25. http://dx.doi.org/10.26438/ijcse/v5i10.2025

[12] S. W. Liu, S. W. Lin, C.W. Wu, *A resubmitted sampling scheme by variables inspection for controlling lot fraction nonconforming*, Int. J. Prod. Res., **52**(12) (2014), 3744-3754. http://dx.doi.org/10.1080/00207543.2014.886028

[13] M. H. Lee, M. B. C. Khoo, X. Chew, P. H. H. Then, *Effect of measurement errors on the performance of coefficient of variation chart with short production runs*, IEEE Access, **8** (2020), 72216-72228. http://dx.doi.org/10.1109/ACCESS.2020.2985410

[14] G. Srinivasa Rao, M. Aslam, R. A. K. Sherwani, M. A. Shehzad, C.H. Jun, *Generalized multiple dependent state sampling plans for coefficient of variation*, Commun. Stat. Theor. M., **51**(20) (2022), 6990-7005. http://dx.doi.org/10.1080/03610926.2020.1869989

[15] G. S. Rao, M. Aslam, F. S. Alamri, C.H. Jun, *Comparing the efficacy of coefficient of variation control charts using generalized multiple dependent state sampling with various run-rule control charts*, Sci. Rep., **14** (2024), 1-17, Article ID 2726. http://dx.doi.org/10.1038/s41598-024-53296-6

[16] U. Shahzad, I. Ahmad, A. V. García-Luengo, T. Zaman, N. H. Al-Noor, A. Kumar, *Estimation of coefficient of variation using calibrated estimators in double stratified random sampling*, Mathematics, **11**(1) (2023), Article ID 252, 17 pages. http://dx.doi.org/10.3390/math11010252

Communications in Advanced Mathematical Sciences
ISSN (Online) 2651-4001

Vol. 8, No. 2, 86-99, 2025
https://doi.org/10.33434/cams.1604629
Research Article

Analytic Approach to non-Newtonian Jeffery Fluid Flow in a Catheterized Curved Artery: Exploring the Impact of Heat, Mass Transfer and Magnetic Field

Gauri Sethi[1], Surendra Kumar Agarwal[1*]

Abstract
This investigation analyzes the physical properties of blood flow via a catheter in a damaged, curved artery while taking mass and heat transfer in a magnetic field. In order to get analytical answers for axial velocity, temperature, and concentration, this study models and solves the set of equations for the incompressible, non-Newtonian Jeffrey fluid under the mild stenosis approximation. The findings show that while there is less barrier to blood flow and concentration, an increase in the parameter of curvature raises shear stress of the artery wall, blood velocity, and temperature. The effect on key factors such as axial velocity, flow rate, resistance impedance, and wall shear stress of arterial geometrical variables such as stenosis, slip parameter, Hartmann number, and catheter parameter is thoroughly and quantitatively analyzed. Moreover, in trapping phenomena, the artery's curvature throws off the symmetry of the trapped bolus.

Keywords: Artery wall, Blood flow, Heat-mass transfer, Jeffery fluid, Magnetic field
2020 AMS: 34B15, 76D05, 76W05

[1] *Department of Mathematics, Inspiration Innovation Synergy University, India, gaurisethi36320@iisuniv.ac.in, surendrakumar.agarwal@iisuniv.ac.in*
*Corresponding author
Received: 20 December 2024, **Accepted:** 01 June 2025, **Available online:** 14 June 2025
How to cite this article: G. Sethi, S. K. Agarwal *Analytic approach to non-Newtonian Jeffery fluid flow in a catheterized curved artery: Exploring the impact of heat, mass transfer and magnetic field*, Commun. Adv. Math. Sci., 8(2) (2025), 86-99.

1. Introduction

These days, no general analytic approaches are accessible for the integration of the Navier-Stokes equations. Moreover, solutions are applicable to all viscosity values, although they are only known for special cases [1]. The cardiovascular system maintains blood flowing convectively through the body's many organs. A serious condition known as atherosclerosis, sometimes referred to as artery stenosis, is brought on by the blood flow's deviation from its typical state [2], [3]. A number of arterial illnesses, including myocardial infarction, artery disease, renal disease, thrombosis, high blood pressure, and strokes, can be brought on by stenosis at one or more key places [4]. When a catheter is placed inside an artery, it modifies the hemodynamic properties and flow pattern. A few theoretical and experimental works examined blood circulation in curved arteries with stenosis. Via mathematical research, Dash et al. (1999) [5] investigated the flow of fluid theory through an intravenous bend an artery stenotic. Blood is modeled as an incompressible Newtonian fluid with a laminar propagation that is supposed to be constant. In his work, the problem-solving analytical method where the resulting boundary conditions were used to solve the governing equations for the predicted model, and the analytic method yielded closed-form solutions for temperature, velocity, and slip velocity.

These days, it is generally accepted that magnetic fields can be used in physiotherapy. With the use of magnetic force, many people are being healed by regulating blood flow and temperature. This model took into account the axis-symmetric blood flow in a bending channel with aberrant growth of stenosis. The moderate stenosis situation has been used to simulate the constitutive equations for an incompressible and steady non-Newtonian tangent hyperbolic fluid. The combined outcome of variable and constant Cu-blood transportation with shape factor was investigated by Ayub et al. (2019) [6]. In this scenario, the blood flow in a bend stenotic artery with balloon is mathematically studied by gathering its behavior as a viscous fluid. Additionally, the Cu-blood medicated form in a bend artery with overlapping stenosis was examined. Using the numerical method, Zaman and Khan (2021) [7] investigated the combined effects of curvature and non-Newtonian flow on unstable nanofluid flow in a curved, overlapping stenosed link. The outcome of the study may serve as a single guideline for a pressure equation that yields a robust solution to blood flow issues. Analytical investigations pertaining to blood flow have been conducted. In the presence of a uniform magnetic field, this study investigates the irregular blood flow via a catheterized artery with overlapping stenosis while taking mass and heat transfer into account.

The comprehension and progression of vascular disorders in general depend heavily on the heat effect phenomena on blood, and the growth and development of atherogenetic processes are more strongly influenced by heat flow in conjunction with the movement of large molecules containing dissolved gases to and through the arterial wall. Research indicates that over 80 percent of deaths from heart disease are related to abnormal blood flow to and from the heart. Thin catheter tubes used in medicine that are constructed of materials of the highest caliber and have a variety of uses [8].

2016, Zaman et al. [9] investigated the unsteady flow of non-Newtonian blood through an inclined and catheterized artery with overlapping stenosis. The results reveal that both slip and inclination angle significantly affect axial velocity, flow rate, wall shear stress, and impedance. Except for wall shear stress, all parameters increase with higher slip or inclination. Hayat et al.(2007) [10] conducted a theoretical study on the peristaltic motion of a Jeffrey fluid within a circular tube, accounting for fluid compressibility and viscoelastic properties. The results reveal that backflow occurs mainly at high relaxation times and low retardation times, and the net flow oscillations in Jeffrey fluid are milder than those in Maxwell fluid.

Chakravarty and Mandal(1996) [11] developed a nonlinear two-dimensional model to study unsteady blood flow through an artery with overlapping stenosis under whole-body acceleration. The artery is modeled as an elastic tube, and blood is treated as a Newtonian fluid influenced by a pulsatile pressure gradient and arterial wall motion. Their findings highlight how body acceleration, stenosis severity, and wall elasticity affect velocity profiles and overall flow behavior during a cardiac cycle. In 2024, M. A. El Kot [12] conducts a theoretical investigation on the behavior of non-Newtonian Jeffrey fluid flowing through a curved, diseased, and catheter-inserted artery, considering the effects of heat and mass transfer. The results indicate that higher arterial curvature leads to an increase in flow velocity, wall shear stress, and temperature, while simultaneously lowering the resistance to flow and solute concentration.

The aforementioned discussions highlight the paucity of research on the mechanics of non-Newtonian blood flow and the dearth of research that considers the impact of magnetic particles, body force, and electrical force on the flow of Jeffrey fluid via a tapering artery that has stenosis in the presence of a magnetic field and wall slip condition. A mathematical model is offered here to study the combined effects of slip velocity, magnetic field, and electrical field on pertinent flow properties for non-Newtonian blood flow in a tapering stenosed artery. The governing equations of motion and energy for the nanofluid model have been determined and simplified, assuming a low Reynolds number and mild stenosis.

2. Problem Formulation

Let us assume that an incompressible non-Newtonian Jeffrey fluid is flowing in a cylindrically curved arterial portion of measure L, with a moderate cramping and radius D_o, wrapped inside a circle with a radius of D^* and centered at the origin o. Also consider another solid circular cylindrical flexible tube (catheter) with a radius of $\bar{a}(<<1)$ is inserted into the artery. $\dot{y}$ stands for an axial direction and $\dot{x}$ for a radial direction in the coordinate system. During the heat and mass transfer process, it is assumed that the artery wall experiences temperature τ_1 and concentration X_1, while the catheter surface experiences temperature τ_0 and concentration X_0, where $\tau_1 > \tau_0$ and $X_1 > X_0$.

The restricted curved region's geometric shape is taken as

$$\frac{D(z)}{D_0} = \begin{cases} 1 - \dfrac{\delta(z-s)}{3D_0 l_0^4}\left[33l_0^3 - 94(z-s)l_0^2 + 96(z-s)^2 l_0 - 32(z-s)^3\right], & \text{for } s \le z \le s + \dfrac{3l_0}{2} \\ 1, & \text{otherwise.} \end{cases}$$

The length of the conflicting stenosis is $\frac{3l_0}{2}$, where d is the position of the stenosis and D_0 is the normal blood vessel's cross sectional radius. In this case, δ represents the critical height of the stenosis, so that at $z = s + \frac{l_0}{2}$ and $z = s + l_0$, the ratio $\frac{\delta}{D_0}$ $<< 1$, appears. $\frac{3\delta}{4}$ is the stenosis thickness at a range from the origin of $z = s + \frac{3l_0}{4}$.

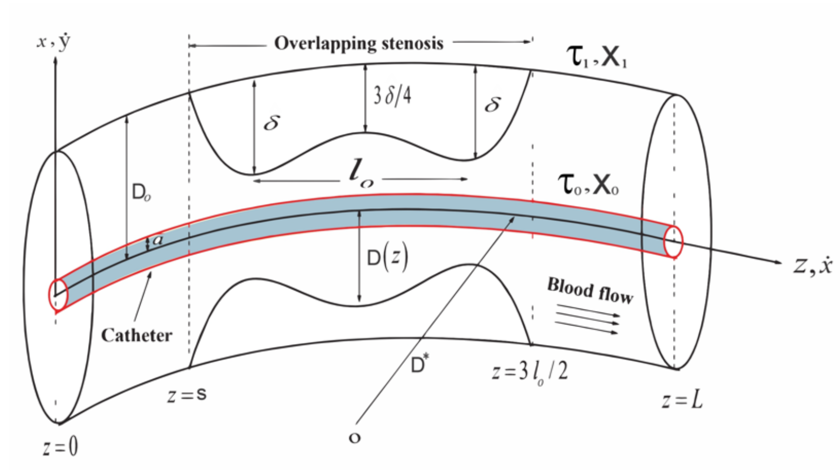

The governing equations stated here may be applied to present the problem's mathematical representation
Continuity Equation

$$\frac{1}{x}\frac{\partial}{\partial x}(x\dot{y})+\frac{\partial \dot{x}}{\partial z}=0 \tag{2.1}$$

Momentum Equation:

$$\rho\left[\frac{\partial \dot{y}}{\partial \xi}+\dot{y}\frac{\partial \dot{y}}{\partial x}+\frac{D^{*}\dot{x}}{x+D^{*}}\frac{\partial \dot{y}}{\partial z}-\frac{\dot{x}^{2}}{x+D^{*}}\right]=-\frac{\partial \Pi}{\partial x}+\frac{1}{x+D^{*}}\frac{\partial}{\partial x}\left[(x+D^{*})S_{xx}\right] +\frac{D^{*}}{x+D^{*}}\frac{\partial S_{xz}}{\partial z}-\frac{\partial S_{zz}}{\partial (x+D^{*})} \tag{2.2}$$

Momentum Equation

$$\rho\left[\frac{\partial \dot{x}}{\partial \xi}+\dot{y}\frac{\partial \dot{x}}{\partial x}+\frac{D^{*}\dot{x}}{x+D^{*}}\frac{\partial \dot{x}}{\partial z}+\frac{\dot{x}\dot{y}}{x+D^{*}}\right]=-\frac{D^{*}}{x+D^{*}}\frac{\partial \Pi}{\partial z}+\frac{1}{(x+D^{*})^{2}}\frac{\partial}{\partial x}\left[(x+D^{*})^{2}S_{xz}\right]+\frac{D^{*}}{x+D^{*}}\frac{\partial S_{zz}}{\partial z}-\sigma B_{0}^{2}\dot{x} \tag{2.3}$$

Energy Equation

$$\rho c_{p}\left[\frac{\partial \Theta}{\partial \xi}+\dot{y}\frac{\partial \Theta}{\partial x}+\frac{D^{*}\dot{x}}{x+D^{*}}\frac{\partial \Theta}{\partial z}\right]=\frac{K}{x+D^{*}}\left[\frac{\partial}{\partial x}\left((x+D^{*})\frac{\partial \Theta}{\partial x}\right)+\frac{\partial}{\partial z}\left(\frac{D^{*2}}{x+D^{*}}\frac{\partial \Theta}{\partial z}\right)\right] +\mu\left[4\left(\frac{\partial \dot{y}}{\partial x}\right)^{2}+\left(\frac{\partial \dot{x}}{\partial x}+\frac{D^{*}}{x+D^{*}}\frac{\partial \dot{y}}{\partial z}-\frac{\dot{x}}{x+D^{*}}\right)^{2}\right] \tag{2.4}$$

Concentration Equation

$$\left[\frac{\partial n}{\partial \xi}+\dot{y}\frac{\partial n}{\partial x}+\frac{D^{*}\dot{x}}{x+D^{*}}\frac{\partial n}{\partial z}\right]=\frac{M_{d}}{x+D^{*}}\left[\frac{\partial}{\partial x}\left((x+D^{*})\frac{\partial n}{\partial x}\right)+\frac{\partial}{\partial z}\left(\frac{D^{*2}}{x+D^{*}}\frac{\partial n}{\partial z}\right)\right] +\frac{M_{d}K_{\tau}}{\tau_{m}}\frac{1}{x+D^{*}}\left[\frac{\partial}{\partial x}\left((x+D^{*})\frac{\partial \Theta}{\partial x}\right)+\frac{\partial}{\partial z}\left(\frac{D^{*}}{x+D^{*}}\frac{\partial \Theta}{\partial z}\right)\right] \tag{2.5}$$

where X is the fluid concentration,τ is the temperature, K signifies the thermal conductivity, c_p is the specific heat at constant pressure, τ_m is the temperature of the medium, M_d is the coefficients of mass diffusivity, and K_τ is the thermal-diffusion ratio. where $\dot{y}$ and $\dot{x}$ are the velocity components in radial and axial directions, respectively, and Π is the fluid pressure, ρ is the fluid density, and μ is the fluid viscosity.

The constitutive equations for the Jeffery fluid are

$$S=\frac{\mu}{1+\lambda}\left(A_{1}+\lambda_{1}\frac{dA_{1}}{dt}\right),$$

where S is the additional stress tensor and The first Rivilin Ericksen tensor is $A_1 = \nabla V + (\nabla V)^T$ the transpose is indicated by T and the Jeffrey fluid parameters are λ (relaxation time) and λ_1 (retardation time).

$$\dot{y} = \dot{x} = 0, \quad \tau = \tau_0, \quad X = X_0 \quad at \quad x = a \tag{2.6}$$

$$\dot{y} = \dot{x} = 0, \quad \tau = \tau_1, \quad X = X_1 \quad at \quad x = D(z) \tag{2.7}$$

Using the following non-dimensional variable:

$$x = D_0 x', \quad z = l_0 z', \quad \dot{y} = \frac{\delta \dot{x}_0 \dot{y}'}{l_0}, \quad D = D_0 D', \quad \dot{x} = \dot{x}_0 \dot{x}', \quad \xi = \frac{l_0 \xi'}{\dot{x}_o}, \quad \Pi = \frac{\dot{x}_o l_0 \mu \Pi'}{D_0^2}, \\ \tau = \tau_0 + (\tau_1 - \tau_0)\Theta, \quad X = X_0 + (X_1 - X_0)n. \tag{2.8}$$

When the dashes are removed from the equations (2.1)-(2.5) using (2.6)-(2.8), the results are:

$$\delta^* \frac{\partial}{\partial x}\left[(x + D_c)\dot{y}\right] + D_c \frac{\partial \dot{x}}{\partial z} = 0 \tag{2.9}$$

$$\frac{\rho \dot{x}_0 D_0^3}{l_0 \mu}\left[\frac{\delta}{l_0^2}\frac{\partial \dot{y}}{\partial \xi} + \frac{\delta^2}{l_0^2 D_0}\dot{y}\frac{\partial \dot{y}}{\partial x} + \frac{\delta}{l_0^2}\frac{D_c \dot{x}}{x + D_c}\frac{\partial \dot{y}}{\partial z} - \frac{1}{D_0}\frac{\dot{x}^2}{x + D_c}\right]$$

$$= -\frac{\partial \Pi}{\partial x} + \frac{D_0^2}{\dot{x}_0 l_0}\frac{\delta}{\dot{x}_0 l_0}\frac{2}{1+\lambda}\frac{1}{x + D_c}\frac{\partial}{\partial x}\left[(x + D_c)\left(1 + \lambda_1 \frac{\dot{x}_0}{l_0}\left(\frac{\delta}{D_0}\dot{y}\frac{\partial}{\partial x} + \frac{D_c \dot{x}}{x + D_c}\frac{\partial}{\partial z}\right)\right)\left(\frac{\partial \dot{y}}{\partial x}\right)\right]$$

$$+ \frac{D_0^3}{\dot{x}_0 l_0^2}\frac{\dot{x}_0}{D_0}\frac{1}{1+\lambda}\frac{D_c}{x + D_c}\frac{\partial}{\partial z}\left[\left(1 + \lambda_1 \frac{\dot{x}_0}{l_0}\left(\frac{\delta}{D_0}\dot{y}\frac{\partial}{\partial x} + \frac{D_c \dot{x}}{x + D_c}\frac{\partial}{\partial z}\right)\right) \times \left(\frac{\partial \dot{x}}{\partial x} + \frac{\delta D_0}{l_0^2}\dot{y}\frac{D_c \dot{x}}{x + D_c}\frac{\partial \dot{y}}{\partial x} - \frac{\dot{x}}{x + D_c}\right)\right]$$

$$- \frac{D_0^2}{\dot{x}_0 l_0^2}\dot{x}_0 \frac{2}{1+\lambda}\frac{1}{x + D_c}\left[\left(1 + \lambda_1 \frac{\dot{x}_0}{l_0}\left(\frac{\delta}{D_0}v\frac{\partial}{\partial x} + \frac{D_c \dot{x}}{x + D_c}\frac{\partial}{\partial z}\right)\right) \times \left(\frac{\dot{x}_0}{l_0}\frac{D_c}{x + D_c}\frac{\partial \dot{y}}{\partial z} - \frac{\delta \dot{x}_0}{l_0 D_0}\frac{\dot{y}}{x + D_c}\right)\right]$$

$$R_e \varepsilon\left[\frac{\delta D_0}{l_0^2}\frac{\partial \dot{y}}{\partial \xi} + \delta^* \varepsilon^2\left(\dot{y}\frac{\partial \dot{y}}{\partial x} + \frac{D_c \dot{x}}{x + D_c}\frac{\partial \dot{y}}{\partial z}\right) - \frac{\dot{x}^2}{x + D_c}\right] = -\frac{\partial \Pi}{\partial x}$$

$$+ \frac{2\delta^* \varepsilon^2}{1+\lambda}\frac{1}{x + D_c}\frac{\partial}{\partial x}\left[(x + D_c)\left(1 + \lambda_1^*\left(\delta^* \dot{y}\frac{\partial}{\partial x} + \frac{D_c \dot{x}}{x + D_c}\frac{\partial}{\partial z}\right)\right)\left(\frac{\partial \dot{y}}{\partial x}\right)\right]$$

$$+ \frac{\varepsilon^2}{1+\lambda}\frac{D_c}{x + D_c}\frac{\partial}{\partial z}\left[\left(1 + \lambda_1^*\left(\delta^* \dot{y}\frac{\partial}{\partial x} + \frac{D_c \dot{x}}{x + D_c}\frac{\partial}{\partial z}\right)\right)\left(\frac{\partial \dot{x}}{\partial x} + \frac{\delta^* \varepsilon^2 D_c}{x + D_c}\frac{\partial \dot{y}}{\partial z} - \frac{\dot{x}}{x + D_c}\right)\right] \tag{2.10}$$

$$- \frac{2\varepsilon^2}{1+\lambda}\frac{1}{x + D_c}\left[\left(1 + \lambda_1^*\left(\delta^* \dot{y}\frac{\partial}{\partial x} + \frac{D_c \dot{x}}{x + D_c}\frac{\partial}{\partial z}\right)\right)\left(\frac{D_c}{x + D_c}\frac{\partial \dot{x}}{\partial z} + \frac{\delta^* \dot{y}}{x + D_c}\right)\right]$$

$$\rho \frac{\dot{x}_0 D_0^2}{l_0 \mu}\left[\frac{\partial \dot{x}}{\partial \xi} + \delta^* \dot{y}\frac{\partial \dot{x}}{\partial x} + \frac{D_c \dot{x}}{x + D_c}\frac{\partial \dot{x}}{\partial z} + \delta^* \frac{\dot{x}\dot{y}}{x + D^*}\right] = -\frac{D_c}{x + D_c}\frac{\partial \Pi}{\partial z}$$

$$+ \frac{1}{1+\lambda} \cdot \frac{1}{(x + D_c)^2}\frac{\partial}{\partial x}\left[(x + D_c)^2\left(1 + \lambda_1^*\left(\delta^* v\frac{\partial}{\partial x} + \frac{D_c \dot{x}}{x + D_c}\frac{\partial}{\partial x}\right)\right) \times \left(\frac{\partial \dot{x}}{\partial x} + \delta^* \varepsilon^2 \frac{D_c}{x + D_c}\frac{\partial \dot{y}}{\partial z} - \frac{\dot{x}}{x + D_c}\right)\right]$$

$$+ \frac{2\varepsilon^2}{1+\lambda} \cdot \frac{D_c}{x + D_c}\frac{\partial}{\partial z}\left[\left(1 + \lambda_1^*\left(\delta^* \dot{y}\frac{\partial}{\partial x} + \frac{D_c \dot{x}}{x + D_c}\frac{\partial}{\partial z}\right)\right) \times \left(\frac{D_c}{x + D_c}\frac{\partial \dot{x}}{\partial z} + \delta^* \frac{\dot{y}}{x + D_c}\right)\right] - \frac{D_0^2}{\mu}\sigma B_0^2 \dot{x}$$

$$R_e\varepsilon\left[\frac{\partial\dot{x}}{\partial\xi}+\delta^*\left(\dot{y}\frac{\partial\dot{x}}{\partial x}+\frac{\dot{x}\dot{y}}{x+D^*}\right)+\frac{D_c\dot{x}}{x+D_c}\frac{\partial\dot{x}}{\partial z}\right]=-\frac{D_c}{x+D_c}\frac{\partial\Pi}{\partial z}$$
$$+\frac{1}{1+\lambda}\cdot\frac{1}{(x+D_c)^2}\frac{\partial}{\partial x}\left[(x+D_c)^2\left(1+\lambda_1^*\left(\delta^* v\frac{\partial}{\partial x}+\frac{D_c\dot{x}}{x+D_c}\frac{\partial}{\partial x}\right)\right)\times\left(\frac{\partial\dot{x}}{\partial x}+\delta^*\varepsilon^2\frac{D_c}{x+D_c}\frac{\partial\dot{y}}{\partial z}-\frac{\dot{x}}{x+D_c}\right)\right] \tag{2.11}$$
$$+\frac{2\varepsilon^2}{1+\lambda}\cdot\frac{D_c}{x+D_c}\frac{\partial}{\partial z}\left[\left(1+\lambda_1^*\left(\delta^*\dot{y}\frac{\partial}{\partial x}+\frac{D_c\dot{x}}{x+D_c}\frac{\partial}{\partial z}\right)\right)\times\left(\frac{D_c}{x+D_c}\frac{\partial\dot{x}}{\partial z}+\delta^*\frac{\dot{y}}{x+D_c}\right)\right]-M^2\dot{x}$$

$$\frac{\rho c_p\dot{x}_0D_0^2}{Kl_0}\left[\frac{\partial\Theta}{\partial\xi}+\delta^*\dot{y}\frac{\partial\Theta}{\partial x}+\frac{D_c\dot{x}}{x+D_c}\frac{\partial\Theta}{\partial z}\right]=\frac{1}{x+D_c}\left[\frac{\partial}{\partial x}\left((x+D_c)\frac{\partial\Theta}{\partial x}\right)+\frac{D_0^2}{l_0^2}\frac{\partial}{\partial z}\left(\frac{D_c}{x+D_c}\frac{\partial\Theta}{\partial z}\right)\right]$$
$$+\frac{\mu\dot{x}_0^2}{D_0^2(\tau_1-\tau_0)}\cdot\frac{1}{K}\left[4\cdot\frac{\delta^*D_0^2}{l_0^2}\left(\frac{\partial\dot{y}}{\partial x}\right)^2+\left(\frac{\partial\dot{x}}{\partial x}+\delta^*\varepsilon^2\frac{D_c}{x+D_c}\frac{\partial\dot{y}}{\partial z}-\frac{\dot{x}}{x+D_c}\right)^2\right]$$

$$R_e\varepsilon P_r\left[\frac{\partial\Theta}{\partial\xi}+\delta^*\dot{y}\frac{\partial\Theta}{\partial x}+\frac{D_c\dot{x}}{x+D_c}\frac{\partial\Theta}{\partial z}\right]=\frac{1}{x+D_c}\left[\frac{\partial}{\partial x}\left((x+D_c)\frac{\partial\Theta}{\partial x}\right)+\varepsilon^2\frac{\partial}{\partial z}\left(\frac{D_c}{x+D_c}\frac{\partial\Theta}{\partial z}\right)\right]$$
$$+B_r\left[4\delta^*\varepsilon^2\left(\frac{\partial\dot{y}}{\partial x}\right)^2+\left(\frac{\partial\dot{x}}{\partial x}+\delta^*\varepsilon^2\frac{D_c}{x+D_c}\frac{\partial\dot{y}}{\partial z}-\frac{\dot{x}}{x+D_c}\right)^2\right] \tag{2.12}$$

$$\frac{D_0^2u_0}{l_0D}\left(\frac{\partial n}{\partial\xi}+\delta^*\dot{y}\frac{\partial n}{\partial x}+\frac{D_c\dot{x}}{x+D_c}\frac{\partial n}{\partial z}\right)=\frac{1}{x+D_c}\left[\frac{\partial}{\partial x}\left((x+D_c)\frac{\partial n}{\partial x}\right)+\varepsilon^2\frac{\partial}{\partial z}\left(\frac{D_c^2}{x+D_c}\frac{\partial n}{\partial z}\right)\right]$$
$$+\frac{K_\tau(\tau_1-\tau_0)}{\tau_m(X_1-X_0)}\cdot\frac{1}{x+D_c}\left[\frac{\partial}{\partial x}\left((x+D_c)\frac{\partial\Theta}{\partial x}\right)+\varepsilon^2\frac{\partial}{\partial z}\left(\frac{D_c^2}{x+D_c}\frac{\partial\Theta}{\partial z}\right)\right]$$

$$R_e\varepsilon S_c\left[\frac{\partial n}{\partial\xi}+\delta^*\dot{y}\frac{\partial n}{\partial x}+\frac{D_c\dot{x}}{x+D_c}\frac{\partial n}{\partial z}\right]=\frac{1}{x+D_c}\left[\frac{\partial}{\partial x}\left((x+D_c)\frac{\partial n}{\partial x}\right)+\varepsilon^2\frac{\partial}{\partial z}\left(\frac{D_c^2}{x+D_c}\frac{\partial n}{\partial z}\right)\right]$$
$$+\frac{S_rS_c}{x+D_c}\left[\frac{\partial}{\partial x}\left((x+D_c)\frac{\partial\Theta}{\partial x}\right)+\varepsilon^2\frac{\partial}{\partial z}\left(\frac{D_c^2}{x+D_c}\frac{\partial\Theta}{\partial z}\right)\right] \tag{2.13}$$

where $P_r=\frac{c_p\mu}{K}$ is Prandtl number $R_e=\frac{\rho\dot{x}_0D_0}{\mu}$ is Reynolds number, $E_c=\frac{\dot{x}_0^2}{c_p(\tau_1-\tau_0)}$ is Eckert number, $D_c=\frac{D^*}{D_0}$ is the curvature parameter, $S_r=\frac{\rho DK_\tau(\tau_1-\tau_0)}{\mu(X_1-X_0)\tau_m}$ is Soret number, $B_r=P_rE_c$ is Brickmann number, $S_c=\frac{\mu}{D\rho}$ is Schmidt number, $M=B_0D_0(\frac{\sigma}{\mu})^{\frac{1}{2}}$ is Hartmann number, where B_0 is the external constant magnetic field in the radial direction, $\lambda^*=\frac{\lambda_1\dot{x}_0}{l_0}$. Now, we make the equations simpler for low grade by deducing the two requirements, stenosis $\delta^*=\frac{\delta}{D_0}<<1$ and $\varepsilon=\frac{D_0}{l_0}\approx o(1)$. For a low Reynolds number flow, in the annulus with mild stenosis, the radial velocity is negligibly tiny and can be disregarded. With these assumptions, equations (2.9)-(2.13) become

$$\frac{\partial\dot{x}}{\partial z}=0 \tag{2.14}$$

$$\frac{\partial\Pi}{\partial x}=0 \tag{2.15}$$

$$D_c(1+\lambda)(x+D_c)\frac{\partial\Pi}{\partial z}=(x+D_c)^2\frac{\partial^2\dot{x}}{\partial x^2}+(x+D_c)\frac{\partial\dot{x}}{\partial x}-M^2\dot{x} \tag{2.16}$$

$$\frac{\partial}{\partial r}\left((x+D_c)\frac{\partial \Theta}{\partial r}\right) = -B_r\left(\frac{\partial \dot{x}}{\partial r} - \frac{\dot{x}}{x+D_c}\right)^2 \tag{2.17}$$

$$\frac{\partial}{\partial x}\left((x+D_c)\frac{\partial n}{\partial x}\right) = -S_r S_c \frac{\partial}{\partial r}\left((x+D_c)\frac{\partial \Theta}{\partial x}\right). \tag{2.18}$$

The boundary conditions are

$$\dot{x} = 0, \quad \Theta = 0, \quad n = 0 \quad on \quad x = \varepsilon, \tag{2.19}$$

$$\dot{x} = 0, \quad \Theta = 1, \quad n = 1 \quad on \quad x = D(z). \tag{2.20}$$

$$D(z) = \begin{cases} 1 + \dfrac{\delta^*(z-s^*)}{3}\left[32(z-s^*)^3 - 96(z-s^*)^2 + 94(z-s^*) - 33\right], & s^* \le z \le s^* + \dfrac{3}{2} \\ 1, & \text{otherwise} \end{cases}$$

where $s^* = \dfrac{s}{l_0}, \quad \varepsilon = \dfrac{\bar{a}}{D_0}$.

Applying the boundary conditions (2.19)-(2.20) for the expressions of axial velocity, temperature, and concentration (2.14)-(2.18) to get

$$\dot{x} = F_1(x+D_c)^M + F_2(x+D_c)^{-M} + \frac{1}{1-M^2}\left\{D_c(1+\lambda)(x+D_c)\frac{d\Pi}{dz}\right\} \tag{2.21}$$

$$\Theta = -B_r\left[\frac{(M-1)^2}{(2M-1)^2}F_1^2(x+D_c)^{2M-1} + \frac{(M+1)^2}{(3-2M)^2}F_2^2(x+D_c)^{3-2M} - 2(M^2-1)F_1F_2(x+D_c)^{-1}\right]$$

$$n = -B_r S_r S_c\left[\frac{(M-1)^2}{(2M-1)^2}F_1^2(x+D_c)^{2M-1} + \frac{(M+1)^2}{(3-2M)^2}F_2^2(x+D_c)^{3-2M} - 2(M^2-1)F_1F_2(x+D_c)^{-1}\right]$$

where the functions $F_1(z), F_2(z)$are given by

$$F_1 = \frac{(D+D_c)^M(\varepsilon+D_c)^M}{(\varepsilon+D_c)^{2M} - (D+D_c)^{2M}}\left[\frac{1}{1-M^2}\left\{D_c(1+\lambda)\frac{d\Pi}{dz}\left((\varepsilon+D_c)(D+D_c)^M - (\varepsilon+D_c)^M(D+D_c)\right)\right\}\right]$$

$$F_2 = \frac{(\varepsilon+D_c)^M(D+D_c)^M}{(D+D_c)^{2M} - (\varepsilon+D_c)^{2M}}\left[\frac{1}{1-M^2}\left\{D_c(1+\lambda)\frac{d\Pi}{dz}\left((\varepsilon+D_c)^M(D+D_c) - (\varepsilon+D_c)(D+D_c)^M\right)\right\}\right].$$

Here, the wall shear stress distribution can be expressed using equation (2.21)

$$W_s = \left[F_1M(x+D_c)^{M-1} - F_2M(x+D_c)^{-M-1} + \frac{1}{1-M^2}\left\{D_c(1+\lambda)\frac{d\Pi}{dz}\right\} - \frac{F_1(x+D_c)^M + F_2(x+D_c)^{-M} + \frac{1}{1-M^2}\left\{D_c(1+\lambda)(x+D_c)\frac{d\Pi}{dz}\right\}}{x+D_c}\right].$$

The stream function is

$$\psi = -\left[\frac{F_1}{M+1}\left((x+D_c)^{M+1}+(\varepsilon+D_c)^{M+1}\right)+\frac{F_2}{1-M}\left((x+D_c)^{1-M}+(\varepsilon+D_c)^{1-M}\right)\right.$$
$$\left.+\frac{1}{1-M^2}\left\{D_c(1+\lambda)\frac{d\Pi}{dz}\left(\frac{(x+D_c)^2}{2}+\frac{(\varepsilon+D_c)^2}{2}\right)\right\}\right].$$

The fluid flow rate is

$$V=\int_{\varepsilon}^{D}\dot{x}\,dx$$

$$V=\frac{F_1}{M+1}\left[(D+D_c)^{M+1}-(\varepsilon+D_c)^{M+1}\right]+\frac{F_2}{1-M}\left[(D+D_c)^{1-M}-(\varepsilon+D_c)^{1-M}\right]$$
$$+\frac{1}{1-M^2}\left\{D_c(1+\lambda)\frac{d\Pi}{dz}\left(\frac{(D+D_c)^2}{2}-\frac{(\varepsilon+D_c)^2}{2}\right)\right\}.$$

The arterial pressure drop is given in the form of

$$\Delta\Pi=\int_0^{L^*}\left(-\frac{d\Pi}{dz}\right)dz.$$

The resistance impedance expression

$$\Lambda=\frac{\Delta\Pi}{V}$$

$$\Lambda=\frac{2(1-M)^2}{D_c(1+\lambda)V\left[(D+D_c)^2-(\varepsilon+D_c)^2\right]}\left[\frac{V-F_1}{M+1}\left((D+D_c)^{M+1}-(\varepsilon+D_c)^{M+1}\right)-\frac{F_2}{1-M}\left((D+D_c)^{1-M}-(\varepsilon+D_c)^{1-M}\right)\right]L^*$$

where $L^*=\dfrac{L}{l_0}$.

3. Results

This section shows the graphical outcomes for the different parameter, so here we study the many characteristics of blood flow across overlapping stenosed arteries with heat, mass transport, and magnetic field by charting the figures of axial velocity $\dot{x}$, wall shear stress W_s, flow rate V, impedance resistance Λ, temperature profile Θ and concentration n. Various graphs are drawn for the different possible values of the parameters like - height of the stenosis, Hartmann number, Brickmann number, Soret number, and Schmidt number, etc.

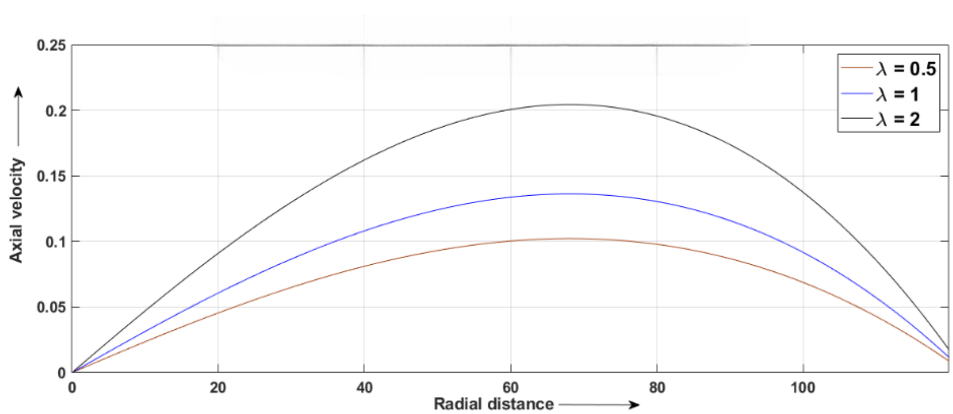

Figure 3.1. Axial velocity with different Jeffery parameter

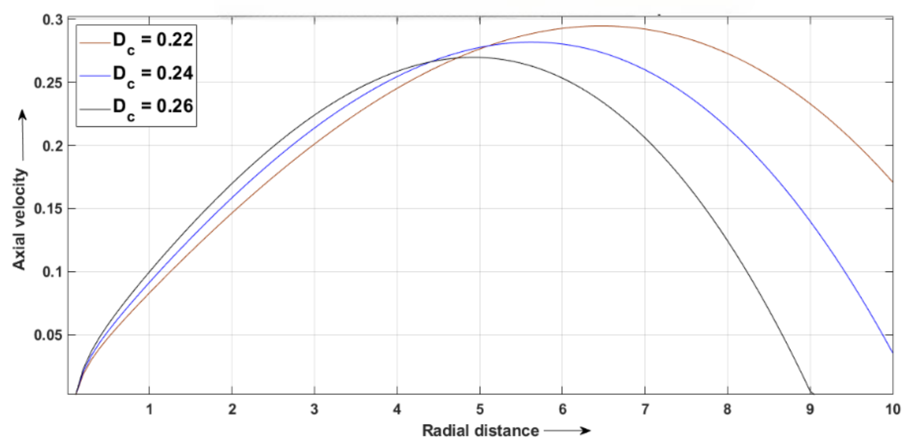

Figure 3.2. Axial velocity for different values of curvature parameter

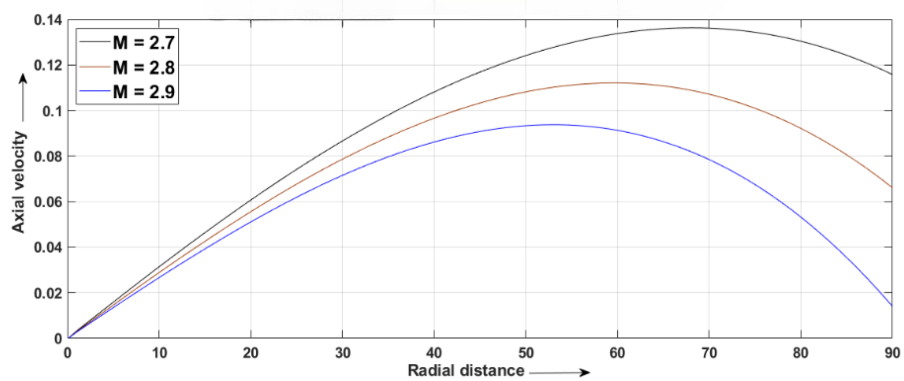

Figure 3.3. Axial velocity for different values of Hartmann number

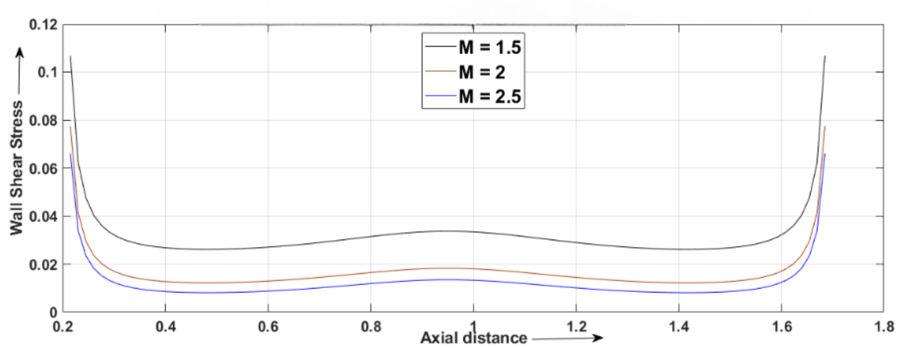

Figure 3.4. Wall shear stress distribution for different values of Hartmann number

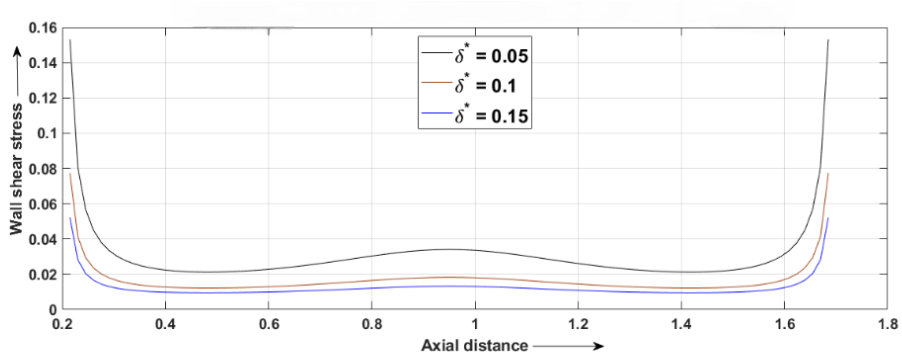

Figure 3.5. Wall shear stress distribution for different values of critical height

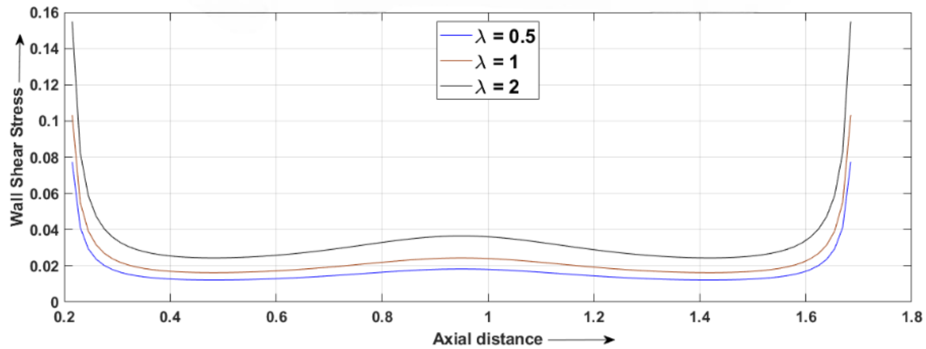

Figure 3.6. Wall shear stress distribution for different Jeffery parameters

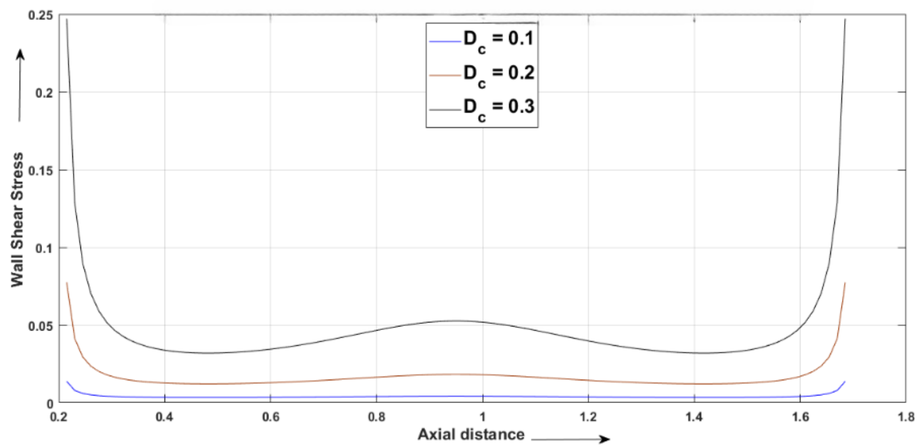

Figure 3.7. Wall shear stress distribution for different values of curvature parameter

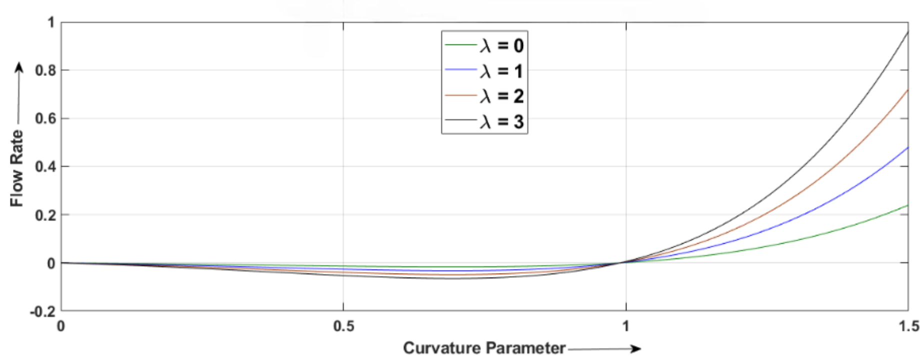

Figure 3.8. Flow rate for different Jeffery parameters

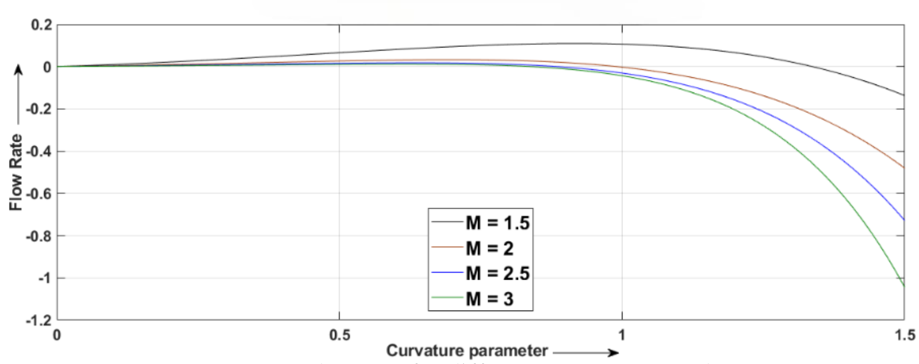

Figure 3.9. Flow rate for different Hartmann numbers

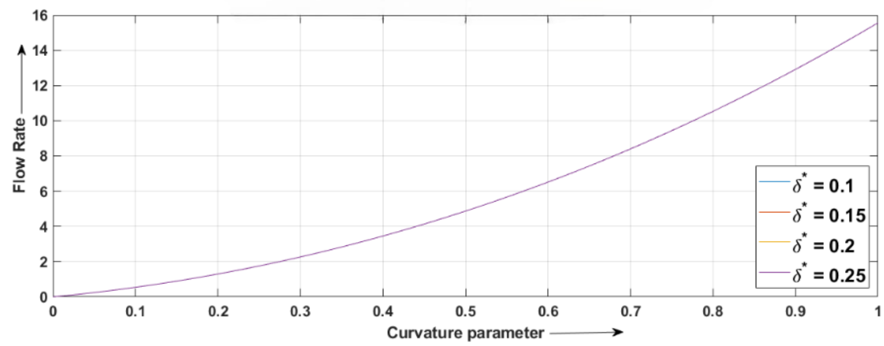

Figure 3.10. Flow rate for different values of critical height

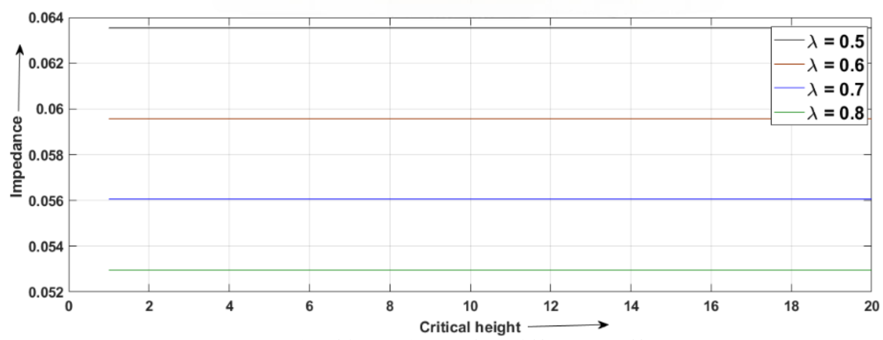

Figure 3.11. Graph of impedance for different Jeffery parameters

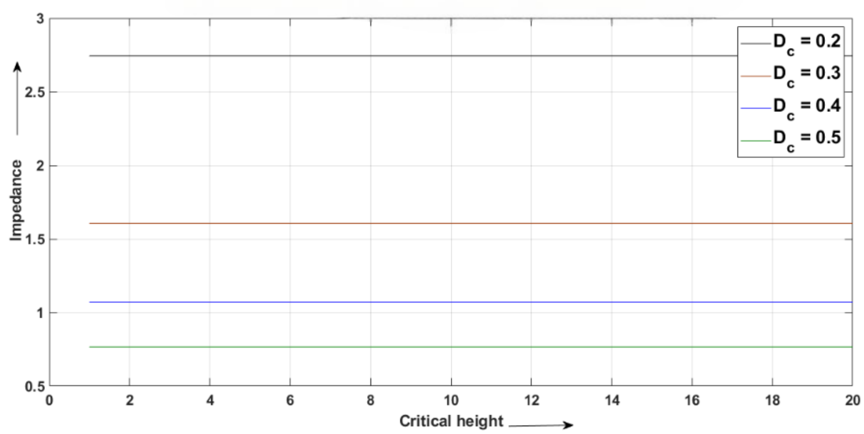

Figure 3.12. Graph of impedance for different values of curvature parameter

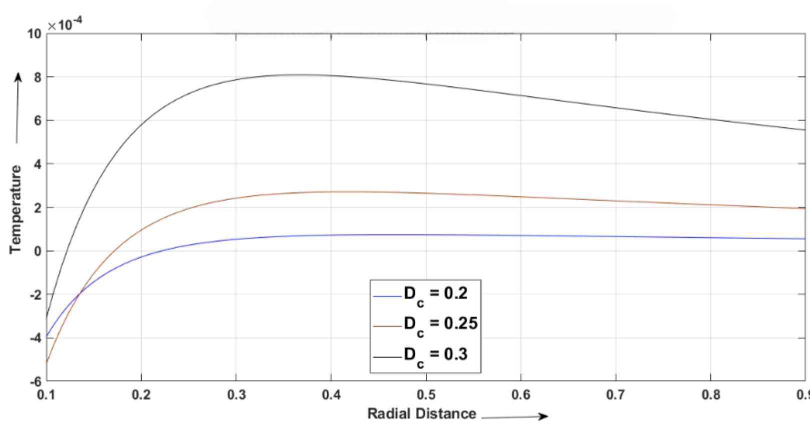

Figure 3.13. Temperature for different curvature parameters

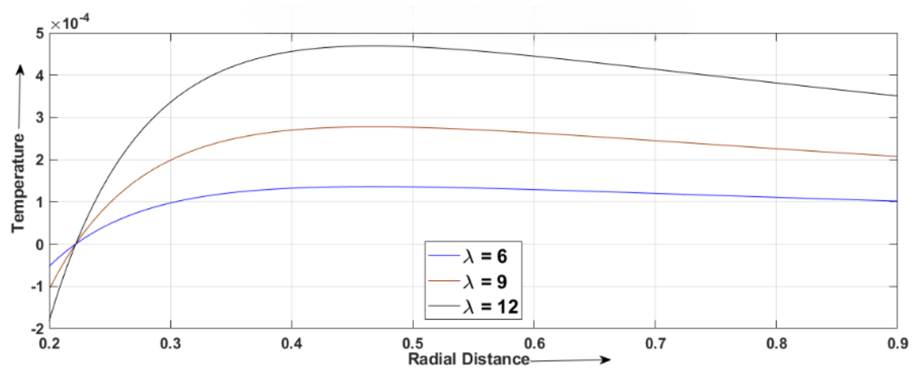

Figure 3.14. Temperature for different Jeffery parameters

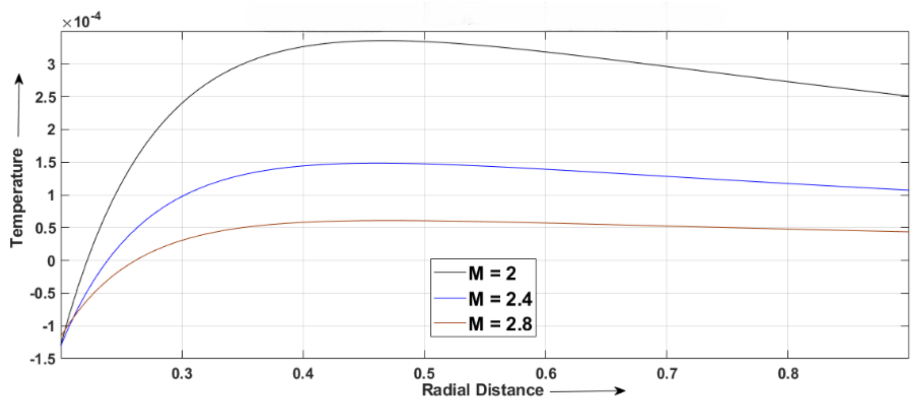

Figure 3.15. Temperature for different Hartmann numbers

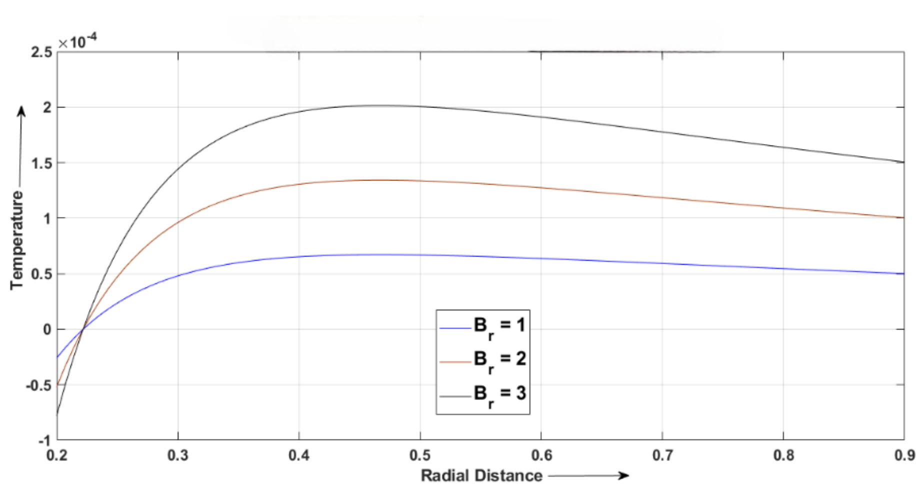

Figure 3.16. Temperature for different Brickmann numbers

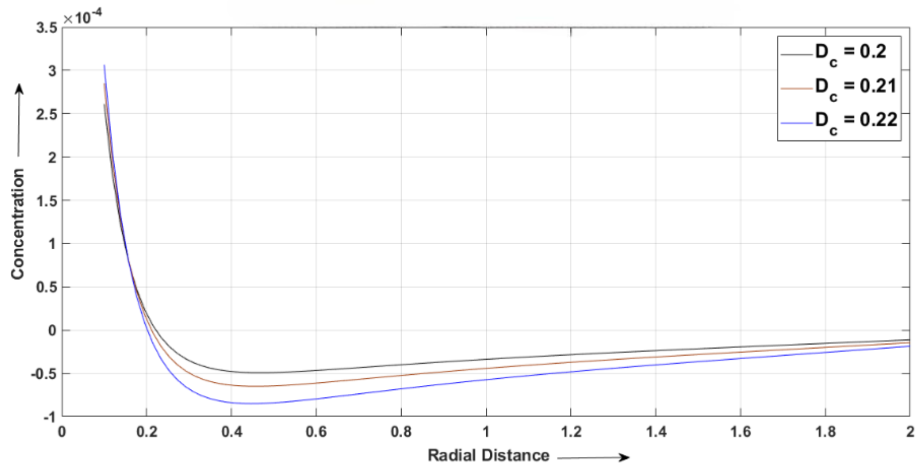

Figure 3.17. Concentration for different curvature parameters

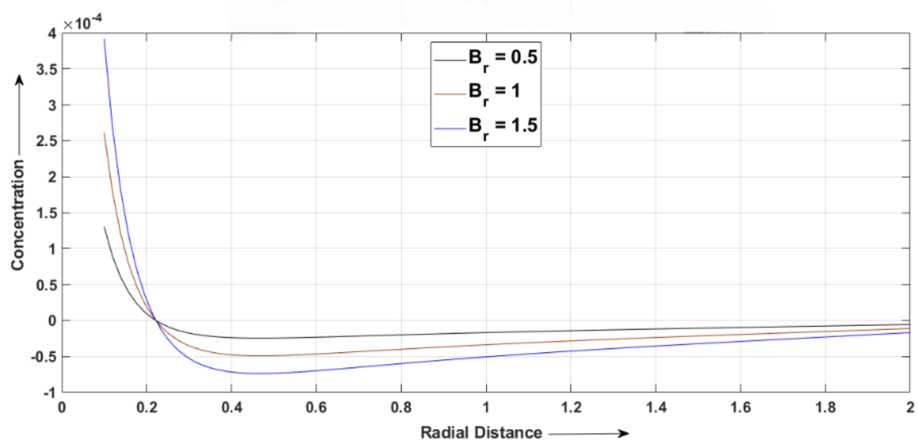

Figure 3.18. Concentration for different Brickmann number

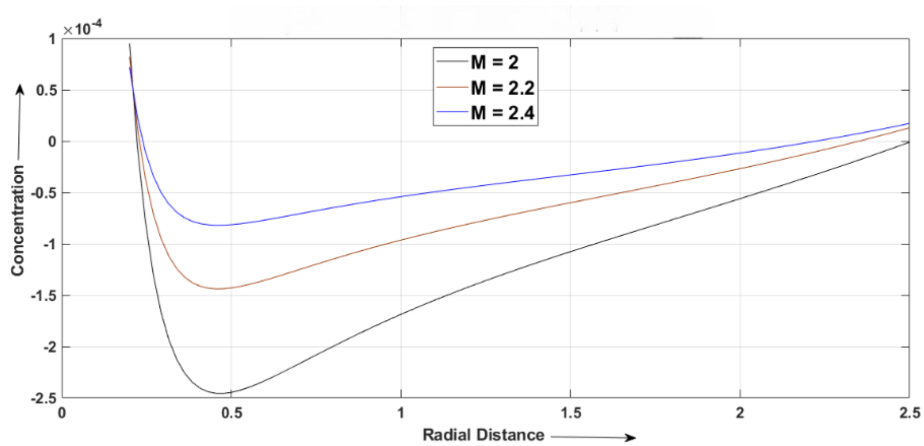

Figure 3.19. Concentration for different Hartmann numbers

We have generated figures to illustrate the effects of the Jeffrey parameter, curvature parameter, and Hartmann number on axial velocity. The results indicate that an increase in both the curvature and Jeffrey parameters leads to an enhancement in axial velocity. This rise in axial velocity suggests that higher viscoelasticity contributes positively to blood flow, potentially reducing the risk of thrombosis. Conversely, an increase in the Hartmann number results in a decrease in axial velocity, implying that the applied magnetic field impedes blood flow.

The plotted figures also depict the distribution of wall shear stress in the region of a bent stenosed artery. It is observed that wall shear stress increases with rising values of the Jeffrey and curvature parameters. However, an inverse relationship is noted with the Hartmann number, and critical height both contribute to a reduction in wall shear stress.

Regarding flow rate, variations with the curvature parameter for different values of critical height, Hartmann number, and Jeffrey parameter reveal that flow rate increases with higher Jeffrey parameter and critical height. In contrast, an increase in the Hartmann number leads to a decline in flow rate. Since an adequate flow rate helps prevent blood pooling, this finding highlights the significance of parameter tuning in maintaining healthy circulation.

The figures also demonstrate how impedance varies in this context. Impedance is found to decrease with increasing curvature parameter but increases with a higher Jeffrey parameter.

Temperature distribution with respect to radial distance is also analyzed for various values of the curvature parameter, Jeffrey parameter, Hartmann number, and Brinkman number. The results show that temperature increases with higher curvature parameter, Jeffrey parameter, and Brinkman number, whereas an increase in the Hartmann number leads to a decrease in temperature.

Finally, concentration profiles are shown for varying values of the Hartmann number, Brinkman number, and curvature parameter. The concentration decreases with increases in the curvature parameter and Brinkman number, while a higher Hartmann number corresponds to an increase in concentration.

4. Conclusion

Jeffrey fluid is a type of non-Newtonian fluid that is significantly used in certain applications as it involves viscous and elastic behaviors, contrary to the Newtonian model, this model considers the relaxation and retardation times, therefore the fluid has a slow response to changes. Thus, Jeffery's model examines the mass and heat transfer in blood flow that is catalyzed by a magnetic field. The trapping phenomenon occurs when an accumulation of blood is caught inside a closed loop of flow, moving along with the main blood, but staying separate. We talk about how different parameters affect temperature, concentration, flow rate, wall shear stress, axial velocity, and resistance to flow.

The main observations are as follows.

1. As a result of the successive increase in Jeffery parameter the axial velocity, wall shear stress, flow rate, and temperature increase.
2. The values of axial velocity, temperature, and wall shear stress increase with increasing curvature parameter, while the inverse effect is observed in concentration.
3. The increase in magnetic field parameter, i.e., Hartmann number, escalates the concentration, whereas flow rate, wall shear stress, axial velocity, and temperature decline.
4. As the critical height increases, both the flow rate and the shear stress decrease.
5. As the Brickmann number increases, the flow rate increases, while the concentration reduces.

5. Article Information

Acknowledgements: The authors express their sincere thanks to the editor and the anonymous reviewers for their helpful comments and suggestions.

Author's Contributions: **G.S.**: Methodology, investigations, software implementation, visualization, and writing. **S. K. A.**: Conceptualization, formal analysis, original draft preparation, validation, review, and editing. All authors read and approved the final manuscript.

Artificial Intelligence Statement: Artificial intelligence techniques were employed in this study to assist in specific tasks, e.g., language correction, some forgotten commands used in Latex.

Conflict of Interest Disclosure: The authors declare that there is no conflict of interest.

Plagiarism Statement: This article was scanned by the plagiarism program.

References

[1] H. Schlichting, *Boundary Layer Theory*, McGraw Hill Education Indian Edition 2014, ISBN-13:978-93-329-0282-4, 7th Edition.

[2] S. Chakravarty, *Effect of stenosis on the flow behavior of blood in an artery,* Int. J. Eng. Sci., **25**(8) (1987), 1003-1016. https://doi.org/10.1016/0020-7225(87)90093-0

[3] M. S. Shabbir, N. Ali, Z. Abbas, *Unsteady blood flow of non-Newtonian fluid through a rigid artery in the presence of multi-irregular stenoses*. J. Braz. Soc. Mech. Sci. Eng., **40** (2018), Article ID 413. https://doi.org/10.1007/s40430-018-1327-x

[4] R. Padma, P. Ponalagusamy, R. T. Selvi, *Mathematical modeling of electro hydrodynamic non-Newtonian fluid flow through tapered arterial stenosis with periodic body acceleration and applied magnetic field*, Appl. Math. Comput., **362** (2019), Article ID 124453. https://doi.org/10.1016/j.amc.2019.05.024

[5] R. K. Dash, G. Jayaraman, K. N. Mehta, *Flow in a catheterized curved artery with stenosis*, J. Biomech., **32**(1) (1999), 49-61. https://doi.org/10.1016/S0021-9290(98)00142-0

[6] M. Ayub, I. Shahzadi, S. Nadeem, *A ballon model analysis with Cu-blood medicated nanoparticles as drug agent through overlapped curved stenotic artery having compliant walls*, Microsyst. Technol., **25** (2019), 2949-2962. https://doi.org/10.1007/s00542-018-4263-x

[7] A. Zaman, A. A. Khan, *Time dependent non-Newtonian nano-fluid (blood) flow in w-shape stenosed channel; with curvature effects*, Math. Comput. Simul., **181** (2021), 82-97. https://doi.org/10.1016/j.matcom.2020.09.017

[8] A. Ahmed, S. Nadeem, *Shape effect of Cu-nanoparticles in unsteady flow through curved artery with catheterized stenosis*, Results Phys., **7** (2017), 677-689. https://doi.org/10.1016/j.rinp.2017.01.015

[9] A. Zaman, N. Ali, M. Sajid, *Slip effects on unsteady non-Newtonian blood flow through an inclined catheterized overlapping stenotic artery*, AIP Adv., **6**(1) (2016), Article ID 015118. https://doi.org/10.1063/1.4941358

[10] T. Hayat, N. Ali, S. Asghar, *An analysis of peristaltic transport for flow of a Jeffrey fluid*, Acta Mech., **193** (2007), 101-112. https://doi.org/10.1007/s00707-007-0468-2

[11] S. Chakravarty, P. K. Mandal, *A Nonlinear two-dimensional model of blood flow in an overlapping arterial stenosis subjected to body acceleration*, Math. Comput. Model., **24**(1) (1996), 43-58. https://doi.org/10.1016/0895-7177(96)00079-9

[12] M. A. El Kot, *Theoretical simulation of blood flow for non-Newtonian Fluid through diseased catheterized curved artery with heat and mass transfer*, (2024), 12 pages. https://doi.org/10.22541/au.170665633.35943336/v1

Communications in Advanced Mathematical Sciences
ISSN (Online) 2651-4001

Vol. 8, No. 2, 100-116, 2025
https://doi.org/10.33434/cams.1673361
Research Article

General Two- and Three-Dimensional Integral Inequalities Based a Change of Variables Methodology

Christophe Chesneau

Abstract
This article establishes new general two- and three-dimensional integral inequalities. The first result involves four functions: two main functions defined on the positive real line and two auxiliary functions defined on the unit interval. As a significant contribution, the upper bound obtained is quite simple; it is expressed only as the product of the unweighted integral norms of these functions. The main ingredient of the proof is an original change of variables methodology. The article also presents a three-dimensional extension of this result. This higher-dimensional version uses a similar structure but with nine functions: three main functions defined on the positive real line and six auxiliary functions defined on the unit interval. It retains the simplicity and sharpness of the upper bound. Both results open up new directions for applications in analysis. This claim is supported by various examples, including some based on power, logarithmic, trigonometric, and exponential functions, as well as some secondary but still general integral inequalities.

Keywords: Change of variables, Gamma function, Hardy-Hilbert-type integral inequalities, Three-dimensional integral inequalities, Two-dimensional integral inequalities
2020 AMS: 26D15, 33E20

Department of Mathematics, LMNO, University of Caen-Normandie, 14032 Caen, France, christophe.chesneau@gmail.com
Received: 10 April 2025, **Accepted:** 27 June 2025, **Available online:** 28 June 2025
How to cite this article: C. Chesneau, *General two- and three-dimensional integral inequalities based a change of variables methodology*, Commun. Adv. Math. Sci., 8(2) (2025), 100-116.

1. Introduction

Multi-dimensional integral inequalities, especially those in two and three dimensions, are fundamental tools in mathematical analysis. In particular, they are essential for understanding the behavior of integral operators and for estimating their bounds. See [1–4]. Among the classical results in two dimensions, the Hardy-Hilbert integral inequality occupies a prominent place. A precise statement is given below. Let $p > 1$, $q = p/(p-1)$ satisfying the Hölder condition $1/p + 1/q = 1$, and $f, g : (0,+\infty) \mapsto (0,+\infty)$ be two functions; they are thus defined on the positive real line, i.e., $(0,+\infty)$, and are positive. Then the Hardy-Hilbert integral inequality states that

$$\int_0^{+\infty}\int_0^{+\infty} \frac{1}{x+y} f(x)g(y)dxdy \leq \frac{\pi}{\sin(\pi/p)} \left[\int_0^{+\infty} f^p(x)dx\right]^{1/p} \left[\int_0^{+\infty} g^q(y)dy\right]^{1/q}, \tag{1.1}$$

provided that the integrals involved converge, i.e., $\int_0^{+\infty} f^p(x)dx < +\infty$ and $\int_0^{+\infty} g^q(y)dy < +\infty$. This result features a sharp constant factor, i.e., $\pi/\sin(\pi/p)$, and the product of two unweighted integral norms of f and g with parameters p and q, respectively. For the basic details, see the classic work by G.H. Hardy in [1]. Over the years, this inequality has inspired extensive research, including numerous extensions and generalizations in higher dimensions. Notable contributions to the development of such extensions include [5–9]. Further generalizations in higher dimensions have been explored in works such as [10–14].

Despite this extensive literature, the derivation of sharp and tractable upper bounds for multidimensional integral inequalities, particularly in two and three dimensions, remains a significant challenge. Many existing results involve sophisticated constants or rely on restrictive assumptions that limit their scope. This motivates the search for new inequalities that offer both structural clarity and wide applicability.

The first inequality established in this article addresses part of this challenge. It gives a sharp and simple upper bound for a two-dimensional integral involving four functions: two main functions defined on $(0,+\infty)$ and two auxiliary functions defined on the unit interval, i.e., $(0,1)$. In a similar framework to that of the Hardy-Hilbert integral inequality, this integral is

$$\int_0^{+\infty}\int_0^{+\infty}\frac{x^{1/p}y^{1/q}}{(x+y)^2}\ell\left(\frac{x}{x+y}\right)m\left(\frac{y}{x+y}\right)f(x)g(y)dxdy,$$

where ℓ and m are the auxiliary functions. The upper bound obtained is quite manageable. It depends only on the unweighted integral norms of f, g, ℓ, and m. Explicitly, it is given by

$$\left[\int_0^1 \ell^p(t)dt\right]^{1/p}\left[\int_0^1 m^q(t)dt\right]^{1/q}\left[\int_0^{+\infty} f^p(x)dx\right]^{1/p}\left[\int_0^{+\infty} g^q(y)dy\right]^{1/q},$$

with a constant factor exactly equal to one. The proof strategy differs from the traditional approaches used in the study of Hardy-Hilbert-type inequalities. It is based on an appropriate factorization of the integrand, the Hölder integral inequality, and a special change of variables that transforms the expression into a simpler form. This change of variables methodology is the main originality of the proof.

In addition to the two-dimensional result, the article introduces a natural extension to three dimensions. This generalized inequality involves a three-dimensional integral that depends on nine functions: three main functions defined on $(0,+\infty)$ and six auxiliary functions defined on $(0,1)$. It has the following general form:

$$\int_0^{+\infty}\int_0^{+\infty}\int_0^{+\infty}\frac{1}{(x+y+z)^2}\left(\frac{x}{x+y}\right)^{1/p}\left(\frac{y}{y+z}\right)^{1/q}\left(\frac{z}{x+z}\right)^{1/r}$$

$$\times\, i\left(\frac{x}{x+y}\right)j\left(\frac{y}{y+z}\right)k\left(\frac{z}{x+z}\right)\ell\left(\frac{x+y}{x+y+z}\right)m\left(\frac{y+z}{x+y+z}\right)n\left(\frac{x+z}{x+y+z}\right)f(x)g(y)h(z)dxdydz,$$

where i, j, k, ℓ, m and n are the auxiliary functions, and r is an additional norm parameter. This extended version retains the simplicity of the two-dimensional case, still with a tractable upper bound depending only on the unweighted integral norms of the functions involved. Explicitly, it is given by

$$\left[\int_0^1 i^p(t)dt\right]^{1/p}\left[\int_0^1 \ell^p(t)dt\right]^{1/p}\left[\int_0^1 j^q(t)dt\right]^{1/q}\left[\int_0^1 m^q(t)dt\right]^{1/q}$$

$$\times\left[\int_0^1 k^r(t)dt\right]^{1/r}\left[\int_0^1 n^r(t)dt\right]^{1/r}\left[\int_0^{+\infty} f^p(x)dx\right]^{1/p}\left[\int_0^{+\infty} g^q(y)dy\right]^{1/q}\left[\int_0^{+\infty} h^r(z)dz\right]^{1/r}.$$

The proof strategy is based on a suitable factorization of the integrand, the generalized Hölder integral inequality (see [15, 16]), and an adapted change of variables that transforms the expression into a simpler form. Again, this change of variables methodology remains the main originality of the proof. The structure of the inequality allows considerable flexibility in the choice of auxiliary functions, providing a unified framework for bounding a large class of complex three-dimensional integrals.

To illustrate the scope and applicability of the results, several concrete examples are given. These include functions of the power, logarithmic, trigonometric, and exponential types. Other new secondary general inequalities are also derived. These highlight the versatility of the proposed inequalities and demonstrate their potential for further applications in analysis.

The rest of the article is as follows: Section 2 is devoted to our main two-dimensional integral result with examples and secondary results. A natural extension to three dimensions is studied in Section 3, again illustrated with examples. Section 4 concludes the article.

2. Two-Dimensional Integral Inequality Results

2.1 Main result

The theorem below gives our general two-dimensional integral inequality result. It is followed by the detailed proof and some discussion.

Theorem 2.1. *Let $p > 1$, $q = p/(p-1)$, and $f, g : (0,+\infty) \mapsto (0,+\infty)$ and $\ell, m : (0,1) \mapsto (0,+\infty)$ be four functions. Then, we have*

$$\int_0^{+\infty}\int_0^{+\infty} \frac{x^{1/p}y^{1/q}}{(x+y)^2}\ell\left(\frac{x}{x+y}\right)m\left(\frac{y}{x+y}\right)f(x)g(y)dxdy \le \Upsilon\left[\int_0^{+\infty} f^p(x)dx\right]^{1/p}\left[\int_0^{+\infty} g^q(y)dy\right]^{1/q},$$

where

$$\Upsilon = \left[\int_0^1 \ell^p(t)dt\right]^{1/p}\left[\int_0^1 m^q(t)dt\right]^{1/q}, \tag{2.1}$$

provided that the integrals involved converge.

Proof. By a well-chosen decomposition of the integrand as the product of two main terms using $1/p+1/q = 1$ and the Hölder integral inequality applied to those terms at the parameters p and $q = p/(p-1)$, we get

$$\begin{aligned}
&\int_0^{+\infty}\int_0^{+\infty} \frac{x^{1/p}y^{1/q}}{(x+y)^2}\ell\left(\frac{x}{x+y}\right)m\left(\frac{y}{x+y}\right)f(x)g(y)dxdy \\
&= \int_0^{+\infty}\int_0^{+\infty} \frac{x^{1/p}}{(x+y)^{2/p}}\ell\left(\frac{x}{x+y}\right)f(x) \times \frac{y^{1/q}}{(x+y)^{2/q}}m\left(\frac{y}{x+y}\right)g(y)dxdy \\
&\le A^{1/p}B^{1/q},
\end{aligned} \tag{2.2}$$

where

$$A = \int_0^{+\infty}\int_0^{+\infty} \frac{x}{(x+y)^2}\ell^p\left(\frac{x}{x+y}\right)f^p(x)dxdy$$

and

$$B = \int_0^{+\infty}\int_0^{+\infty} \frac{y}{(x+y)^2}m^q\left(\frac{y}{x+y}\right)g^q(y)dxdy.$$

We can now find the exact expressions for A and B, starting with A. Using the Fubini-Tonelli integral theorem to permutate the two integral signs and changing the variables as $u = x/(x+y)$, so $du = [-x/(x+y)^2]dy$, $y = 0 \Rightarrow u = 1$ and $y \to +\infty \Rightarrow u = 0$, we obtain

$$\begin{aligned}
A &= \int_0^{+\infty} f^p(x)\left[\int_0^{+\infty} \frac{x}{(x+y)^2}\ell^p\left(\frac{x}{x+y}\right)dy\right]dx = \int_0^{+\infty} f^p(x)\left[\int_0^1 \ell^p(u)du\right]dx \\
&= \left[\int_0^1 \ell^p(t)dt\right]\left[\int_0^{+\infty} f^p(x)dx\right].
\end{aligned} \tag{2.3}$$

In a similar way, but with the change of variables $v = y/(x+y)$ with $dv = [-y/(x+y)^2]dx$, $x = 0 \Rightarrow v = 1$ and $x \to +\infty \Rightarrow v = 0$, we get

$$\begin{aligned}
B &= \int_0^{+\infty} g^q(y)\left[\int_0^{+\infty} \frac{y}{(x+y)^2}m^q\left(\frac{y}{x+y}\right)dx\right]dy = \int_0^{+\infty} g^q(y)\left[\int_0^1 m^q(v)dv\right]dy \\
&= \left[\int_0^1 m^q(t)dt\right]\left[\int_0^{+\infty} g^q(y)dy\right].
\end{aligned} \tag{2.4}$$

Combining Equations (2.2), (2.3) and (2.4), and using $1/p+1/q=1$, we get

$$\int_0^{+\infty}\int_0^{+\infty}\frac{x^{1/p}y^{1/q}}{(x+y)^2}\ell\left(\frac{x}{x+y}\right)m\left(\frac{y}{x+y}\right)f(x)g(y)dxdy$$

$$\leq\left\{\left[\int_0^1\ell^p(t)dt\right]\left[\int_0^{+\infty}f^p(x)dx\right]\right\}^{1/p}\left\{\left[\int_0^1 m^q(t)dt\right]\left[\int_0^{+\infty}g^q(y)dy\right]\right\}^{1/q}$$

$$=\left[\int_0^1\ell^p(t)dt\right]^{1/p}\left[\int_0^1 m^q(t)dt\right]^{1/q}\left[\int_0^{+\infty}f^p(x)dx\right]^{1/p}\left[\int_0^{+\infty}g^q(y)dy\right]^{1/q}$$

$$=\Upsilon\left[\int_0^{+\infty}f^p(x)dx\right]^{1/p}\left[\int_0^{+\infty}g^q(y)dy\right]^{1/q},$$

where Υ is indicated in Equation (2.1). This concludes the proof of Theorem 2.1. □

The main interest of this theorem is the generality of the two-dimensional integral. It includes two auxiliary functions, ℓ and m, which provide additional flexibility. Another major strength is the simplicity of the upper bound. It depends only on the integral norms of the functions involved. Given the wide variety of known integral formulas (see [17]), the structure of this upper bound allows for easy adaptation. In particular, it allows the derivation of tractable two-dimensional integral inequalities. These may have useful applications in operator theory and related areas.

In the rest of this section, we support these claims with several examples considering different types of auxiliary functions, and with established secondary results derived more or less directly from Theorem 2.1.

2.2 Examples

Some specific examples of applications of Theorem 2.1 are given below. They deal with different functions ℓ and m.

Example 1. Applying Theorem 2.1 with $\ell(t)=t^{\alpha}$, $\alpha>0$, and $m(t)=t^{\beta}$, $\beta>0$, we get

$$\int_0^{+\infty}\int_0^{+\infty}\frac{x^{\alpha+1/p}y^{\beta+1/q}}{(x+y)^{\alpha+\beta+2}}f(x)g(y)dxdy=\int_0^{+\infty}\int_0^{+\infty}\frac{x^{1/p}y^{1/q}}{(x+y)^2}\ell\left(\frac{x}{x+y}\right)m\left(\frac{y}{x+y}\right)f(x)g(y)dxdy$$
$$\leq\Upsilon\left[\int_0^{+\infty}f^p(x)dx\right]^{1/p}\left[\int_0^{+\infty}g^q(y)dy\right]^{1/q},$$

where

$$\Upsilon=\left[\int_0^1\ell^p(t)dt\right]^{1/p}\left[\int_0^1 m^q(t)dt\right]^{1/q}=\left(\int_0^1 t^{\alpha p}dt\right)^{1/p}\left(\int_0^1 t^{\beta q}dt\right)^{1/q}=\frac{1}{(\alpha p+1)^{1/p}(\beta q+1)^{1/q}}.$$

This upper bound is thus determined in a straightforward manner, despite the relative complexity of the two main two-dimensional integrals. In summary, thanks to Theorem 2.1, we have established that

$$\int_0^{+\infty}\int_0^{+\infty}\frac{x^{\alpha+1/p}y^{\beta+1/q}}{(x+y)^{\alpha+\beta+2}}f(x)g(y)dxdy\leq\frac{1}{(\alpha p+1)^{1/p}(\beta q+1)^{1/q}}\left[\int_0^{+\infty}f^p(x)dx\right]^{1/p}\left[\int_0^{+\infty}g^q(y)dy\right]^{1/q}.$$

This inequality can also be manipulated to derive other integral inequality results. For example, if we take $p=2$, $\alpha=\gamma/2$, $\gamma>0$, and $\beta=\gamma/2=\alpha$, it simplifies to

$$\int_0^{+\infty}\int_0^{+\infty}\frac{\sqrt{xy}}{(x+y)^2}\left(\frac{\sqrt{xy}}{x+y}\right)^{\gamma}f(x)g(y)dxdy\leq\frac{1}{\gamma+1}\sqrt{\int_0^{+\infty}f^2(x)dx}\sqrt{\int_0^{+\infty}g^2(y)dy}.$$

This result has the advantage of being tractable with a simple constant factor. For example, considering γ as a variable and integrating both sides for $\gamma \in (0,\tau)$ with $\tau > 0$, and using the Fubini-Tonelli integral theorem, we get

$$\int_0^{+\infty}\int_0^{+\infty} \frac{\sqrt{xy}}{(x+y)^2} \times \frac{1}{\log[(x+y)/\sqrt{xy}]}\left[1-\left(\frac{\sqrt{xy}}{x+y}\right)^{\tau}\right] f(x)g(y)dxdy$$
$$= \int_0^{+\infty}\int_0^{+\infty} \frac{\sqrt{xy}}{(x+y)^2}\left[\int_0^{\tau}\left(\frac{\sqrt{xy}}{x+y}\right)^{\gamma} d\gamma\right] f(x)g(y)dxdy$$
$$= \int_0^{\tau}\left[\int_0^{+\infty}\int_0^{+\infty} \frac{\sqrt{xy}}{(x+y)^2}\left(\frac{\sqrt{xy}}{x+y}\right)^{\gamma} f(x)g(y)dxdy\right] d\gamma$$
$$\leq \left[\int_0^{\tau}\frac{1}{\gamma+1}d\gamma\right]\sqrt{\int_0^{+\infty} f^2(x)dx}\sqrt{\int_0^{+\infty} g^2(y)dy}$$
$$= \log(\tau+1)\sqrt{\int_0^{+\infty} f^2(x)dx}\sqrt{\int_0^{+\infty} g^2(y)dy}.$$

More directly, we have

$$\int_0^{+\infty}\int_0^{+\infty} \frac{\sqrt{xy}}{(x+y)^2\log[(x+y)/\sqrt{xy}]}\left[1-\left(\frac{\sqrt{xy}}{x+y}\right)^{\tau}\right] f(x)g(y)dxdy \leq \log(\tau+1)\sqrt{\int_0^{+\infty} f^2(x)dx}\sqrt{\int_0^{+\infty} g^2(y)dy}.$$

To the best of our knowledge, this is a new two-dimensional integral inequality in the literature.

Example 2. Applying Theorem 2.1 with $\ell(t) = [-\log(t)]^{\alpha}$, $\alpha > 0$, and $m(t) = [-\log(t)]^{\beta}$, $\beta > 0$, we get

$$\int_0^{+\infty}\int_0^{+\infty} \frac{x^{1/p}y^{1/q}}{(x+y)^2}\left[-\log\left(\frac{x}{x+y}\right)\right]^{\alpha}\left[-\log\left(\frac{y}{x+y}\right)\right]^{\beta} f(x)g(y)dxdy$$
$$= \int_0^{+\infty}\int_0^{+\infty} \frac{x^{1/p}y^{1/q}}{(x+y)^2}\ell\left(\frac{x}{x+y}\right)m\left(\frac{y}{x+y}\right) f(x)g(y)dxdy$$
$$\leq \Upsilon\left[\int_0^{+\infty} f^p(x)dx\right]^{1/p}\left[\int_0^{+\infty} g^q(y)dy\right]^{1/q},$$

where, using the formula of the gamma function in [17, Entry 4.2726], i.e., $\Gamma(x) = \int_0^1 [-\log(t)]^{x-1}dt$, $x > 0$,

$$\Upsilon = \left[\int_0^1 \ell^p(t)dt\right]^{1/p}\left[\int_0^1 m^q(t)dt\right]^{1/q} = \left[\int_0^1 [-\log(t)]^{\alpha p}dt\right]^{1/p}\left[\int_0^1 [-\log(t)]^{\beta q}dt\right]^{1/q}$$
$$= \Gamma^{1/p}(\alpha p+1)\Gamma^{1/q}(\beta q+1).$$

As a more direct presentation, we have

$$\int_0^{+\infty}\int_0^{+\infty} \frac{x^{1/p}y^{1/q}}{(x+y)^2}\left[-\log\left(\frac{x}{x+y}\right)\right]^{\alpha}\left[-\log\left(\frac{y}{x+y}\right)\right]^{\beta} f(x)g(y)dxdy$$
$$\leq \Gamma^{1/p}(\alpha p+1)\Gamma^{1/q}(\beta q+1)\left[\int_0^{+\infty} f^p(x)dx\right]^{1/p}\left[\int_0^{+\infty} g^q(y)dy\right]^{1/q}.$$

We emphasize again the originality of the main two-dimensional integral and the simplicity of the constant factor.

Example 3. Trigonometric functions can also be used as auxiliary functions in Theorem 2.1. In particular, applying this theorem with $p=2$, $\ell(t)=\sin[\theta(\pi/2)t]$, $\theta\in[0,1]$, and $m(t)=\sin[\theta(\pi/2)t]=\ell(t)$, $\theta\in[0,1]$, we obtain

$$\begin{aligned}
&\int_0^{+\infty}\int_0^{+\infty}\frac{\sqrt{xy}}{(x+y)^2}\sin\left[\theta\frac{\pi}{2}\left(\frac{x}{x+y}\right)\right]\sin\left[\theta\frac{\pi}{2}\left(\frac{y}{x+y}\right)\right]f(x)g(y)dxdy\\
&=\int_0^{+\infty}\int_0^{+\infty}\frac{x^{1/p}y^{1/q}}{(x+y)^2}\ell\left(\frac{x}{x+y}\right)m\left(\frac{y}{x+y}\right)f(x)g(y)dxdy\\
&\leq \Upsilon\left[\int_0^{+\infty}f^p(x)dx\right]^{1/p}\left[\int_0^{+\infty}g^q(y)dy\right]^{1/q}\\
&=\Upsilon\sqrt{\int_0^{+\infty}f^2(x)dx}\sqrt{\int_0^{+\infty}g^2(y)dy},
\end{aligned}$$

where

$$\begin{aligned}
\Upsilon&=\left[\int_0^{+\infty}f^p(x)dx\right]^{1/p}\left[\int_0^{+\infty}g^q(y)dy\right]^{1/q}=\sqrt{\int_0^1\sin^2\left(\theta\frac{\pi}{2}t\right)dt}\sqrt{\int_0^1\sin^2\left(\theta\frac{\pi}{2}t\right)dt}\\
&=\int_0^1\sin^2\left(\theta\frac{\pi}{2}t\right)dt=\frac{1}{2}\left[1-\frac{\sin(\theta\pi)}{\theta\pi}\right].
\end{aligned}$$

Therefore, we have

$$\begin{aligned}
&\int_0^{+\infty}\int_0^{+\infty}\frac{\sqrt{xy}}{(x+y)^2}\sin\left[\theta\frac{\pi}{2}\left(\frac{x}{x+y}\right)\right]\sin\left[\theta\frac{\pi}{2}\left(\frac{y}{x+y}\right)\right]f(x)g(y)dxdy\\
&\leq\frac{1}{2}\left[1-\frac{\sin(\theta\pi)}{\theta\pi}\right]\sqrt{\int_0^{+\infty}f^2(x)dx}\sqrt{\int_0^{+\infty}g^2(y)dy}.
\end{aligned}$$

We can also express the constant factor in terms of the sine cardinal function, as $(1/2)[1-\mathrm{sinc}(\theta\pi)]$, with $\mathrm{sinc}(a)=\sin(a)/a$ for $a\neq 0$, and $\mathrm{sinc}(0)=1$.

Example 4. Complementing the logarithmic functions considered in the second example, exponential functions can be investigated. Applying Theorem 2.1 with $\ell(t)=e^{\alpha t}$, $\alpha>0$, and $m(t)=e^{\beta t}$, $\beta>0$, we get

$$\begin{aligned}
\int_0^{+\infty}\int_0^{+\infty}\frac{x^{1/p}y^{1/q}}{(x+y)^2}e^{(\alpha x+\beta y)/(x+y)}f(x)g(y)dxdy&=\int_0^{+\infty}\int_0^{+\infty}\frac{x^{1/p}y^{1/q}}{(x+y)^2}\ell\left(\frac{x}{x+y}\right)m\left(\frac{y}{x+y}\right)f(x)g(y)dxdy\\
&\leq\Upsilon\left[\int_0^{+\infty}f^p(x)dx\right]^{1/p}\left[\int_0^{+\infty}g^q(y)dy\right]^{1/q},
\end{aligned}$$

where

$$\Upsilon=\left[\int_0^1\ell^p(t)dt\right]^{1/p}\left[\int_0^1 m^q(t)dt\right]^{1/q}=\left(\int_0^1 e^{\alpha pt}dt\right)^{1/p}\left(\int_0^1 e^{\beta qt}dt\right)^{1/q}=\frac{1}{(\alpha p)^{1/p}(\beta q)^{1/q}}\left(e^{\alpha p}-1\right)^{1/p}\left(e^{\beta q}-1\right)^{1/q}.$$

Thus, we have

$$\int_0^{+\infty}\int_0^{+\infty}\frac{x^{1/p}y^{1/q}}{(x+y)^2}e^{(\alpha x+\beta y)/(x+y)}f(x)g(y)dxdy\leq\frac{1}{(\alpha p)^{1/p}(\beta q)^{1/q}}\left(e^{\alpha p}-1\right)^{1/p}\left(e^{\alpha q}-1\right)^{1/q}\left[\int_0^{+\infty}f^p(x)dx\right]^{1/p}\left[\int_0^{+\infty}g^q(y)dy\right]^{1/q}.$$

2.3 Secondary results

We can use Theorem 2.1 to establish other new general two-dimensional integral inequality results. Three such results are presented and proved below.

The proposition below can be viewed as a variant of Theorem 2.1.

Proposition 2.2. *Let $p > 1$, $q = p/(p-1)$, and $f, g : (0, +\infty) \mapsto (0, +\infty)$ and $\ell, m : (0, 1) \mapsto (0, +\infty)$ be four functions. Then, we have*

$$\int_0^{+\infty}\int_0^{+\infty} \frac{1}{(x+y)^2}\ell\left(\frac{x}{x+y}\right) m\left(\frac{y}{x+y}\right) f(x)g(y)dxdy \leq \Upsilon \left[\int_0^{+\infty} \frac{1}{x} f^p(x)dx\right]^{1/p} \left[\int_0^{+\infty} \frac{1}{y} g^q(y)dy\right]^{1/q},$$

where Υ is given by Equation (2.1), provided that the integrals involved converge.

Proof. We can express the main two-dimensional integral as follows:

$$\int_0^{+\infty}\int_0^{+\infty} \frac{1}{(x+y)^2}\ell\left(\frac{x}{x+y}\right) m\left(\frac{y}{x+y}\right) f(x)g(y)dxdy = \int_0^{+\infty}\int_0^{+\infty} \frac{x^{1/p}y^{1/q}}{(x+y)^2}\ell\left(\frac{x}{x+y}\right) m\left(\frac{y}{x+y}\right) f_\dagger(x)g_\dagger(y)dxdy,$$

where

$$f_\dagger(x) = \frac{1}{x^{1/p}} f(x), \quad g_\dagger(y) = \frac{1}{y^{1/q}} g(y).$$

Applying Theorem 2.1 to these functions, we get

$$\int_0^{+\infty}\int_0^{+\infty} \frac{x^{1/p}y^{1/q}}{(x+y)^2}\ell\left(\frac{x}{x+y}\right) m\left(\frac{y}{x+y}\right) f_\dagger(x)g_\dagger(y)dxdy \leq \Upsilon \left[\int_0^{+\infty} f_\dagger^p(x)dx\right]^{1/p} \left[\int_0^{+\infty} g_\dagger^q(y)dy\right]^{1/q}$$

$$= \Upsilon \left[\int_0^{+\infty} \frac{1}{x} f^p(x)dx\right]^{1/p} \left[\int_0^{+\infty} \frac{1}{y} g^q(y)dy\right]^{1/q},$$

where Υ is given by Equation (2.1). So we have

$$\int_0^{+\infty}\int_0^{+\infty} \frac{1}{(x+y)^2}\ell\left(\frac{x}{x+y}\right) m\left(\frac{y}{x+y}\right) f(x)g(y)dxdy \leq \Upsilon \left[\int_0^{+\infty} \frac{1}{x} f^p(x)dx\right]^{1/p} \left[\int_0^{+\infty} \frac{1}{y} g^q(y)dy\right]^{1/q}.$$

This ends the proof of Proposition 2.2. □

This result thus relativizes the importance of the power functions $x^{1/p}$ and $y^{1/q}$ in Theorem 2.1; they can be transposed to the integral norms of f and g, leading to appropriate weighted integral norms with suitable definitions of the weight functions.

The proposition below gives a framework that unifies the Hardy-Hilbert integral inequality and Theorem 2.1.

Proposition 2.3. *Let $p > 1$, $q = p/(p-1)$, $\sigma \in [0, 1]$, and $f, g : (0, +\infty) \mapsto (0, +\infty)$ and $\ell, m : (0, 1) \mapsto (0, +\infty)$ be four functions. Then, we have*

$$\int_0^{+\infty}\int_0^{+\infty} \frac{x^{(1-\sigma)/p}y^{(1-\sigma)/q}}{(x+y)^{2-\sigma}}\ell^{1-\sigma}\left(\frac{x}{x+y}\right) m^{1-\sigma}\left(\frac{y}{x+y}\right) f(x)g(y)dxdy$$
$$\leq \frac{\pi^\sigma}{\sin^\sigma(\pi/p)}\Upsilon^{1-\sigma} \left[\int_0^{+\infty} f^p(x)dx\right]^{1/p} \left[\int_0^{+\infty} g^q(y)dy\right]^{1/q},$$

where Υ is given by Equation (2.1), provided that the integrals involved converge.

Proof. The case $\sigma = 0$ corresponds to Theorem 2.1, and the case $\sigma = 1$ corresponds to the Hardy-Hilbert integral inequality as recalled in Equation (1.1). So let us assume $\sigma \in (0, 1)$. We can express the main two-dimensional integral as follows:

$$\int_0^{+\infty}\int_0^{+\infty} \frac{x^{(1-\sigma)/p}y^{(1-\sigma)/q}}{(x+y)^{2-\sigma}}\ell^{1-\sigma}\left(\frac{x}{x+y}\right) m^{1-\sigma}\left(\frac{y}{x+y}\right) f(x)g(y)dxdy$$
$$= \int_0^{+\infty}\int_0^{+\infty} \left[\frac{1}{x+y} f(x)g(y)\right]^\sigma \times \left[\frac{x^{1/p}y^{1/q}}{(x+y)^2}\ell\left(\frac{x}{x+y}\right) m\left(\frac{y}{x+y}\right) f(x)g(y)\right]^{1-\sigma} dxdy.$$

Using the Hölder integral inequality applied to the two main terms at the parameters $1/\sigma$ and $1/(1-\sigma)$, the Hardy-Hilbert integral inequality and Theorem 2.1, we get

$$\int_0^{+\infty}\int_0^{+\infty}\left[\frac{1}{x+y}f(x)g(y)\right]^{\sigma}\times\left[\frac{x^{1/p}y^{1/q}}{(x+y)^2}\ell\left(\frac{x}{x+y}\right)m\left(\frac{y}{x+y}\right)f(x)g(y)\right]^{1-\sigma}dxdy$$

$$\leq\left[\int_0^{+\infty}\int_0^{+\infty}\frac{1}{x+y}f(x)g(y)dxdy\right]^{\sigma}\left[\int_0^{+\infty}\int_0^{+\infty}\frac{x^{1/p}y^{1/q}}{(x+y)^2}\ell\left(\frac{x}{x+y}\right)m\left(\frac{y}{x+y}\right)f(x)g(y)dxdy\right]^{1-\sigma}$$

$$\leq\left\{\frac{\pi}{\sin(\pi/p)}\left[\int_0^{+\infty}f^p(x)dx\right]^{1/p}\left[\int_0^{+\infty}g^q(y)dy\right]^{1/q}\right\}^{\sigma}\left\{\Upsilon\left[\int_0^{+\infty}f^p(x)dx\right]^{1/p}\left[\int_0^{+\infty}g^q(y)dy\right]^{1/q}\right\}^{1-\sigma}$$

$$=\frac{\pi^{\sigma}}{\sin^{\sigma}(\pi/p)}\Upsilon^{1-\sigma}\left[\int_0^{+\infty}f^p(x)dx\right]^{1/p}\left[\int_0^{+\infty}g^q(y)dy\right]^{1/q}.$$

So we have

$$\int_0^{+\infty}\int_0^{+\infty}\frac{x^{(1-\sigma)/p}y^{(1-\sigma)/q}}{(x+y)^{2-\sigma}}\ell^{1-\sigma}\left(\frac{x}{x+y}\right)m^{1-\sigma}\left(\frac{y}{x+y}\right)f(x)g(y)dxdy\leq\frac{\pi^{\sigma}}{\sin^{\sigma}(\pi/p)}\Upsilon^{1-\sigma}\left[\int_0^{+\infty}f^p(x)dx\right]^{1/p}\left[\int_0^{+\infty}g^q(y)dy\right]^{1/q}.$$

This concludes the proof of Proposition 2.3. □

As indicated in the proof, the case $\sigma=0$ corresponds to Theorem 2.1, and the case $\sigma=1$ corresponds to the Hardy-Hilbert integral inequality. To the best of our knowledge, all intermediate cases lead to new two-dimensional integral inequalities.

The proposition below presents a different formulation of Theorem 2.1, dealing with only one main function.

Proposition 2.4. *Let $p>1$, $q=p/(p-1)$, $\sigma\in[0,1]$, and $f:(0,+\infty)\mapsto(0,+\infty)$ and $\ell,m:(0,1)\mapsto(0,+\infty)$ be three functions. Then the inequality in Theorem 2.1 is equivalent to the following inequality:*

$$\int_0^{+\infty}\left[\int_0^{+\infty}\frac{x^{1/p}y^{1/q}}{(x+y)^2}\ell\left(\frac{x}{x+y}\right)m\left(\frac{y}{x+y}\right)f(x)dx\right]^p dy\leq\Upsilon^p\int_0^{+\infty}f^p(x)dx,$$

where Υ is given by Equation (2.1), provided that the integrals involved converge.

Proof. We start by proving that Theorem 2.1 implies the stated inequality. We can write the main two-dimensional integral term as follows:

$$\int_0^{+\infty}\left[\int_0^{+\infty}\frac{x^{1/p}y^{1/q}}{(x+y)^2}\ell\left(\frac{x}{x+y}\right)m\left(\frac{y}{x+y}\right)f(x)dx\right]^p dy$$

$$=\int_0^{+\infty}\left[\int_0^{+\infty}\frac{x^{1/p}y^{1/q}}{(x+y)^2}\ell\left(\frac{x}{x+y}\right)m\left(\frac{y}{x+y}\right)f(x)dx\right]^{p-1}\times\left[\int_0^{+\infty}\frac{x^{1/p}y^{1/q}}{(x+y)^2}\ell\left(\frac{x}{x+y}\right)m\left(\frac{y}{x+y}\right)f(x)dx\right]dy$$

$$=\int_0^{+\infty}\int_0^{+\infty}\frac{x^{1/p}y^{1/q}}{(x+y)^2}\ell\left(\frac{x}{x+y}\right)m\left(\frac{y}{x+y}\right)f(x)g_\star(y)dxdy, \tag{2.5}$$

where

$$g_\star(y)=\left[\int_0^{+\infty}\frac{x^{1/p}y^{1/q}}{(x+y)^2}\ell\left(\frac{x}{x+y}\right)m\left(\frac{y}{x+y}\right)f(x)dx\right]^{p-1}.$$

Applying Theorem 2.1 to the functions f and $g_\star$, we obtain

$$\int_0^{+\infty}\int_0^{+\infty}\frac{x^{1/p}y^{1/q}}{(x+y)^2}\ell\left(\frac{x}{x+y}\right)m\left(\frac{y}{x+y}\right)f(x)g_\star(y)dxdy\leq\Upsilon\left[\int_0^{+\infty}f^p(x)dx\right]^{1/p}\left[\int_0^{+\infty}g_\star^q(y)dy\right]^{1/q}. \tag{2.6}$$

Let us now investigate the second integral term of this upper bound. Since $q(p-1)=p$, we get

$$\int_0^{+\infty} g_\star^q(y)dy = \int_0^{+\infty}\left[\int_0^{+\infty}\frac{x^{1/p}y^{1/q}}{(x+y)^2}\ell\left(\frac{x}{x+y}\right)m\left(\frac{y}{x+y}\right)f(x)dx\right]^{q(p-1)}dy$$
$$=\int_0^{+\infty}\left[\int_0^{+\infty}\frac{x^{1/p}y^{1/q}}{(x+y)^2}\ell\left(\frac{x}{x+y}\right)m\left(\frac{y}{x+y}\right)f(x)dx\right]^{p}dy. \tag{2.7}$$

Combining Equations (2.5), (2.6) and (2.7), we get

$$\int_0^{+\infty}\left[\int_0^{+\infty}\frac{x^{1/p}y^{1/q}}{(x+y)^2}\ell\left(\frac{x}{x+y}\right)m\left(\frac{y}{x+y}\right)f(x)dx\right]^{p}dy$$
$$\leq \Upsilon\left[\int_0^{+\infty} f^p(x)dx\right]^{1/p}\left\{\int_0^{+\infty}\left[\int_0^{+\infty}\frac{x^{1/p}y^{1/q}}{(x+y)^2}\ell\left(\frac{x}{x+y}\right)m\left(\frac{y}{x+y}\right)f(x)dx\right]^{p}dy\right\}^{1/q}.$$

Simplifying both sides and using $1/p+1/q=1$, we have

$$\left\{\int_0^{+\infty}\left[\int_0^{+\infty}\frac{x^{1/p}y^{1/q}}{(x+y)^2}\ell\left(\frac{x}{x+y}\right)m\left(\frac{y}{x+y}\right)f(x)dx\right]^{p}dy\right\}^{1/p}\leq \Upsilon\left[\int_0^{+\infty} f^p(x)dx\right]^{1/p},$$

which implies that

$$\int_0^{+\infty}\left[\int_0^{+\infty}\frac{x^{1/p}y^{1/q}}{(x+y)^2}\ell\left(\frac{x}{x+y}\right)m\left(\frac{y}{x+y}\right)f(x)dx\right]^{p}dy\leq \Upsilon^p\int_0^{+\infty} f^p(x)dx.$$

This is the desired inequality.

Let us now assume that this inequality holds and implies Theorem 2.1.

We can express the main two-dimensional integral inequality of Theorem 2.1 as follows:

$$\int_0^{+\infty}\int_0^{+\infty}\frac{x^{1/p}y^{1/q}}{(x+y)^2}\ell\left(\frac{x}{x+y}\right)m\left(\frac{y}{x+y}\right)f(x)g(y)dxdy=\int_0^{+\infty}\left[\int_0^{+\infty}\frac{x^{1/p}y^{1/q}}{(x+y)^2}\ell\left(\frac{x}{x+y}\right)m\left(\frac{y}{x+y}\right)f(x)\right]g(y)dxdy.$$

Applying the Hölder integral inequality to the two main terms with respect to y at the parameters p and q, and using the supposed inequality, we get

$$\int_0^{+\infty}\left[\int_0^{+\infty}\frac{x^{1/p}y^{1/q}}{(x+y)^2}\ell\left(\frac{x}{x+y}\right)m\left(\frac{y}{x+y}\right)f(x)\right]g(y)dxdy$$
$$\leq\left\{\int_0^{+\infty}\left[\int_0^{+\infty}\frac{x^{1/p}y^{1/q}}{(x+y)^2}\ell\left(\frac{x}{x+y}\right)m\left(\frac{y}{x+y}\right)f(x)\right]^{p}dy\right\}^{1/p}\left[\int_0^{+\infty} g^q(y)dy\right]^{1/q}$$
$$=\left\{\Upsilon^p\int_0^{+\infty} f^p(x)dx\right\}^{1/p}\left[\int_0^{+\infty} g^q(y)dy\right]^{1/q}$$
$$=\Upsilon\left[\int_0^{+\infty} f^p(x)dx\right]^{1/p}\left[\int_0^{+\infty} g^q(y)dy\right]^{1/q}.$$

So we have

$$\int_0^{+\infty}\int_0^{+\infty}\frac{x^{1/p}y^{1/q}}{(x+y)^2}\ell\left(\frac{x}{x+y}\right)m\left(\frac{y}{x+y}\right)f(x)g(y)dxdy\leq \Upsilon\left[\int_0^{+\infty} f^p(x)dx\right]^{1/p}\left[\int_0^{+\infty} g^q(y)dy\right]^{1/q},$$

which is the inequality in Theorem 2.1. The equivalence is shown, which concludes the proof of Proposition 2.4. □

This result is of particular interest in operator theory, as it gives a guarantee of continuity in the sense of the integral norm for operators of the following form:

$$\mathscr{T}(f)(y)=\left[\int_0^{+\infty}\frac{x^{1/p}y^{1/q}}{(x+y)^2}\ell\left(\frac{x}{x+y}\right)m\left(\frac{y}{x+y}\right)f(x)dx\right]^p,$$

where ℓ and m can be adapted to different mathematical scenarios.

The rest of the article is devoted to a new three-dimensional perspective of integral inequality, inspired by our two-dimensional results.

3. Three-Dimensional Integral Inequality Results

3.1 Main result

The theorem below can be seen as a natural three-dimensional extension of Theorem 2.1. The addition of one dimension also allows for the use of more auxiliary functions while still having a manageable upper bound. The detailed proof, a complementary version of the theorem, and some discussion follow.

Theorem 3.1. *Let $p>1$, $q>1$ and $r=pq/(pq-p-q)$, and $f,g,h:(0,+\infty)\mapsto(0,+\infty)$ and $i,j,k,\ell,m,n:(0,1)\mapsto(0,+\infty)$ be nine functions. Then, we have*

$$\int_0^{+\infty}\int_0^{+\infty}\int_0^{+\infty}\frac{1}{(x+y+z)^2}\left(\frac{x}{x+y}\right)^{1/p}\left(\frac{y}{y+z}\right)^{1/q}\left(\frac{z}{x+z}\right)^{1/r}$$
$$\times i\left(\frac{x}{x+y}\right)j\left(\frac{y}{y+z}\right)k\left(\frac{z}{x+z}\right)\ell\left(\frac{x+y}{x+y+z}\right)m\left(\frac{y+z}{x+y+z}\right)n\left(\frac{x+z}{x+y+z}\right)f(x)g(y)h(z)dxdydz$$
$$\leq\Xi\left[\int_0^{+\infty}f^p(x)dx\right]^{1/p}\left[\int_0^{+\infty}g^q(y)dy\right]^{1/q}\left[\int_0^{+\infty}h^r(z)dz\right]^{1/r},$$

where

$$\Xi=\left[\int_0^1 i^p(t)dt\right]^{1/p}\left[\int_0^1 \ell^p(t)dt\right]^{1/p}\left[\int_0^1 j^q(t)dt\right]^{1/q}\left[\int_0^1 m^q(t)dt\right]^{1/q}\left[\int_0^1 k^r(t)dt\right]^{1/r}\left[\int_0^1 n^r(t)dt\right]^{1/r},\tag{3.1}$$

provided that the integrals involved converge.

Proof. By a well-chosen decomposition of the integrand as the product of three main terms using $1/p+1/q+1/r=1$, and the generalized Hölder integral inequality applied to those terms at the parameters p, q, and $r=pq/(pq-p-q)$, we get

$$\int_0^{+\infty}\int_0^{+\infty}\int_0^{+\infty}\frac{1}{(x+y+z)^2}\left(\frac{x}{x+y}\right)^{1/p}\left(\frac{y}{y+z}\right)^{1/q}\left(\frac{z}{x+z}\right)^{1/r}$$
$$\times i\left(\frac{x}{x+y}\right)j\left(\frac{y}{y+z}\right)k\left(\frac{z}{x+z}\right)\ell\left(\frac{x+y}{x+y+z}\right)m\left(\frac{y+z}{x+y+z}\right)n\left(\frac{x+z}{x+y+z}\right)f(x)g(y)h(z)dxdydz$$
$$=\int_0^{+\infty}\int_0^{+\infty}\int_0^{+\infty}\frac{1}{(x+y+z)^{2/p}}\left(\frac{x}{x+y}\right)^{1/p}i\left(\frac{x}{x+y}\right)\ell\left(\frac{x+y}{x+y+z}\right)f(x)$$
$$\times\frac{1}{(x+y+z)^{2/q}}\left(\frac{y}{y+z}\right)^{1/q}j\left(\frac{y}{y+z}\right)m\left(\frac{y+z}{x+y+z}\right)g(y)$$
$$\times\frac{1}{(x+y+z)^{2/r}}\left(\frac{z}{x+z}\right)^{1/r}k\left(\frac{z}{x+z}\right)n\left(\frac{x+z}{x+y+z}\right)h(z)dxdydz$$
$$\leq C^{1/p}D^{1/q}E^{1/r},\tag{3.2}$$

where

$$C=\int_0^{+\infty}\int_0^{+\infty}\int_0^{+\infty}\frac{1}{(x+y+z)^2}\times\frac{x}{x+y}i^p\left(\frac{x}{x+y}\right)\ell^p\left(\frac{x+y}{x+y+z}\right)f(x)dxdydz,$$

$$D=\int_0^{+\infty}\int_0^{+\infty}\int_0^{+\infty}\frac{1}{(x+y+z)^2}\times\frac{y}{y+z}j^q\left(\frac{y}{y+z}\right)m^q\left(\frac{y+z}{x+y+z}\right)g(y)dxdydz$$

and

$$E=\int_0^{+\infty}\int_0^{+\infty}\int_0^{+\infty}\frac{1}{(x+y+z)^2}\times\frac{z}{x+z}k^r\left(\frac{z}{x+z}\right)n^r\left(\frac{x+z}{x+y+z}\right)h(z)dxdydz.$$

For more details on the generalized Hölder integral inequality, we refer to [15, 16].

We can now find the exact expressions for C, D, and E, starting with C. Applying the Fubini-Tonelli integral theorem to permutate the three integral signs, introducing the term $1=(x+y)/(x+y)$ and changing the variables as $u=(x+y)/(x+y+z)$, so $du=[-(x+y)/(x+y+z)^2]dz$, $z=0\Rightarrow u=1$ and $z\rightarrow+\infty\Rightarrow u=0$, followed by the change of variables $v=x/(x+y)$, so $dv=[-x/(x+y)^2]dy$, $y=0\Rightarrow v=1$ and $y\rightarrow+\infty\Rightarrow v=0$, we get

$$\begin{aligned}
C&=\int_0^{+\infty}f(x)\left\{\int_0^{+\infty}\frac{x}{(x+y)^2}i^p\left(\frac{x}{x+y}\right)\left[\int_0^{+\infty}\frac{x+y}{(x+y+z)^2}\ell^p\left(\frac{x+y}{x+y+z}\right)dz\right]dy\right\}dx\\
&=\int_0^{+\infty}f(x)\left\{\int_0^{+\infty}\frac{x}{(x+y)^2}i^p\left(\frac{x}{x+y}\right)\left[\int_0^{1}\ell^p(u)du\right]dy\right\}dx\\
&=\left[\int_0^1\ell^p(u)du\right]\int_0^{+\infty}f(x)\left[\int_0^{+\infty}\frac{x}{(x+y)^2}i^p\left(\frac{x}{x+y}\right)dy\right]dx\\
&=\left[\int_0^1\ell^p(u)du\right]\int_0^{+\infty}f(x)\left[\int_0^{1}i^p(v)dv\right]dx\\
&=\left[\int_0^1\ell^p(t)dt\right]\left[\int_0^1 i^p(t)dt\right]\int_0^{+\infty}f(x)dx.
\end{aligned}\tag{3.3}$$

In a similar way, but with the introduction of the term $1=(y+z)/(y+z)$, the change of variables $u=(y+z)/(x+y+z)$ with $du=[-(y+z)/(x+y+z)^2]dx$, $x=0\Rightarrow u=1$ and $x\rightarrow+\infty\Rightarrow u=0$, and the change of variables $v=y/(y+z)$ with $dv=[-y/(y+z)^2]dz$, $z=0\Rightarrow v=1$ and $z\rightarrow+\infty\Rightarrow v=0$, we get

$$\begin{aligned}
D&=\int_0^{+\infty}g(y)\left\{\int_0^{+\infty}\frac{y}{(y+z)^2}j^q\left(\frac{y}{y+z}\right)\left[\int_0^{+\infty}\frac{y+z}{(x+y+z)^2}m^q\left(\frac{y+z}{x+y+z}\right)dx\right]dz\right\}dy\\
&=\int_0^{+\infty}g(y)\left\{\int_0^{+\infty}\frac{y}{(y+z)^2}j^q\left(\frac{y}{y+z}\right)\left[\int_0^{1}m^q(u)du\right]dz\right\}dy\\
&=\left[\int_0^1 m^q(u)du\right]\int_0^{+\infty}g(y)\left[\int_0^{+\infty}\frac{y}{(y+z)^2}j^q\left(\frac{y}{y+z}\right)dz\right]dy\\
&=\left[\int_0^1 m^q(u)du\right]\int_0^{+\infty}g(y)\left[\int_0^{1}j^q(v)dv\right]dy\\
&=\left[\int_0^1 m^q(t)dt\right]\left[\int_0^1 j^q(t)dt\right]\int_0^{+\infty}g(y)dy.
\end{aligned}\tag{3.4}$$

Adopting a similar approach, but with the introduction of the term $1=(x+z)/(x+z)$, the change of variables $u=(x+z)/(x+y+z)$ with $du=[-(x+z)/(x+y+z)^2]dy$, $y=0\Rightarrow u=1$ and $y\rightarrow+\infty\Rightarrow u=0$, and the change of variables $v=z/(x+z)$

with $dv = [-z/(x+z)^2]dx$, $x = 0 \Rightarrow v = 1$ and $x \to +\infty \Rightarrow v = 0$, we get

$$\begin{aligned}
E &= \int_0^{+\infty} h(z) \left\{ \int_0^{+\infty} \frac{z}{(x+z)^2} k^r \left(\frac{z}{x+z}\right) \left[\int_0^{+\infty} \frac{x+z}{(x+y+z)^2} n^r \left(\frac{x+z}{x+y+z}\right) dy \right] dx \right\} dz \\
&= \int_0^{+\infty} h(z) \left\{ \int_0^{+\infty} \frac{z}{(x+z)^2} k^r \left(\frac{z}{x+z}\right) \left[\int_0^{1} n^r(u) du \right] dx \right\} dz \\
&= \left[\int_0^1 n^r(u) du \right] \int_0^{+\infty} h(z) \left[\int_0^{+\infty} \frac{z}{(x+z)^2} k^r \left(\frac{z}{x+z}\right) dx \right] dz \\
&= \left[\int_0^1 n^r(u) du \right] \int_0^{+\infty} h(z) \left[\int_0^1 k^r(v) dv \right] dz \\
&= \left[\int_0^1 n^r(t) dt \right] \left[\int_0^1 k^r(t) dt \right] \int_0^{+\infty} h(z) dz. \qquad (3.5)
\end{aligned}$$

Combining Equations (3.2), (3.3), (3.4) and (3.5), and using $1/p + 1/q + 1/r = 1$, we get

$$\begin{aligned}
&\int_0^{+\infty} \int_0^{+\infty} \int_0^{+\infty} \frac{1}{(x+y+z)^2} \left(\frac{x}{x+y}\right)^{1/p} \left(\frac{y}{y+z}\right)^{1/q} \left(\frac{z}{x+z}\right)^{1/r} \\
&\times i\left(\frac{x}{x+y}\right) j\left(\frac{y}{y+z}\right) k\left(\frac{z}{x+z}\right) \ell\left(\frac{x+y}{x+y+z}\right) m\left(\frac{y+z}{x+y+z}\right) n\left(\frac{x+z}{x+y+z}\right) f(x)g(y)h(z) dxdydz \\
&\leq \left\{ \left[\int_0^1 \ell^p(t) dt \right] \left[\int_0^1 i^p(t) dt \right] \int_0^{+\infty} f(x) dx \right\}^{1/p} \left\{ \left[\int_0^1 m^q(t) dt \right] \left[\int_0^1 j^q(t) dt \right] \int_0^{+\infty} g(y) dy \right\}^{1/q} \\
&\times \left\{ \left[\int_0^1 n^r(t) dt \right] \left[\int_0^1 k^r(t) dt \right] \int_0^{+\infty} h(z) dz \right\}^{1/r} \\
&= \left[\int_0^1 i^p(t) dt \right]^{1/p} \left[\int_0^1 \ell^p(t) dt \right]^{1/p} \left[\int_0^1 j^q(t) dt \right]^{1/q} \left[\int_0^1 m^q(t) dt \right]^{1/q} \\
&\times \left[\int_0^1 k^r(t) dt \right]^{1/r} \left[\int_0^1 n^r(t) dt \right]^{1/r} \left[\int_0^{+\infty} f^p(x) dx \right]^{1/p} \left[\int_0^{+\infty} g^q(y) dy \right]^{1/q} \left[\int_0^{+\infty} h^r(z) dz \right]^{1/r} \\
&= \Xi \left[\int_0^{+\infty} f^p(x) dx \right]^{1/p} \left[\int_0^{+\infty} g^q(y) dy \right]^{1/q} \left[\int_0^{+\infty} h^r(z) dz \right]^{1/r},
\end{aligned}$$

where Ξ is indicated in Equation (3.1). This concludes the proof of Theorem 3.1. □

Another version of Theorem 3.1 can be presented by thoroughly changing the order of the variables x, y, and z. It is given below.

Theorem 3.2. *Let $p > 1$, $q > 1$ and $r = pq/(pq - p - q)$, and $f, g, h : (0, +\infty) \mapsto (0, +\infty)$ and $i, j, k, \ell, m, n : (0, 1) \mapsto (0, +\infty)$ be nine functions. Then, we have*

$$\begin{aligned}
&\int_0^{+\infty} \int_0^{+\infty} \int_0^{+\infty} \frac{1}{(x+y+z)^2} \left(\frac{x}{x+z}\right)^{1/p} \left(\frac{y}{x+y}\right)^{1/q} \left(\frac{z}{y+z}\right)^{1/r} \\
&\times i\left(\frac{x}{x+z}\right) j\left(\frac{y}{x+y}\right) k\left(\frac{z}{y+z}\right) \ell\left(\frac{x+z}{x+y+z}\right) m\left(\frac{x+y}{x+y+z}\right) n\left(\frac{y+z}{x+y+z}\right) f(x)g(y)h(z) dxdydz \\
&\leq \Xi \left[\int_0^{+\infty} f^p(x) dx \right]^{1/p} \left[\int_0^{+\infty} g^q(y) dy \right]^{1/q} \left[\int_0^{+\infty} h^r(z) dz \right]^{1/r},
\end{aligned}$$

where Ξ is given by Equation (3.1), provided that the integrals involved converge.

Proof. The proof is almost identical to that of Theorem 3.1. There are only slight modifications in the management of the variables x, y, and z. For the sake of redundancy, we omit the full development. □

The main interest of Theorems 3.1 and 3.2 is the generality of the three-dimensional integral. They include six auxiliary functions, i, j, k, ℓ, m and n, which provide additional flexibility. Another major strength is the simplicity of the upper bound. It depends only on the unweighted integral norms of the functions involved, allowing tractable three-dimensional integral inequalities to be derived. These can have useful applications in operator theory dealing with three-dimensional operators and related areas.

In the rest of this section, several examples are given involving different types of auxiliary functions.

3.2 Examples

Some specific examples of applications of Theorem 3.1 are given below. They deal with different functions i, j, k, ℓ, m and n. Similar examples can be given for Theorem 3.2. We omit them for the sake of redundancy.

Example 1. We start with the use of standard power functions. Applying Theorem 3.1 with $i(t) = t^{\alpha}$, $\alpha > 0$, $j(t) = t^{\beta}$, $\beta > 0$, $k(t) = t^{\gamma}$, $\gamma > 0$, $\ell(t) = t^{\kappa}$, $\kappa > 0$, $m(t) = t^{\theta}$, $\theta > 0$, and $n(t) = t^{\upsilon}$, $\upsilon > 0$, we get

$$\int_0^{+\infty}\int_0^{+\infty}\int_0^{+\infty} \frac{x^{1/p}y^{1/q}z^{1/r}(x+y)^{\kappa-\alpha-1/p}(y+z)^{\theta-\beta-1/q}(x+z)^{\upsilon-\gamma-1/r}}{(x+y+z)^{2+\kappa+\theta+\upsilon}} f(x)g(y)h(z)dxdydz$$

$$= \int_0^{+\infty}\int_0^{+\infty}\int_0^{+\infty} \frac{1}{(x+y+z)^2}\left(\frac{x}{x+y}\right)^{1/p}\left(\frac{y}{y+z}\right)^{1/q}\left(\frac{z}{x+z}\right)^{1/r}$$

$$\times\, i\left(\frac{x}{x+y}\right) j\left(\frac{y}{y+z}\right) k\left(\frac{z}{x+z}\right) \ell\left(\frac{x+y}{x+y+z}\right) m\left(\frac{y+z}{x+y+z}\right) n\left(\frac{x+z}{x+y+z}\right) f(x)g(y)h(z)dxdydz$$

$$\le \Xi\left[\int_0^{+\infty} f^p(x)dx\right]^{1/p}\left[\int_0^{+\infty} g^q(y)dy\right]^{1/q}\left[\int_0^{+\infty} h^r(z)dz\right]^{1/r},$$

where

$$\Xi = \left[\int_0^1 i^p(t)dt\right]^{1/p}\left[\int_0^1 \ell^p(t)dt\right]^{1/p}\left[\int_0^1 j^q(t)dt\right]^{1/q}\left[\int_0^1 m^q(t)dt\right]^{1/q}\left[\int_0^1 k^r(t)dt\right]^{1/r}\left[\int_0^1 n^r(t)dt\right]^{1/r}$$

$$= \left(\int_0^1 t^{\alpha p}dt\right)^{1/p}\left(\int_0^1 t^{\kappa p}dt\right)^{1/p}\left(\int_0^1 t^{\beta q}dt\right)^{1/q}\left(\int_0^1 t^{\theta q}dt\right)^{1/q}\left(\int_0^1 t^{\gamma r}dt\right)^{1/r}\left(\int_0^1 t^{\upsilon r}dt\right)^{1/r}$$

$$= \frac{1}{(\alpha p+1)^{1/p}(\kappa p+1)^{1/p}(\beta q+1)^{1/q}(\theta q+1)^{1/q}(\gamma r+1)^{1/r}(\upsilon r+1)^{1/r}}.$$

As a result, we have

$$\int_0^{+\infty}\int_0^{+\infty}\int_0^{+\infty} \frac{x^{1/p}y^{1/q}z^{1/r}(x+y)^{\kappa-\alpha-1/p}(y+z)^{\theta-\beta-1/q}(x+z)^{\upsilon-\gamma-1/r}}{(x+y+z)^{2+\kappa+\theta+\upsilon}} f(x)g(y)h(z)dxdydz$$

$$\le \frac{1}{(\alpha p+1)^{1/p}(\kappa p+1)^{1/p}(\beta q+1)^{1/q}(\theta q+1)^{1/q}(\gamma r+1)^{1/r}(\upsilon r+1)^{1/r}}$$

$$\times\left[\int_0^{+\infty} f^p(x)dx\right]^{1/p}\left[\int_0^{+\infty} g^q(y)dy\right]^{1/q}\left[\int_0^{+\infty} h^r(z)dz\right]^{1/r}.$$

This provides a new manageable three-dimensional integral inequality, with numerous adjustable parameters, which can be adapted to different contexts.

Example 2. Applying Theorem 3.1 with $i(t)=1$, $j(t)=1$, $k(t)=1$, $\ell(t)=[-\log(t)]^{\alpha}$, $\alpha>0$, $m(t)=[-\log(t)]^{\beta}$, $\beta>0$, and $n(t)=[-\log(t)]^{\gamma}$, $\gamma>0$, we get

$$\int_0^{+\infty}\int_0^{+\infty}\int_0^{+\infty}\frac{1}{(x+y+z)^2}\left(\frac{x}{x+y}\right)^{1/p}\left(\frac{y}{y+z}\right)^{1/q}\left(\frac{z}{x+z}\right)^{1/r}$$

$$\times\left[-\log\left(\frac{x+y}{x+y+z}\right)\right]^{\alpha}\left[-\log\left(\frac{y+z}{x+y+z}\right)\right]^{\beta}\left[-\log\left(\frac{x+z}{x+y+z}\right)\right]^{\gamma}f(x)g(y)h(z)dxdydz$$

$$=\int_0^{+\infty}\int_0^{+\infty}\int_0^{+\infty}\frac{1}{(x+y+z)^2}\left(\frac{x}{x+y}\right)^{1/p}\left(\frac{y}{y+z}\right)^{1/q}\left(\frac{z}{x+z}\right)^{1/r}$$

$$\times\, i\left(\frac{x}{x+y}\right)j\left(\frac{y}{y+z}\right)k\left(\frac{z}{x+z}\right)\ell\left(\frac{x+y}{x+y+z}\right)m\left(\frac{y+z}{x+y+z}\right)n\left(\frac{x+z}{x+y+z}\right)f(x)g(y)h(z)dxdydz$$

$$\leq \Xi\left[\int_0^{+\infty}f^p(x)dx\right]^{1/p}\left[\int_0^{+\infty}g^q(y)dy\right]^{1/q}\left[\int_0^{+\infty}h^r(z)dz\right]^{1/r},$$

where

$$\Xi=\left[\int_0^1 i^p(t)dt\right]^{1/p}\left[\int_0^1 \ell^p(t)dt\right]^{1/p}\left[\int_0^1 j^q(t)dt\right]^{1/q}\left[\int_0^1 m^q(t)dt\right]^{1/q}\left[\int_0^1 k^r(t)dt\right]^{1/r}\left[\int_0^1 n^r(t)dt\right]^{1/r}$$

$$=\left[\int_0^1[-\log(t)]^{\alpha p}dt\right]^{1/p}\left[\int_0^1[-\log(t)]^{\beta q}dt\right]^{1/q}\left[\int_0^1[-\log(t)]^{\gamma r}dt\right]^{1/r}$$

$$=\Gamma^{1/p}(\alpha p+1)\Gamma^{1/q}(\beta q+1)\Gamma^{1/r}(\gamma r+1).$$

More directly, we have

$$\int_0^{+\infty}\int_0^{+\infty}\int_0^{+\infty}\frac{1}{(x+y+z)^2}\left(\frac{x}{x+y}\right)^{1/p}\left(\frac{y}{y+z}\right)^{1/q}\left(\frac{z}{x+z}\right)^{1/r}$$

$$\times\left[-\log\left(\frac{x+y}{x+y+z}\right)\right]^{\alpha}\left[-\log\left(\frac{y+z}{x+y+z}\right)\right]^{\beta}\left[-\log\left(\frac{x+z}{x+y+z}\right)\right]^{\gamma}f(x)g(y)h(z)dxdydz$$

$$\leq\Gamma^{1/p}(\alpha p+1)\Gamma^{1/q}(\beta q+1)\Gamma^{1/r}(\gamma r+1)\left[\int_0^{+\infty}f^p(x)dx\right]^{1/p}\left[\int_0^{+\infty}g^q(y)dy\right]^{1/q}\left[\int_0^{+\infty}h^r(z)dz\right]^{1/r}.$$

We emphasize the crucial role of the gamma function in the constant factor and the relative complexity of the integrand.

Example 3. Theorem 3.1 can involve trigonometric functions. For example, applying it with $p=3$, $q=3$, $i(t)=1$, $j(t)=1$, $k(t)=1$, $\ell(t)=\sin[\theta(\pi/2)t]$, $\theta\in[0,1]$, $m(t)=\sin[\theta(\pi/2)t]=\ell(t)$, $\theta\in[0,1]$, and $n(t)=\sin[\theta(\pi/2)t]=\ell(t)=m(t)$, $\theta\in[0,1]$, we get

$$\int_0^{+\infty}\int_0^{+\infty}\int_0^{+\infty}\frac{1}{(x+y+z)^2}\left(\frac{x}{x+y}\right)^{1/3}\left(\frac{y}{y+z}\right)^{1/3}\left(\frac{z}{x+z}\right)^{1/3}$$

$$\times\sin\left[\theta\frac{\pi}{2}\left(\frac{x+y}{x+y+z}\right)\right]\sin\left[\theta\frac{\pi}{2}\left(\frac{y+z}{x+y+z}\right)\right]\sin\left[\theta\frac{\pi}{2}\left(\frac{x+z}{x+y+z}\right)\right]f(x)g(y)h(z)dxdydz$$

$$=\int_0^{+\infty}\int_0^{+\infty}\int_0^{+\infty}\frac{1}{(x+y+z)^2}\left(\frac{x}{x+y}\right)^{1/p}\left(\frac{y}{y+z}\right)^{1/q}\left(\frac{z}{x+z}\right)^{1/r}$$

$$\times\, i\left(\frac{x}{x+y}\right)j\left(\frac{y}{y+z}\right)k\left(\frac{z}{x+z}\right)\ell\left(\frac{x+y}{x+y+z}\right)m\left(\frac{y+z}{x+y+z}\right)n\left(\frac{x+z}{x+y+z}\right)f(x)g(y)h(z)dxdydz$$

$$\leq \Xi \left[\int_0^{+\infty} f^p(x)dx\right]^{1/p} \left[\int_0^{+\infty} g^q(y)dy\right]^{1/q} \left[\int_0^{+\infty} h^r(z)dz\right]^{1/r}$$

$$= \Xi \left[\int_0^{+\infty} f^3(x)dx\right]^{1/3} \left[\int_0^{+\infty} g^3(y)dy\right]^{1/3} \left[\int_0^{+\infty} h^3(z)dz\right]^{1/3},$$

where

$$\Xi = \left[\int_0^1 i^p(t)dt\right]^{1/p} \left[\int_0^1 \ell^p(t)dt\right]^{1/p} \left[\int_0^1 j^q(t)dt\right]^{1/q} \left[\int_0^1 m^q(t)dt\right]^{1/q} \left[\int_0^1 k^r(t)dt\right]^{1/r} \left[\int_0^1 n^r(t)dt\right]^{1/r}$$
$$= \left[\int_0^1 \sin^3\left(\theta\frac{\pi}{2}t\right)dt\right]^{1/3} \left[\int_0^1 \sin^3\left(\theta\frac{\pi}{2}t\right)dt\right]^{1/3} \left[\int_0^1 \sin^3\left(\theta\frac{\pi}{2}t\right)dt\right]^{1/3}$$
$$= \int_0^1 \sin^3\left(\theta\frac{\pi}{2}t\right)dt = \frac{8}{3\theta\pi}\sin^4\left(\theta\frac{\pi}{4}\right)\left[2+\cos\left(\theta\frac{\pi}{2}\right)\right].$$

Therefore, we have

$$\int_0^{+\infty}\int_0^{+\infty}\int_0^{+\infty} \frac{1}{(x+y+z)^2}\left(\frac{x}{x+y}\right)^{1/3}\left(\frac{y}{y+z}\right)^{1/3}\left(\frac{z}{x+z}\right)^{1/3}$$

$$\times \sin\left[\theta\frac{\pi}{2}\left(\frac{x+y}{x+y+z}\right)\right]\sin\left[\theta\frac{\pi}{2}\left(\frac{y+z}{x+y+z}\right)\right]\sin\left[\theta\frac{\pi}{2}\left(\frac{x+z}{x+y+z}\right)\right] f(x)g(y)h(z)dxdydz$$

$$\leq \frac{8}{3\theta\pi}\sin^4\left(\theta\frac{\pi}{4}\right)\left[2+\cos\left(\theta\frac{\pi}{2}\right)\right]\left[\int_0^{+\infty} f^3(x)dx\right]^{1/3}\left[\int_0^{+\infty} g^3(y)dy\right]^{1/3}\left[\int_0^{+\infty} h^3(z)dz\right]^{1/3}.$$

Example 4. As a last simple example, applying Theorem 3.1 with $i(t) = e^{\alpha t}$, $\alpha > 0$, $j(t) = e^{\beta t}$, $\beta > 0$, $k(t) = e^{\gamma t}$, $\gamma > 0$, $\ell(t) = e^{\kappa t}$, $\kappa > 0$, $m(t) = e^{\theta t}$, $\theta > 0$, and $n(t) = e^{\upsilon t}$, $\upsilon > 0$, we get

$$\int_0^{+\infty}\int_0^{+\infty}\int_0^{+\infty} \frac{1}{(x+y+z)^2}\left(\frac{x}{x+y}\right)^{1/p}\left(\frac{y}{y+z}\right)^{1/q}\left(\frac{z}{x+z}\right)^{1/r}$$

$$\times e^{\alpha x/(x+y)+\beta y/(y+z)+\gamma z/(x+z)+[(\kappa+\upsilon)x+(\kappa+\theta)y+(\theta+\upsilon)z]/(x+y+z)} f(x)g(y)h(z)dxdydz$$

$$= \int_0^{+\infty}\int_0^{+\infty}\int_0^{+\infty} \frac{1}{(x+y+z)^2}\left(\frac{x}{x+y}\right)^{1/p}\left(\frac{y}{y+z}\right)^{1/q}\left(\frac{z}{x+z}\right)^{1/r}$$

$$\times i\left(\frac{x}{x+y}\right) j\left(\frac{y}{y+z}\right) k\left(\frac{z}{x+z}\right) \ell\left(\frac{x+y}{x+y+z}\right) m\left(\frac{y+z}{x+y+z}\right) n\left(\frac{x+z}{x+y+z}\right) f(x)g(y)h(z)dxdydz$$

$$\leq \Xi \left[\int_0^{+\infty} f^p(x)dx\right]^{1/p} \left[\int_0^{+\infty} g^q(y)dy\right]^{1/q} \left[\int_0^{+\infty} h^r(z)dz\right]^{1/r},$$

where

$$\Xi = \left[\int_0^1 i^p(t)dt\right]^{1/p} \left[\int_0^1 \ell^p(t)dt\right]^{1/p} \left[\int_0^1 j^q(t)dt\right]^{1/q} \left[\int_0^1 m^q(t)dt\right]^{1/q} \left[\int_0^1 k^r(t)dt\right]^{1/r} \left[\int_0^1 n^r(t)dt\right]^{1/r}$$

$$= \left(\int_0^1 e^{\alpha pt}dt\right)^{1/p}\left(\int_0^1 e^{\kappa pt}dt\right)^{1/p}\left(\int_0^1 e^{\beta qt}dt\right)^{1/q}\left(\int_0^1 e^{\theta qt}dt\right)^{1/q}\left(\int_0^1 e^{\gamma rt}dt\right)^{1/r}\left(\int_0^1 e^{\upsilon rt}dt\right)^{1/r}$$

$$= \frac{1}{(\alpha p)^{1/p}(\kappa p)^{1/p}(\beta q)^{1/q}(\theta q)^{1/q}(\gamma r)^{1/r}(\upsilon r)^{1/r}}$$

$$\times (e^{\alpha p}-1)^{1/p}(e^{\kappa p}-1)^{1/p}(e^{\alpha q}-1)^{1/q}\left(e^{\theta q}-1\right)^{1/q}(e^{\gamma r}-1)^{1/r}(e^{\upsilon r}-1)^{1/r}.$$

More directly, we have

$$\int_0^{+\infty}\int_0^{+\infty}\int_0^{+\infty}\frac{1}{(x+y+z)^2}\left(\frac{x}{x+y}\right)^{1/p}\left(\frac{y}{y+z}\right)^{1/q}\left(\frac{z}{x+z}\right)^{1/r}$$

$$\times e^{\alpha x/(x+y)+\beta y/(y+z)+\gamma z/(x+z)+[(\kappa+\upsilon)x+(\kappa+\theta)y+(\theta+\upsilon)z]/(x+y+z)}f(x)g(y)h(z)dxdydz$$

$$\leq \frac{1}{(\alpha p)^{1/p}(\kappa p)^{1/p}(\beta q)^{1/q}(\theta q)^{1/q}(\gamma r)^{1/r}(\upsilon r)^{1/r}}$$

$$\times\left(e^{\alpha p}-1\right)^{1/p}\left(e^{\kappa p}-1\right)^{1/p}\left(e^{\alpha q}-1\right)^{1/q}\left(e^{\theta q}-1\right)^{1/q}\left(e^{\gamma r}-1\right)^{1/r}\left(e^{\upsilon r}-1\right)^{1/r}$$

$$\times\left[\int_0^{+\infty}f^p(x)dx\right]^{1/p}\left[\int_0^{+\infty}g^q(y)dy\right]^{1/q}\left[\int_0^{+\infty}h^r(z)dz\right]^{1/r}.$$

To the best of our knowledge, this is again a new three-dimensional integral inequality in the literature. We can also think of using the exponential function to establish various inequalities of the Laplace transform of three-dimensional functions.

4. Conclusion

In conclusion, this article offers new tools to the theory of two- and three-dimensional integral inequalities by establishing two general theorems. This is characterized by the presence of several auxiliary functions. The first theorem focuses on the two-dimensional case and gives a simple upper bound for two-dimensional integrals of a certain form. This upper bound is based on the integral norms of the function involved. The second theorem can be seen as a natural extension of the first to three dimensions. It still provides tractable, sharp, and general upper bounds. They may lead to further developments in mathematical analysis in three dimensions. The theory has been illustrated by several examples dealing with specific auxiliary functions. Some complementary results beyond the standard framework have also been established.

Future work may explore refined inequalities under additional structural conditions. Applications to operator theory, functional analysis, and partial differential equations are also anticipated. Furthermore, the flexibility of the approach suggests possible generalizations to higher dimensions. We will explore these perspectives in future articles.

Article Information

Acknowledgements: The author would like to express their sincere thanks to the editor and the anonymous reviewers for their helpful comments and suggestions.

Artificial Intelligence Statement: No artificial intelligence has been used in the article.

Conflict of Interest Disclosure: No potential conflict of interest was declared by the author.

Plagiarism Statement: This article was scanned by the plagiarism program.

References

[1] G. H. Hardy, J. E. Littlewood, G. Polya, *Inequalities*, Cambridge University Press, Cambridge, 1934.

[2] E. F. Beckenbach, R. Bellman, *Inequalities*, Springer, Berlin, 1961.

[3] W. Walter, *Differential and Integral Inequalities*, Springer, Berlin, 1970.

[4] D. Bainov, P. Simeonov, *Integral Inequalities and Applications, Mathematics and Its Applications*, Vol. 57. Kluwer Academic, Dordrecht, 1992.

[5] B. C. Yang, *Hilbert-Type Integral Inequalities*, Bentham Science Publishers, The United Arab Emirates, 2009.

[6] Z. T. Xie, Z. Zeng, Y. F. Sun, *A new Hilbert-type inequality with the homogeneous kernel of degree -2*, Adv. Appl. Math. Sci., **12** (2013), 391-401.

[7] V. Adiyasuren, T. Batbold, M. Krnić, *Hilbert-type inequalities involving differential operators, the best constants and applications*, Math. Inequal. Appl., **18** (2015), 111-124. https://doi.org/10.7153/mia-18-07

[8] C. Chesneau, *Some four-parameter trigonometric generalizations of the Hilbert integral inequality*, Asia Math., **8** (2024), 45-59. https://doi.org/10.5281/zenodo.13949386

[9] C. Chesneau, *Study of two three-parameter non-homogeneous variants of the Hilbert integral inequality*, Lobachevskii J. Math., **45** (2024), 4931-4953. https://doi.org/10.1134/S1995080224605526

[10] Q. Chen, B. C. Yang, *A survey on the study of Hilbert-type inequalities*, J. Inequal. Appl., **2015** (2015), 1-29. https://doi.org/10.1186/s13660-015-0829-7

[11] W. T. Sulaiman, *New types of Hardy-Hilbert's integral inequality*, Gen. Math. Notes, **2** (2011), 111-118.

[12] W. W. Wei, X. Y. Lei, *Some more generalizations of the integral inequalities of Hardy and Hilbert*, Hacet. J. Math. Stat., **40** (2011), 863-869.

[13] Z. Huang, B. C. Yang, A multidimensional Hilbert-type integral inequality, J. Inequal. Appl., **2015** (2015), Article ID 151, 13 pages. https://doi.org/10.1186/s13660-015-0673-9

[14] M. Z. Sarikaya, M. S. Bingol, *Recent developments of integral inequalities of the Hardy-Hilbert type*, Turkish J. Ineq., **8**(2) (2024), 43-54.

[15] J. F. Tian, *Properties of generalized Hölder's inequalities*, J. Math. Ineq., **9**(2) (2015), 473-480. https://doi.org/10.7153/jmi-09-40

[16] B. Benaissa, M. Z. Sarikaya, *On the refinements of some important inequalities with a finite set of positive numbers*, Math. Methods Appl. Sci., **47**(12) (2024), 9589-9599. https://doi.org/10.1002/mma.10084

[17] I. S. Gradshteyn, I. M. Ryzhik, *Table of Integrals, Series, and Products*, 7th Edition, Academic Press, Amsterdam, 2007.

Communications in Advanced Mathematical Sciences
ISSN (Online) 2651-4001

Vol. 8, No. 2, 117-124, 2025
https://doi.org/10.33434/cams.1660609
Research Article

Characteristically Near Stable Vector Fields in the Polar Complex Plane

James F. Peters[1*], Enze Cui[1]

Abstract
This paper introduces results for characteristically proximal vector fields that are stable or non-stable in the polar complex plane $\mathbb{C}$. All characteristic vectors (aka eigenvectors) emanate from the same fixed point in $\mathbb{C}$, namely, 0. Stable characteristic vector fields satisfy an extension of the Krantz stability condition, namely, the maximal eigenvalue of a stable system lies within or on the boundary of the unit circle in $\mathbb{C}$. An application is given for stable vector fields detected in motion waveforms in infrared video frames. AI is used to separate the changing from the unchanging parts of each video frame.

Keywords: Characteristic, Complex Plane, Eigenvalue, Eigenvector, Proximity, Stability
2020 AMS: 32Q26, 15A18, 54E05

[1] *Department of Electrical & Computer Engineerig, University of Manitoba, Winnipeg, Manitoba, Canada, James.Peters3@umanitoba.ca, cuie@myumanitoba.ca*
*Corresponding author
Received: 18 March 2025, **Accepted:** 29 June 2025, **Available online:** 01 July 2025
How to cite this article: J. F. Peters, E. Cui, *Characteristically near stable vector fields in the polar complex plane*, Commun. Adv. Math. Sci., 8(2) (2025), 117-124.

1. Introduction

This paper introduces proximities of characteristic vector fields that are stable in the polar complex plane. A dynamical system is a 1-1 mapping from a set of points M to itself [1, §9.1.1], which describes the time-dependence of a point in a complex ambient system. In its earliest incarnation by Poincaré, the focus was on the stability of the solar system [2]. More recently, dynamical system behaviour is in the form of varying oscillations in motion waveforms [3, 4]. Typically, vector fields are used to construct dynamical systems (see, e.g., [5, §4], [6]).

The focus here is on dynamical systems generated by stable characteristic vector fields (cVfs) in $\mathbb{C}$ and their corresponding semigroups. Comparison of cVf characteristics leads to the detection of proximal cVf semigroups. In general, a characteristic of an object X is a mapping $\varphi : X \to \mathbb{C}$ with values $\varphi(x \in X)$ that provide an object profile. Proximal objects X, Y require $|\varphi(x \in X) - \varphi(y \in Y)| = 0$. All characteristic vectors (aka eigenvectors) emanate from the same fixed point in $\mathbb{C}$, namely, 0. Stable characteristic vector fields satisfy the Krantz stability condition, namely, all eigenvalues lie inside the unit circle in $\mathbb{C}$.

An application of the proposed approach is given in measuring system stability in terms of vector fields emanating from oscillatory waveforms derived from the up-and-down movements of a walker, runner, or biker recorded in a sequence of infrared video frames. We prove that system stability occurs when its maximum eigenvalue occurs within or on the boundary of the unit circle in the complex plane (See Theorem 2.11). This result extends results in [7, 8]) as well as in [9–11].

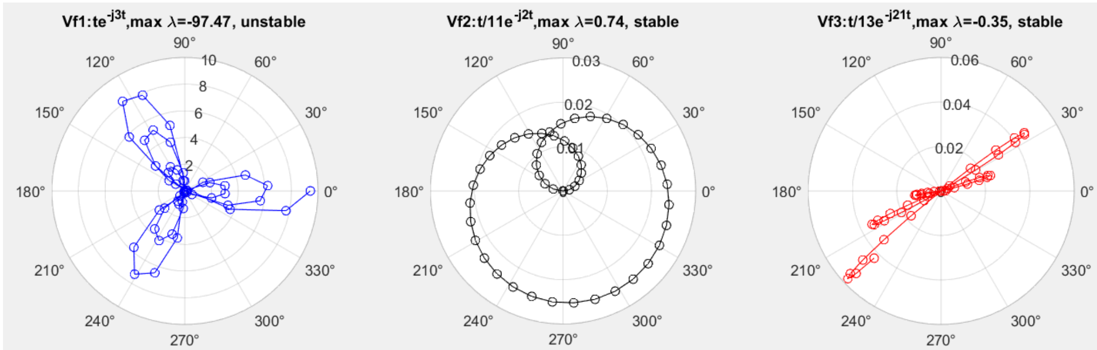

Figure 1.1. Three vector fields in polar complex plane: (leftmost,unstable) $\vec{V}f_1$, (middle,stable) $\vec{V}f_2$,(rightmost,stable) $\vec{V}f_3$

Symbol	Meaning
$\mathbb{C}$	Complex plane
j	Imaginary unit, defined by $j^2 = -1$
$\vec{0}$	Center of the unit circle in the complex polar plane
z	A complex number: $z = a + jb = e^{j\theta}$, where $a,\ jb \in \mathbb{C}$
2^X	Collection of subsets in set X
$A\,\widetilde{\delta}_\Phi\,B$	A is characteristically near B
$\varphi(a \in A) \in \mathbb{C}$	Characteristic value of element $a \in A$
$\Phi(A)$	$\{\varphi(a_1),\ldots,\varphi(a_n) : a_1,\ldots,a_n \in A\} \in 2^{\mathbb{C}}$
$d^{\Phi}(A,B)$	Characteristic distance between sets A and B

Table 1.1. Principal symbols used in this study

2. Preliminaries

Detected affinities between vector fields for stable systems result from determining the infimum of the distances between pairs of system characteristics.

Definition 2.1. (Vector)
A **vector** *v (denoted by $\vec{v}$) is a quantity that has magnitude and direction in the complex plane $\mathbb{C}$.*

Definition 2.2. (Vector Field in the Complex Plane)
Let $U = \{p \in \mathbb{C}\}$ be a bounded region in the complex plane containing points $p(x, jy) \in U$. A **vector field** *is a mapping $F : U \to 2^{\mathbb{C}}$ defined by*

$$F(p(x, jy)) = \{\vec{v}\} \in 2^{\mathbb{C}} \text{ denoted by } \vec{V}f.$$

Remark 2.3. *A complex number z in polar form (discovered by Euler [12]) is written $z = re^{j\theta}$.*

Example 2.4. *Three examples of vector fields in polar form are given in Figure 1.1.*

Definition 2.5. (Vector Field in the Complex Plane)
Let $U = \{z \in \mathbb{C}\}$ be a bounded region in the complex plane containing points $z(x, jy) \in U \subset \mathbb{C}$. A **vector field** *is a mapping $F : U \to 2^{\mathbb{C}}$ defined by*

$$F(z(x, yj)) = \left\{\vec{v} \in 2^{\mathbb{C}}\right\} \text{ denoted by } \vec{V}f.$$

Definition 2.6. (Eigenvalue λ(aka Characteristic value))
The eigenvalues (characteristic values) of a matrix A are solutions to the determinant $\mathbf{det}(\mathbf{A} - \lambda\mathbf{I}), \mathbf{I} = \begin{bmatrix} 1 & 0 \\ 0 & 1 \end{bmatrix}$ *identity matrix.*

Example 2.7. (Sample Eigenvalues)
$A = \begin{bmatrix} 4 & 8 \\ 6 & 26 \end{bmatrix}, I = \begin{bmatrix} 1 & 0 \\ 0 & 1 \end{bmatrix}$: $det(A - \lambda I) = \begin{vmatrix} 4-\lambda & 8 \\ 6 & 26-\lambda \end{vmatrix} = (4-\lambda)(26-\lambda) - (8)(6) = 0$

$104 - 30\lambda + \lambda^2 - 48 = \lambda^2 - 30\lambda + 56 = (\lambda - 28)(\lambda - 2) = 0$
$\lambda_1 = 28, \lambda_2 = 2$ (**eigen values of**) A

Definition 2.8. (Eigenvector)
Given a matrix A, then $\vec{v}$ is an eigenvector, provided $A\vec{v} - \lambda\vec{v} = 0 \in \mathbb{C}$.

1^{st} $\mathbb{C}$ quadrant	1^{st} $\mathbb{C}$ quadrant	3^{rd} $\mathbb{C}$ quadrant
$\vec{z_{11}} = 0.1500 + 0.0498j$	$\vec{z_{12}} = 0.0106 + 0.0035j$	$\vec{z_{13}} = -0.0754 - 0.0250j$
$\vec{z_{21}} = 0.1586 + 0.0471j$	$\vec{z_{22}} = 0.0333 + 0.0091j$	$\vec{z_{23}} = -0.0418 - 0.0124j$

Table 2.1. *Eigenvectors derived from $\frac{t}{11}e^{j2t}Vf$*

Example 2.9. (Sample eigenvectors in center $\frac{t}{11}e^{j2t}$ $\vec{V}$f in Figure 1.1)
A selection of eigenvectors from the first and third quadrants in the polar complex plane in the center vector field in Figure 1.1 are given in Table 2.1.

Definition 2.10. (Krantz Vector Field Stability Condition [1])
A vector field $\vec{V}f$ in the complex plane is stable, provided all of the eigenvalues of $\vec{V}f$ are either within or on the boundary of the unit circle centered 0 in $\mathbb{C}$.

Theorem 2.11. (Vector Field Stability Condition)
A vector field $\vec{V}f$ in the complex plane is stable, provided the maximal eigenvalue of $\vec{V}f$ lies within or on the boundary of the unit circle in $\mathbb{C}$.

Proof. From Definition 2.10, all eigenvalues $D = \{\lambda\}$ for a stable vector field lie either within or on the boundary of the unit circle in $\mathbb{C}$. Hence, $max(\lambda) \in D$ lies either within or on the boundary of the unit circle in $\mathbb{C}$. □

λ_{max}	λ_{max-1}	λ_{max-2}	λ_{max-3}	λ_{max-4}
-0.7384	-0.2328	-0.0823	-0.0488	-0.0298

Table 2.2. *Eigenvalues derived from $\frac{t}{11}e^{j2t}Vf$*

Example 2.12. (Largest λ values for the center $\frac{t}{11}e^{j2t}$ vector field in Figure 1.1)
The 5 bigest eigenvalues derived from the center vector field Vf in Figure 1.1 are given in Table 2.2. From Theorem 2.11, Vf is stable, since λ_{max}=-0.7384 in Table 2.2 lies within the unit circle in the complex plane $\mathbb{C}$.

Definition 2.13. *A characteristic of an object (aka sets, systems) X is a mapping φ:*

$$\varphi : X \to \mathbb{C} \text{ defined by } \varphi(x \in X) \in \mathbb{C}.$$

Definition 2.14. (Characteristic Distance)
Let X,Y be nonempty sets and $a \in A \in 2^X, b \in B \in 2^Y$ and let $\varphi(a), \varphi(b)$ be numerical characteristics inherent in A and B. The nearness mapping $d^{\Phi} : 2^X \times 2^Y \to \mathbb{R}$ is defined by

$$d^{\Phi}(A,B) = \inf_{\substack{\varphi(a) \in \Phi(A) \\ \varphi(b) \in \Phi(B)}} \{|\varphi(a) - \varphi(b)|\} = \varepsilon \in [0,1] \in \mathbb{C}.$$

In effect, A and B are characteristically near, provided $0 \leq d^{\Phi}(A,B) \leq 1$ in the first quadrant of the unit circle in the complex plane $\mathbb{C}$.

Definition 2.15. (Characteristic Nearness of Systems [13])
Let X,Y be a pair of systems. For nonempty subsets $A \in 2^X, B \in 2^Y$, the characteristic nearness of A,B (denoted by $A \ \widetilde{\delta}_{\Phi} \ B$) is defined by

$$A \ \widetilde{\delta}_{\Phi} \ B \Leftrightarrow d^{\widetilde{\Phi}}(A,B) = \varepsilon \in [0,1].$$

Theorem 2.16. (Fundamental Theorem of Near Systems)
Let X,Y be a pair of systems with $A \in 2^X, B \in 2^Y$.

$$A\, \widetilde{\delta}_{\Phi}\, B \Leftrightarrow \exists a \in A,\, b \in B : |\varphi(a) - \varphi(b)| = \varepsilon \in [0,1]$$

Proof. $\Rightarrow$: From Definition 2.14, $A\, \widetilde{\delta}_{\Phi}\, B$ implies that there is at least one pair $a \in A$, $b \in B$ such that $d^{\tilde{\Phi}}(A,B) = |\varphi(a) - \varphi(b)| = \varepsilon \in [0,1]$..
$\Leftarrow$: Given $d^{\Phi}(A,B) = \varepsilon \in [0,1]$, we know that $\inf_{\substack{a\in A\\ b\in B}} \sup|\varphi(a) - \varphi(b)| = \varepsilon \in [0,1] \in \mathbb{C}$. Hence, from Definition 2.15, $A\, \widetilde{\delta}_{\Phi}\, B$, also. That is, sufficient nearness of at least one pair characteristics $\varphi(a \in A), \varphi(b \in B) \in [0,1] \in \mathbb{C}$ indicates the characteristic nearness of the sets, i.e., we conclude $A\, \widetilde{\delta}_{\Phi}\, B$. □

Theorem 2.17. (Characteristically Close Systems)
Systems X,Y are characteristically near if and only X,Y contain subsystems that are characteristically near.

Proof. Immediate from Theorem 2.16. □

Theorem 2.18. (Stable Systems Extreme Closeness Condition)
Let $\vec{V}f1, \vec{V}f2$ be vector fields representing a pair of stable systems and let $max\lambda_{vecVf1}, max\lambda_{vecVf2}$ be the maximum λ (eigenvalues) for the pair of systems. If $\left|\max\lambda_{\vec{v}f1} - \max\lambda_{\vec{v}f2}\right| \in [0,0.5]$., then $\vec{V}f1\, \widetilde{\delta}_{\Phi}\, \vec{V}f2$.

Proof. From Theorem 2.11, for the vector field $\vec{V}f$ for a stable system, $max\lambda_{vecVf} \in [0,\pm 1]$. For a pair of system vector fields $\vec{V}f1, \vec{V}f2$, assume that $\left|\max\lambda_{\vec{v}f1} - \max\lambda_{\vec{v}f2}\right| \in [0,0.5] \in [0,1]$.. Hence, from Theorem 2.16, we have $\vec{V}f1\, \widetilde{\delta}_{\Phi}\, \vec{V}f2$. □

Remark 2.19. (Magiros Stable System Motions Condition)
Let the extreme closeness stability condition Theorem 2.18 corresponds to a pair of vector fields $\vec{V}f1, \vec{V}f1 : \vec{V}f1\, \widetilde{\delta}_{\Phi}\, \vec{V}f1$ derived from motion waveforms of a pair of physical systems. In that case, the maximal λ different requirement would represent a pair of motion waveforms that are very stable. That is, any small disturbance results in a small variation in the original waveform [14].

Remark 2.20. (Vector Field Characteristics)
We have the followig characteristics for a vector field $(\vec{V}f,+)$ to work with. Let $\vec{V}f =$ vector field in $\mathbb{C}$. $Sg = (\vec{V}f,+)$ Surface group in $\mathbb{C}$.

$\varphi_1(S_g) = (\max\varphi(\lambda)) \notin$ *unit circle* $\Rightarrow$ *unstable vector field.*

$\varphi_2(S_g) = (\max\varphi(\lambda)) \in$ *unit circle* $\Rightarrow$ *stable vector field.*

$\varphi_3(S_g) = \left\| \varphi(\lambda_{\vec{V}f_1}) - \varphi(\lambda_{\vec{V}f_2}) \right\| \in [0,0.5] \Rightarrow \vec{V}f_1\, \widetilde{\delta}_{\Phi}\, \vec{V}f_2.$

$\Phi(S_g) = \left\{\varphi_1(S_g), \varphi_2(S_g), \varphi_3(S_g)\right\}.$

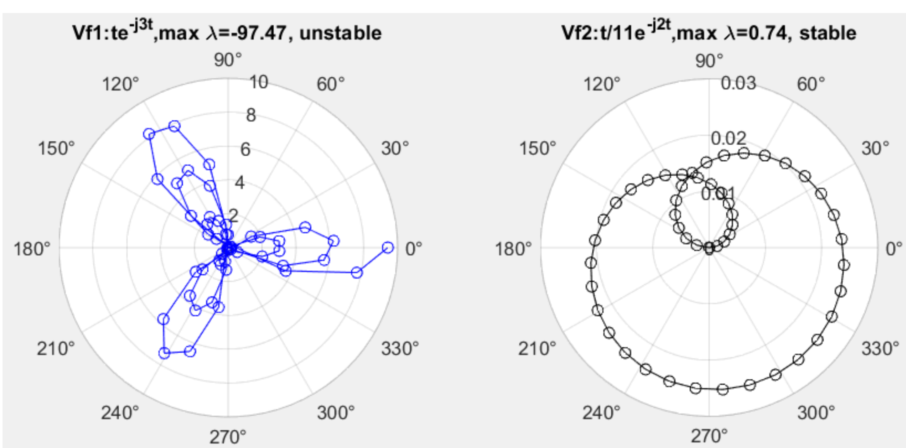

Figure 2.1. Case 1: Characteristically non-near vector fields

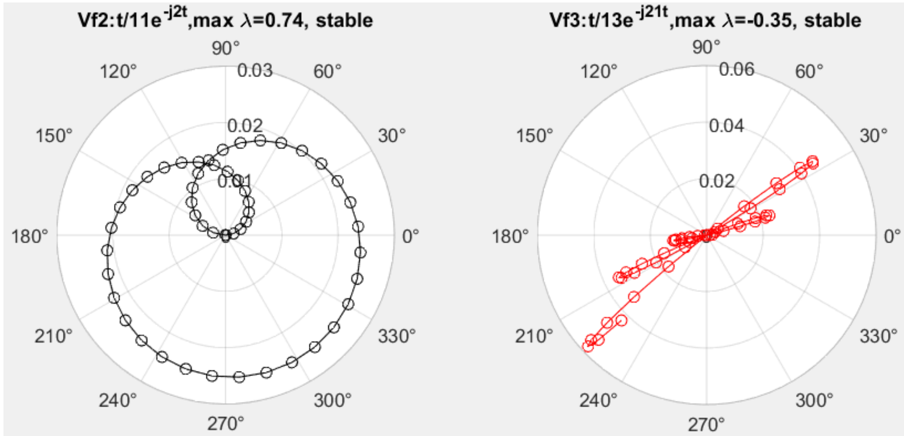

Figure 2.2. Case 2: Characteristically near vector fields

Example 2.21. (Characteristically Non-Near Vector Fields)
In Figure 2.1, (not)$(Vf1 \ \widetilde{\delta_\Phi} \ Vf2)$*, since*

$$\varphi_6(Sg_{Vf1})(max)\lambda = -97.47 \ \Rightarrow \ \textbf{unstable vector field}$$
$$\varphi_6(Sg_{Vf2})(max)\lambda = 0.74 \ \Rightarrow \textbf{stable vector field}.$$

Example 2.22. (Characteristically Near Vector Fields)
In Figure 2.2, $Vf2 \ \widetilde{\delta_\Phi} \ Vf3$*, since*

$$\varphi_5(Sg_{Vf2,Vf3}) = \left\| \varphi((\max)\lambda_{\vec{V}f_2} = 0.74) - \varphi(\lambda_{\vec{V}f_3} = -0.035) \right\| \in [0, 0.5] \Rightarrow \textbf{\textit{stable vector field}}.$$

$$\varphi_6(Sg_{Vf2})(\max)\lambda = 0.74 \Rightarrow \textbf{\textit{stable vector field}}.$$

$$\varphi_6(Sg_{Vf3})(\max)\lambda = -0.35 \Rightarrow \textbf{\textit{stable vector field}}.$$

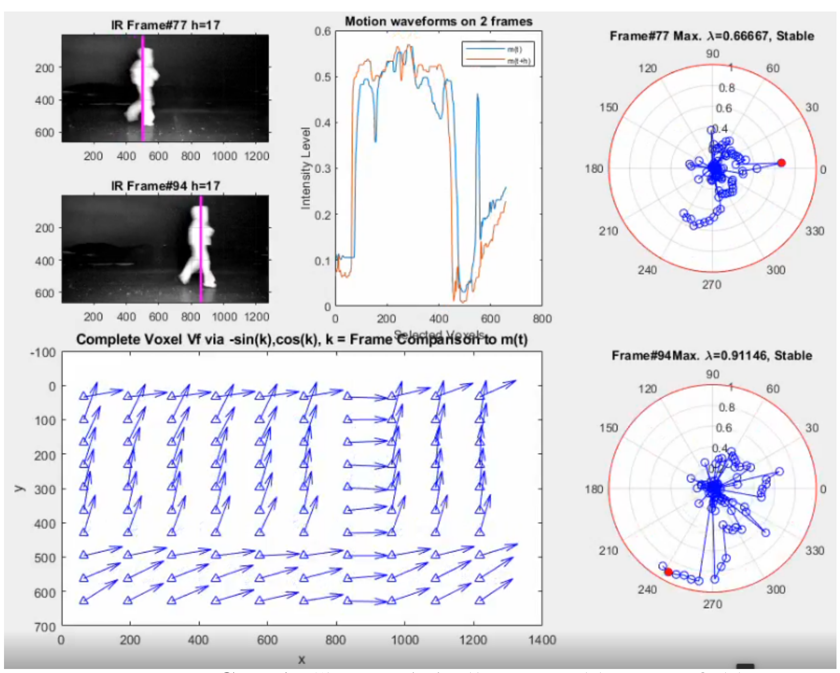

Figure 2.3. Case 1: Characteristically near stable vector fields

Theorem 2.23. (Characteristically Close Systems Are Proximally Close)
Characteristic close systems are proximal.

Proof. This is an immediate consequence of the fundamental near systems Theorem 2.16. □

3. Application: Detection of Characteristically Near Stable Vector Fields on Motion Waveforms in Infrared Video Frames

This section illustrates how to identify characteristically near motion waveforms in stable or unstable vector fields recorded in sequences of infrared video frames. This application presents an advance over the method of evaluating motion waveforms in video frames that was introduced in [16]. In the following example, the vector fields emanate from seqiences of runner waveforms is recorded in frame sequences in infrared videos. Be comparing the stability characteristics of the runner vector fields in pairs of video frames, we can then determine the overall stability of the runner. This approach carries over in assessing the characteristic closeness of the overall stability of the vector fields emanating from any vibrating system at different times. For simplicity, we consider only the maximum eigenvalues of the vector field in each video frame.

Example 3.1. (Case 1: Pair of Characteristically Close Stable Vector Fields)
In Figure 2.3, contains a pair of characteristically near stable vector fields $\vec{V}f_{fr77}, \vec{V}f_{fr94}$ in frames 77 and 94. Observe

$$max\lambda_{fr77} = 0.67,$$

$$max\lambda_{fr94} = 0.91,$$

$$||0.67| - |-0.91|| = 0.24 \in [0, 0.5];\ \textit{Hence, from characteristic } \varphi_3(S_g),$$

$$\vec{V}f_{fr77}\ \widetilde{\delta}_\Phi\ \vec{V}f_{fr94}.$$

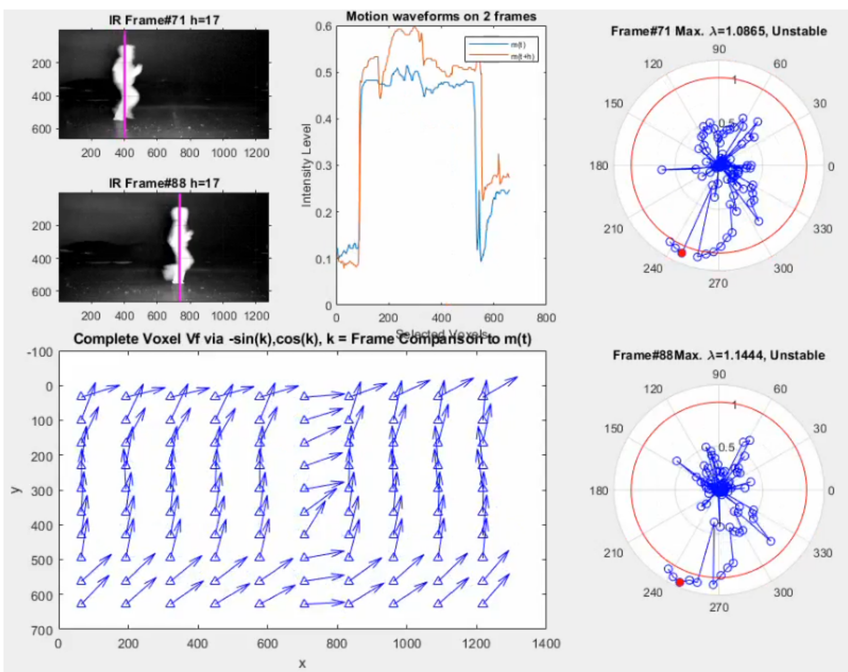

Figure 3.1. Case 2: Pair of Characteristically near unstable vector fields

Example 3.2. (Case 2: Pair of Characteristically Close Unstable Vector Fields)
In Figure 3.1, contains a pair of unstable vector fields $\vec{V}f_{fr71}, \vec{V}f_{fr88}$ in frames 71 and 88. Observe

$$max\lambda_{fr71} = 1.09,$$

$$max\lambda_{fr88} = 1.44,$$

$$||1.09| - |1.44|| = 0.35 \in [0, 0.5];\ \textit{Hence, from characteristic } \varphi_3(Sg),$$

$$\vec{V}f_{fr71}\ \widetilde{\delta}_\Phi\ \vec{V}f_{fr88}.$$

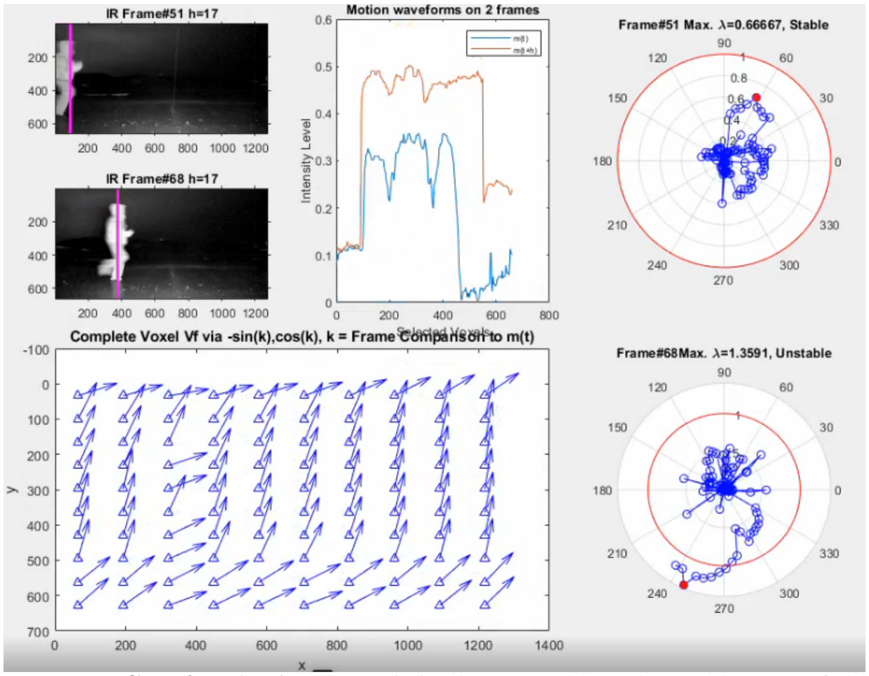

Figure 3.2. Case 3: Pair of Characteristically near stable and unstable vector fields

Example 3.3. (Case 3: Characteristically Close Stable and Unstable Vector Fields)
In Figure 3.2, contains a stable vector field $\vec{V}f_{fr51}$ *and unstable* $\vec{V}f_{fr68}$ *in frames 51 and 68. Observe*

$$max\lambda_{fr51} = 0.67,$$

$$max\lambda_{fr51} = 0.67,$$

$$max\lambda_{fr68} = 1.36,$$

$$||0.67| - |1.36|| = 0.69 \not\in [0, 0.5]; \textit{Hence, from characteristic } \varphi_3(Sg),$$

$$\vec{V}f_{fr51}\ (not)\widetilde{\delta}_{\Phi}\ \vec{V}f_{fr68}.$$

Remark 3.4. (Significance of Characteristically Non-Close Stable and Unstable Vector Fields in Case 3)
Stable vector fields characteristically non-close to unstable vector fields are represented in Case 3 in Figure 3.2. The vector fields in Example 3.3 have underlying systems that have the potential to be modulated to obtain a pair of characteristically close stable systems, since

$$||0.67| - |1.36|| = 0.69 \in [0, 1]\ (satisfies Theorem\ 2.16).$$

That is, even though the vector field $\vec{V}f_{fr68}$ *is unstable in Case 3, it is characteristically close to the stable vector field* $\vec{V}f_{fr51}$ *in Figure 3.2. That characteristic closeness suggests the possibility of modulating the waveform slightly to change the vector field* $\vec{V}f_{fr68}$ *from unstable to unstable.*

Unlike the temporal proximities of systems in the study in [8], the characteristically close systems in Figure 3.2 are within the same video, but are separated by 10 frames and, hence, are not temporally close. The form of characteristic closeness introduced in this paper corroborates the results in [13]. Cases 1 and 2 illustrate the result in Theorem 2.23, namely, characteristically close systems are proximal.

Acknowledgements

Acknowledgements: We extend our thanks to Tane Vergili for sharing her profound insights concerning the proximity space theory in this paper. In addition, we extend our thanks to Andrzej Skowron, Mirosław Pawlak, Divagar Vakeesan, William Hankley, Brent Clark and Sheela Ramanna for sharing their insights concerning time-constrained dynamical systems. In some ways, this paper is a partial answer to the question 'How [temporally] Near?' put forward in 2002 [15].

This research has been supported by the Natural Sciences & Engineering Research Council of Canada (NSERC) discovery grant 185986 and Instituto Nazionale di Alta Matematica (INdAM) Francesco Severi, Gruppo Nazionale per le Strutture Algebriche, Geometriche e Loro Applicazioni grant 9 920160 000362, n.prot U 2016/000036 and Scientific and Technological Research Council of Turkey (TÜBİTAK) Scientific Human Resources Development (BIDEB) under grant no: 2221-1059B211301223.

Author's Contributions: The Abstract and Introduction were written by J. F. Peters and edited by E. Cui. The definitions, remarks, examples and theorems that appear in Section 2 were introduced by J.F. Peters and edited by E. Cui. The examples in Section 3 were introduced by E. Cui and edited by J.F. Peters. All authors read and approved the final manuscript.

Artificial Intelligence Statement: AI is used to separate the changing from the unchanging parts of each video frame.

Conflict of Interest Disclosure: No potential conflict of interest was declared by the authors.

Plagiarism Statement: This article was scanned by the plagiarism program.

References

[1] S. G. Krantz, *Essentials of topology with applications*, CRC Press, New York, 2009. http://dx.doi.org/10.1201/b12333

[2] H. Poincaré, *Sur les équations de la dynamique et le problème des trois corps*, Acta Math., **13** (1890), 1-272.

[3] R. De Leo, J. A. Yorke, *Streams and graphs of dynamical systems*, Qual. Theory Dyn. Syst., **24** (2024), Article ID 1, 53 pages. https://doi.org/10.1007/s12346-024-01112-x

[4] M. Feldman, *Hilbert Transform Applications in Mechanical Vibration*, John Wiley and Sons, 2011. http://doi.org/10.1002/9781119991656

[5] P. Pokorny, A. Klic, *Dynamical systems generated by two alternating vector fields*, Eur. Phys. J. Special Top., **165** (2008), 61-71. https://doi.org/10.1140/epjst/e2008-00849-9

[6] R. Forman, *Combinatorial vector fields and dynamical systems*, Mathematische Zeitschrift, **228** (1998), 629–681. https://doi.org/10.1007/PL00004638

[7] S. Tiwari, J. F. Peters, *Proximal groups: Extension of topological groups. Application in the concise representation of Hilbert envelopes on oscillatory motion waveforms*, Comm. Algebra, **52**(9) (2024), 3904–3914. https://doi.org/10.1080/00927872.2024.2334895

[8] M. S. Haider, J. F. Peters, *Temporal proximities: Self-similar temporally close shapes*, Chaos Solitons Fractals, **151** (2021), Article ID 111237, 10 pages. https://doi.org/10.1016/j.chaos.2021.111237

[9] J. F. Peters, T. Vergili, *Good coverings of proximal Alexandrov spaces. Path cycles in the extension of the Mitsuishi-Yamaguchi good covering and Jordan curve theorems*, Appl. Gen. Topol., **24**(1) (2023), 25–45. https://doi.org/10.4995/agt.2023.17046

[10] E. Ozkan, B. Kuloglu, J. F. Peters, *k-Narayana sequence self-similarity. Flip graph views of k-Narayana self-similarity*, Chaos Solitons Fractals, **153**(2) (2021), Article ID 111473. https://doi.org/10.1016/j.chaos.2021.111473

[11] E. Erdag, J. F. Peters, O. Deveci, *The Jacobsthal-Padovan-Fibonacci p-sequence and its application in the concise representation of vibrating systems with dual proximal groups*, J. Supercomput., **81** (2025), Article ID 197. https://doi.org/10.1007/s11227-024-06608-6

[12] L. Euler, *Introductio in Analysin Infinitorum. (Latin)*, Sociedad Andaluza de Educacion Matematica Thales, Springer, New York, 1748.

[13] J. F. Peters, T. Vergili, F. Ucan, D. Vakeesan, *Indefinite descriptive proximities inherent in dynamical systems. An Axiomatic Approach*, arXiv, (2025). https://doi.org/10.48550/arXiv.2501.02585

[14] D. G. Magiros, *On stability definitions of dynamical systems*, Proc. Nat. Acad. Sci. U.S.A., **53**(6) (1965), 1288–1294,

[15] Z. Pawlak, J. F. Peters, Jak bliski? [Polish] (How near?). In: *Systemy Wspomagania Decyzji*, vol. I, 2007, pp. 57–109, University of Silesia, Katowice, ISBN 83-920730-4-5.

[16] J. F. Peters, T. U. Liyanage, *Energy Dissipation in Hilbert Envelopes on Motion Waveforms Detected in Vibrating Systems: An Axiomatic Approach*, Commun. Adv. Math. Sci., **7**(4) (2024), 178–186. https://doi.org/10.33434/cams.1549815